

INFORMATION TO USERS

This reproduction was made from a copy of a document sent to us for microfilming. While the most advanced technology has been used to photograph and reproduce this document, the quality of the reproduction is heavily dependent upon the quality of the material submitted.

The following explanation of techniques is provided to help clarify markings or notations which may appear on this reproduction.

1. The sign or "target" for pages apparently lacking from the document photographed is "Missing Page(s)". If it was possible to obtain the missing page(s) or section, they are spliced into the film along with adjacent pages. This may have necessitated cutting through an image and duplicating adjacent pages to assure complete continuity.
2. When an image on the film is obliterated with a round black mark, it is an indication of either blurred copy because of movement during exposure, duplicate copy, or copyrighted materials that should not have been filmed. For blurred pages, a good image of the page can be found in the adjacent frame. If copyrighted materials were deleted, a target note will appear listing the pages in the adjacent frame.
3. When a map, drawing or chart, etc., is part of the material being photographed, a definite method of "sectioning" the material has been followed. It is customary to begin filming at the upper left hand corner of a large sheet and to continue from left to right in equal sections with small overlaps. If necessary, sectioning is continued again—beginning below the first row and continuing on until complete.
4. For illustrations that cannot be satisfactorily reproduced by xerographic means, photographic prints can be purchased at additional cost and inserted into your xerographic copy. These prints are available upon request from the Dissertations Customer Services Department.
5. Some pages in any document may have indistinct print. In all cases the best available copy has been filmed.

**University
Microfilms
International**

300 N. Zeeb Road
Ann Arbor, MI 48106

8514202

Paracha, Obed-ur-Rahman

**AN EXPERIMENTAL INVESTIGATION OF THE EFFECT OF CARBON DIOXIDE
ON STEAM DRIVE RECOVERY**

The University of Oklahoma

PH.D. 1985

**University
Microfilms
International** 300 N. Zeeb Road, Ann Arbor, MI 48106

PLEASE NOTE:

In all cases this material has been filmed in the best possible way from the available copy.
Problems encountered with this document have been identified here with a check mark ✓.

1. Glossy photographs or pages _____
2. Colored illustrations, paper or print _____
3. Photographs with dark background _____
4. Illustrations are poor copy _____
5. Pages with black marks, not original copy _____
6. Print shows through as there is text on both sides of page _____
7. Indistinct, broken or small print on several pages ✓
8. Print exceeds margin requirements _____
9. Tightly bound copy with print lost in spine _____
10. Computer printout pages with indistinct print _____
11. Page(s) _____ lacking when material received, and not available from school or author.
12. Page(s) _____ seem to be missing in numbering only as text follows.
13. Two pages numbered _____. Text follows.
14. Curling and wrinkled pages _____
15. Dissertation contains pages with print at a slant, filmed as received _____
16. Other _____

University
Microfilms
International

THE UNIVERSITY OF OKLAHOMA
GRADUATE COLLEGE

AN EXPERIMENTAL INVESTIGATION
OF THE EFFECT OF CARBON DIOXIDE ON STEAM DRIVE
RECOVERY

A DISSERTATION
SUBMITTED TO THE GRADUATE FACULTY
in partial fulfillment of the requirements for the
degree of
DOCTOR OF PHILOSOPHY

by
OBED-UR-RAHMAN PARACHA
Norman, Oklahoma
1985

AN EXPERIMENTAL INVESTIGATION
OF THE EFFECT OF CARBON DIOXIDE ON STEAM DRIVE
RECOVERY
A DISSERTATION
APPROVED FOR THE DEPARTMENT OF PETROLEUM AND
GEOLOGICAL ENGINEERING

BY

Hebban Tiab
Akhtar S. Khan
Chaudhry
D. E. Menzie

ACKNOWLEDGMENTS

The author wishes to express his sincere appreciations to his advisor Dr. Djebbar Tiab for his guidance, invaluable suggestions and encouragement in completing this study. The moral support and valuable advice of Dr. Donald E. Menzie, Dr. A.S. Khan, Dr. Erle C. Donaldson and Dr. Faruk Civan are gratefully acknowledged.

The author feels greatly indebted to Dr. Roy Knapp for continued support, encouragement and guidance during the years of his graduate study.

I would also like to express my appreciations to my parents and friends for their continued support, love and concern during the preparation of this thesis.

A last but most significant debt goes to my wife for her patient efforts in typing and retyping this thesis. Forever appreciating her help, love and concern I dedicate this thesis to her.

ABSTRACT

A laboratory study was undertaken to evaluate the effects of carbon dioxide injection with steam on heavy to intermediate oil recovery. The effects of other operating parameters, such as pressure, temperature, injection rate, oil viscosity, and pH on oil recovery were also investigated.

A large number of displacement tests were conducted on unconsolidated sand packs of 3 inches in diameter and 24 inches in length. The sand packs were saturated with crude oils of gravities 15, 20, and 26°API. A mixture of varying concentration of carbon dioxide in steam, ranging from 0.0 to 0.006 SCF CO₂/cm.³ steam (water equivalent), was injected at different steam temperatures, rates, and pH to evaluate the effect of each individual parameter on oil recovery.

The examination of the results obtained indicated that: (1) the injection of carbon dioxide with steam increases the rate of recovery significantly, (2) the recovery is affected by the concentration of carbon dioxide in the injected steam and is maximized at a concentration of about 0.004 standard cubic feet of carbon dioxide per cubic centimeter of cold water equivalent steam, (3) the overall recovery depends on oil viscosity and hence the API gravity. It improves by 8 % in case of 15°API oil, 4% in case of 20°API oil, whereas no

significant improvement in ultimate recovery, over the conventional steam flooding process, was observed in case of 26°API oil, (4) the recovery decreases with increasing pressure and hence the temperature, (5) the recovery is rate dependent and is maximized at a steam injection rate of 30 cm.³/minute, (6) the recovery is not affected by pH, when steam and carbon dioxide are injected simultaneously.

TABLE OF CONTENTS

	Page
ACKNOWLEDGEMENTS.....	iii
ABSTRACT.....	iv
LIST OF TABLES	vii
LIST OF FIGURES	xi
Chapter	
I. INTRODUCTION	1
Statement of the problem.....	3
II. LITERATURE REVIEW	11
Mechanisms	23
III. MATHEMATICAL FORMULATION	31
Energy balance equation	31
Continuity equation.....	36
Dimensional analysis.....	48
IV. EXPERIMENTAL EQUIPMENT AND MATERIALS.....	73
Linear displacement cell	73
Porous medium	75
Pressure and temperature monitoring system.....	77
Production system	77
V. EXPERIMENTAL PROCEDURE	79
VI. RESULTS AND INTERPRETATIONS	85
Determination of recovery by conventional steamflooding.....	87

Determination of CO ₂ concentration in injected steam to maximize recovery	88
Determination of the steam injection rate to maximize recovery.....	91
Effect of oil gravity on ultimate recovery..	93
Effect of pH on ultimate recovery.....	96
Effect of pressure on ultimate recovery....	99
Comparison with theory.....	101
VI. SUMMARY AND CONCLUSIONS.....	109
REFERENCES	116
NOMENCLATURE	122
APPENDICES	127
A. Properties of oil and porous media....	130
B1. Summary of displacement test results (Phase 1).....	139
B2. Summary of displacement test results (Phase 2).....	161
C. Summary of displacement test results (Phase 3).....	166
D. Summary of displacement test results (Phase 4).....	176
E. Summary of displacement test results (Phase 5).....	182
F. Summary of temperature distribution results with distance.....	201
G. Plots of laboratory results.....	

LIST OF TABLES

Table	Page
3.1. Similarity Parameters for Steam Processes.....	63
3.2. Scaling Parameters for Steam Processes.....	64
A1. Crude Oil Physical Properties.....	123
A2. Mineral Content by Percent Weight of the Porous Media used for Displacement Tests.....	129
B11. Properties of the Sandpack and Fluids (Runs 1 through 6).....	132
B12. Displacement Test Results (Run 1).....	133
B13. Displacement Test Results (Run 2).....	134
B14. Displacement Test Results (Run 3).....	135
B15. Displacement Test Results (Run 4).....	136
B16. Displacement Test Results (Run 5).....	137
B17. Displacement Test Results (Run 6).....	138
B21. Properties of the Sandpack and Fluids (Runs 7 through 12).....	140
B22. Displacement Test Results (Run 7).....	141
B23. Displacement Test Results (Run 8).....	142
B24. Displacement Test Results (Run 9).....	143
B25. Displacement Test Results (Run 10).....	144
B26. Displacement Test Results (Run 11).....	145
B27. Displacement Test Results (Run 12).....	146

B31.	Properties of the Sandpack and Fluids (Runs 13 through 18).....	147
B32.	Displacement Test Results (Run 13).....	148
B33.	Displacement Test Results (Run 14).....	149
B34.	Displacement Test Results (Run 15).....	150
B35.	Displacement Test Results (Run 16).....	151
B36.	Displacement Test Results (Run 17).....	152
B37.	Displacement Test Results (Run 18).....	153
B41.	Properties of the Sandpack and Fluids (Runs 19 through 24).....	154
B42.	Displacement Test Results (Run 19).....	155
B43.	Displacement Test Results (Run 20).....	156
B44.	Displacement Test Results (Run 21).....	157
B45.	Displacement Test Results (Run 22).....	158
B46.	Displacement Test Results (Run 23).....	159
B47.	Displacement Test Results (Run 24).....	160
C11.	Properties of the Sandpack and Fluids (Runs 25 through 27).....	162
C12.	Displacement Test Results (Run 25).....	163
C13.	Displacement Test Results (Run 26).....	164
C14.	Displacement Test Results (Run 27).....	165
D11.	Properties of the Sandpack and Fluids (Runs 28 through 35).....	167
D12.	Displacement Test Results (Run 28).....	168
D13.	Displacement Test Results (Run 29).....	169
D14.	Displacement Test Results (Run 30).....	170
D15.	Displacement Test Results (Run 31).....	171
D16.	Displacement Test Results (Run 32).....	172
D17.	Displacement Test Results (Run 33).....	173

D18.	Displacement Test Results (Run 34).....	174
D19.	Displacement Test Results (Run 35).....	175
E11.	Properties of the Sandpack and Fluids (Runs 36 through 39).....	177
E12.	Displacement Test Results (Run 36).....	178
E13.	Displacement Test Results (Run 37).....	179
E14.	Displacement Test Results (Run 38).....	180
E15.	Displacement Test Results (Run 39).....	181
F1.	Temperature Distribution with Distance (Runs 1 through 3).....	183
F2.	Temperature Distribution with Distance (Runs 4 through 6).....	184
F3.	Calculated Temperature Distribution with Distance using Lauwriers Methods (Run 1 through 6).....	187

LIST OF FIGURES

Figure	Page
1.1. Carbon dioxide Effect on Mead Strawn Crude Oil.....	7
1.2. Viscosity of Crude Oils Saturated with CO ₂	7
1.3. Carbon dioxide Density Required for Miscible Displacement.....	9
2.1. Willman et al Steam Drive Model.....	13
2.2. Schematic Drawing of Baker's Flow Model.....	15
2.3. Effect of Steam Quality on Oil Recovery.....	20
2.4. Effect of Steam Injection Rate on Oil Recovery.....	20
2.5. Effect of Permeability on Oil Recovery	21
2.6. Effect of Dip on Oil Recovery.....	22
2.7. Effect of Well Location on Oil Recovery.....	22
2.8. Schematic Diagram of Steam Drive.....	25
2.9. Effect of Temperature on Irreducible Water Saturation.....	28
2.10. Effect of Temperature on Relative Permeability Ratio.	29
2.11. Effect of Temperature on Residual Oil Saturation.....	30
2.12. Individual Relative Permeability as a Function of Temperature.....	30
3.1. Schematic Diagram For Mass And Heat Balance.....	32
4.1. Schematic of Experimental Setup.....	74
4.2. Schematic of the Displacement Cell.....	76

Figure	Page
6.1. Effect of CO ₂ on Steam Drive Recovery (Steam Injection Temperature = 300°F).....	86
6.2. Effect of Injection Rate on Steam Drive Recovery.....	92
6.3. Effect of Gravity on Steam Drive Recovery.....	95
6.4. Effect of Pressure on Steam Drive Recovery.....	100
6.5. Comparison of Experimental Results with Those Obtained by Using Myhill and Stegemeier Method.....	107
6.6. Temperature Distribution with Distance for Run No.1..	108
G1. Effect of CO ₂ on Steam Drive Recovery (Steam Injection Temperature = 350°F).....	202
G2. Effect of CO ₂ on Steam Drive Recovery (Steam Injection Temperature = 400°F).....	203
G3. Effect of CO ₂ on Steam Drive Recovery (Steam Injection Temperature = 450°F).....	204
G4. Effect of CO ₂ on Steam Drive Recovery (Steam Injection Temperature = 500°F).....	205
G5. Effect of CO ₂ on Steam Drive Recovery (Steam Injection Temperature = 550°F).....	206
G6. Effect of CO ₂ on Steam Drive Recovery (Steam Temperature = 400°F, Oil Gravity = 15°API)....	207
G7. Effect of CO ₂ on Steam Drive Recovery (Steam Temperature = 400°F, Oil Gravity = 26°API)....	208
G8. Effect of pH on Steam Drive Recovery (CO ₂ /Steam Ratio = 0.00 SCF CO ₂ /cm ³ Steam).....	209
G9. Effect of pH on Steam Drive Recovery (CO ₂ /Steam Ratio = .002 SCF CO ₂ /cm ³ Steam).....	210
G10. Effect of pH on Steam Drive Recovery (CO ₂ /Steam Ratio = .004 SCF CO ₂ /cm ³ Steam).....	211
G11. Effect of pH on Steam Drive Recovery (CO ₂ /Steam Ratio = .006 SCF CO ₂ /cm ³ Steam).....	212
G12. Holm-Josendal Dynamic Miscibility Displacement Correlation.....	213

Figure	Page
G13. Pressure Required for Miscible Displacement in CO ₂ Flooding.....	214
G14. Physical System Representing CO ₂ /Steam Flooding.....	215
G15. Chart for Temperature Variation of Crude Oil Viscosity.....	216
G16. Effect of Oil Viscosity on Development of Vertical Sweep.....	217
G17. Swelling Factor Comparison of Heavy Oils.....	218
G18. Temperature Distribution with Distance for Run No.2...	219
G19. Temperature Distribution with Distance for Run No.3...	220
G20. Temperature Distribution with Distance for Run No.4...	221
G21. Temperature Distribution with Distance for Run No.5...	222
G22. Temperature Distribution with Distance for Run No.6...	223
G23. Fraction of Heat Injected in Steamflood Remaining in Steam Zone.....	224

CHAPTER I

INTRODUCTION

Throughout the entire world a considerable amount of oil is classified as unrecoverable by existing primary and secondary recovery techniques. The magnitude of this resource together with the declining world oil reserves prompted the petroleum engineers and researchers to develop enhanced oil recovery methods, which are separated into three major categories:

1. Thermal recovery
 - a. Steam stimulation
 - b. Steam drive
 - c. In situ combustion
2. Chemical flooding
 - a. Surfactant/Polymer Injection
 - b. Polymer Flooding
 - c. Caustic Flooding
3. Miscible Displacement
 - a. Miscible Hydrocarbon Displacement
 - b. CO₂ Injection
 - c. Inert Gas Injection

Steam drive and CO₂ injection are the most widespread commercial processes. Steam flooding, the most profitable enhanced oil recovery method today, has proved a powerful recovery process in heavy oil reservoirs. Recently it was applied successfully to a relatively low viscosity oil reservoir.¹

Carbon dioxide flooding is the next most promising among the enhanced oil recovery methods. Miscible displacement with CO_2 has been applied successfully to reservoir oils with API gravities of greater than 25° API, while its application with low API gravity oils has been restricted because of the complex phase behavior, including the possible deposition of asphaltene, which might damage the permeability of the reservoir. Immiscible displacement with CO_2 applies efficiently to the heavier, viscous, reservoir oils through the mechanisms of oil swelling and oil viscosity reduction. For all heavy oil reservoirs the major mechanism of the enhanced oil recovery method is the reduction of reservoir oil viscosity which results in a pronounced increase in the mobility of the oils and a corresponding improvement of oil production rates. Welker and Dunlop² published the viscosity reduction effects of CO_2 in 1963. They concluded that viscosity reduction is as high as 98% for a 4800-cp heavy crude oil at 80°F.

Pursley³ and Weinstein⁴ were the first to suggest the addition of gas to cyclic steam stimulation. They found a 50%, or more, increase in oil recovery from gas/steam stimulation compared with steam alone in physical and computer models. They also matched field results for steam stimulation with and without gas. Recently Redford⁵ investigated the effects of solvent addition to steam with highly positive results.

The motivation for this study comes from the promising results of earlier studies mentioned above and the enhanced oil recovery projects where exhaust gases from the steam generators are injected into the reservoir along with the steam. The

emphasis of this study will be on the recovery by steam/CO₂ flooding processes.

Statement of the Problem

1. Steam Flooding:

The two most widely used and profitable enhanced oil recovery techniques available today are cyclic steam stimulation and steam flooding (or steam drive). Current oil production from these methods exceeds 550,000 barrels per day which accounts for more than 80% of the total enhanced oil recovery production. Considering the huge proven reserves of heavy viscous oil, discovered to date, which exceed one trillion barrels, the potential for future production by these methods is still higher.

Cyclic steam stimulation process consists of injecting steam into the producing well for a certain specified period of time followed by shutting-in the well to allow sufficient time for the heat to dissipate and spread into the reservoir and then placing the well on production. This process allows the immediate surroundings of the production well to be maintained at a higher temperature thus improving the flow of oil near the well bore. Oil production stabilizes at a much higher level due to the pronounced increase in the mobility of the heavy oil. In addition to the viscosity reduction resulting from steam injection, other factors contributing to the stimulated production are:

- a. Thermal expansion
- b. Compression of solution gas
- c. Well bore clean-up effects

In a steam flooding process, steam is injected into a number of injection wells and oil is produced from the adjacent wells. As the steam moves forward towards the producing well, its temperature drops and at some distance from the injection well it starts condensing forming a hot water bank. The hot water condensed from the steam tends to settle below the steam vapor because of its relative higher density and the steam travels preferentially along the top of the bed as it moves towards the producing well.

Three principal zones develop in this process which are identified as:

1. Saturated steam zone
2. Condensation zone
3. Hot water zone

Each of these zones makes positive contributions towards the enhancement of oil displacement. In the saturated steam region, oil displacement is enhanced by effects of steam distillation, gas drive and solvent extraction, in addition to the viscosity reduction, thermal expansion and reduction in residual oil saturation etc. active in other heated regions too. Oil displacement is also enhanced by the increasing relative permeability to oil with increased temperature.^{6,7,8}

There is little or no information in published literature on failures of the steam flooding process, which would have given valuable data in defining the limits of applications of these processes. Among the parameters to be considered before any practical application, the following are of particular

importance.

1. Permeability should be high, no lower than 1 darcy for full scale displacement.
2. Oil in place should be about 1200-1700 bbl/acre-foot.
3. The oil gravity should be in the range of 15-30°API.
4. Formation thickness should be greater than 30 ft. and its depth should be less than 3000 ft. to minimize heat losses. The reservoir depth is also limited by the technical aspects of high pressure injection.

2. Carbon Dioxide Flooding:

The idea of oil displacement by CO₂ originated during the late twenties.^{9,10} Through intensive laboratory research and field tests this idea turned into a proven recovery process with the potential of recovering more than 90% of the oil contacted in a reservoir. The factors contributing to the enhanced production as a result of CO₂ injection are identified as:

1. Oil Swelling
2. Viscosity Reduction
3. Miscibility Effects
4. Solution Gas Drive
5. Reaction with Reservoir Rock

The various mechanisms by which it displaces oil from the porous media include:

1. Miscible Drive
2. Immiscible Drive
3. Trapped Gas Effect

A miscible displacement is one in which the displacing and the displaced fluids become miscible in all proportions, at least to a local extent, without formation of an interface between the two fluids. Miscibility depends upon the pressure, temperature, the composition of the oil and the composition of the displacing fluid. Miscible displacement theoretically recovers all of the reservoir oil contacted because of the elimination of the capillary and interfacial forces which are responsible for retaining substantial quantities of oil under immiscible conditions.

Carbon dioxide has the potential of not only eliminating the capillary and interfacial forces above certain reservoir pressures and thus creating miscible flow conditions, it also is, highly soluble in crude oils at moderate pressures which causes considerable swelling and reduction in the viscosity, thereby increasing recovery efficiency (see figures, 1.1, & 1.2).^{12,13}

The pressure range in this type of displacements varies from about 700 psia necessary to achieve substantial CO₂ solubility, to a certain higher value (ranging from 2000 to more than 5000 psi depending on composition of oil and reservoir temperature) at which the solubility of CO₂ causes sufficient extraction of hydrocarbons to promote miscible displacement. This higher pressure is termed by some investigators¹⁴ as the minimum miscibility pressure and is defined as the pressure at which the recovery is 94% of the oil contacted at a given temperature and above which essentially no additional oil is recovered. A number of correlations are available in the literature for determining

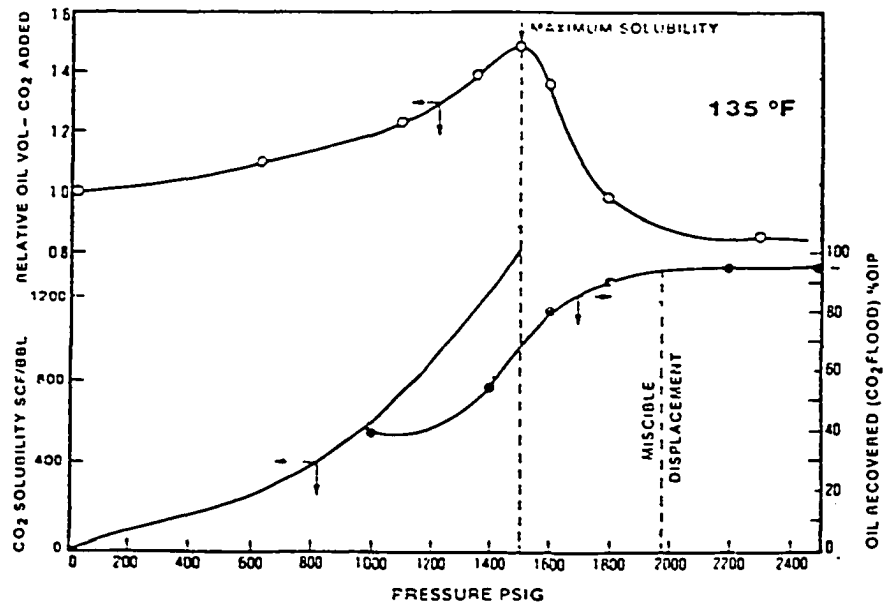


Figure 1.1: Mead Strawn Crude oil (after Ref.12)

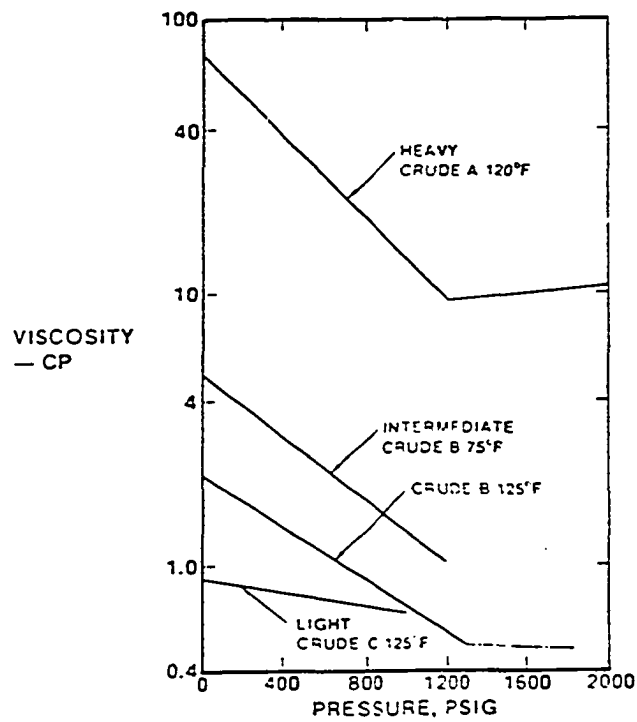


Figure 1.2: Viscosity of Crude oils Saturated with CO₂ (after Ref.13)

the optimum pressure required for maximum oil displacement efficiency by miscible displacement.^{15,16,17}

It has been reported that lower miscibility pressure is required for lighter oils, while for heavier oils the pressure requirement is quite high to create miscibility conditions (see fig. 1.3).¹⁸ The purity of the injected CO_2 , also affects the miscibility pressure. Its contamination with N_2 or CH_4 causes an increase, whereas C_3H_8 or H_2 causes a decrease in the pressure required for miscible displacement. Reservoir oils with gravities of more than 25° API are the best candidates for CO_2 miscible displacement.

Since the pressure and amount of CO_2 required for miscible displacement of heavier oils is too high, the economic factors do not dictate this type of displacement process. These oils can still be recovered by immiscible CO_2 displacement through the mechanisms of oil swelling and oil viscosity reduction because of the high solubility of CO_2 at reservoir pressures. Oils of gravities as low as 15° API are efficiently recovered by CO_2 immiscible displacement.

During the above mentioned displacement processes by CO_2 (miscible or immiscible), some oil is also recovered by the trapped gas effect. The injection of CO_2 creates a free gas saturation which replaces a part of the residual oil that would not have been otherwise recovered.

Applications of the CO_2 displacement processes also have some limitations given as follows:

1. The principal difficulty in any CO_2 displacement

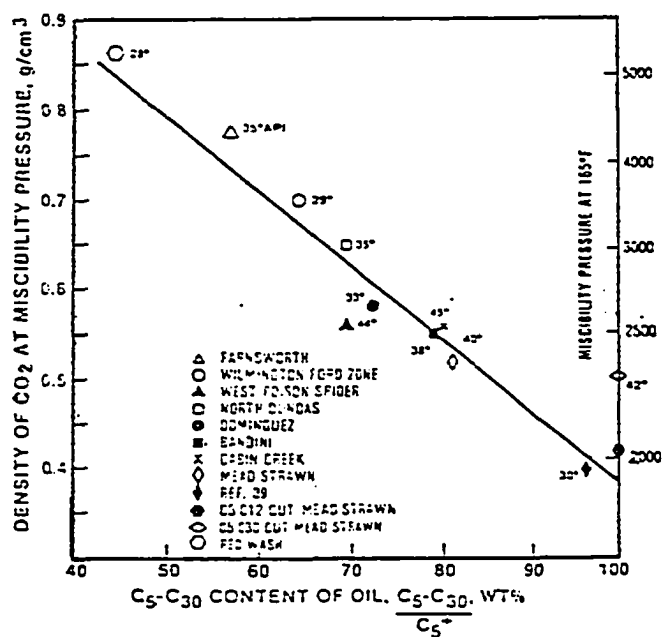


Figure 1.3: Carbon dioxide density required for miscible displacement vs. C₅ through C₃₀ content of crude oils (after Ref. 17).

process is contact of a large fraction of the oil. Because of the very high mobility¹⁹ of CO₂ due to its very low viscosity, the displacement of oil is unstable giving rise to the following problems:

- a. CO₂ fingers through the more viscous fluid
- b. Sweep efficiency is lower than desirable
- c. Early breakthrough of CO₂ into producing wells

Consequently substantial amount of reservoir oil is not contacted, not swelled and its viscosity is not reduced.

2. Thin pay zones and low vertical permeability are preferred to prevent gravity override.
3. Oil saturations should be greater than 25% and its gravity not be less than 15° API.
4. Reservoir must be deep enough so that its pressure is greater than the miscibility pressure of CO₂. Most of these limitations may be eliminated if steam is injected along with CO₂.

In this experimental study these two most promising enhanced oil recovery processes, steam flooding and CO₂ flooding, were combined to: (1) investigate the effect of CO₂ on steam drive performance, (2) establish a CO₂/steam ratio which would maximize recovery.

CHAPTER II

LITERATURE REVIEW

Steam flooding has been employed successfully to recover oil from medium to heavy oil reservoirs for the past three decades and has emerged as one of the most efficient processes in the field of Petroleum Engineering. Since its inception the steam drive process has been and is being studied in the laboratory, field and by the use of mathematical models. The ultimate objective of all this work is to develop a reliable engineering scheme to estimate oil recovery for a given set of conditions which could be altered to optimize steam flood design.

Willman et al²⁰ took the lead in conducting experimental research on linear laboratory cores when subjected to steam flooding and as a result concluded that:

1. The recovery by steam injection is significantly higher than hot water flooding which in turn is more efficient than the conventional cold water flooding.
2. The mechanisms responsible for the increased recovery are thermal expansion of oil, viscosity reduction and steam distillation with its related gas drive and solvent extraction effects.

They also suggested a procedure for estimating steam drive

performance based on the classical heat balance equations first presented by Marx and Langenheim²¹ assuming that the flow of heat from the steam zone into the hot liquid zone ahead of the condensation front is negligible (see fig. 2.1). This method of solution, in spite of its restrictive assumptions, has found considerable applications.

Lauwerier²² presented a model to predict the temperature distribution and thermal efficiency of a hot, non-condensable, fluid injection process by assuming thermal conductivities to be zero in the direction of flow and infinite over the longitudinal cross-section of the reservoir. Spillette²³ and Thomas²⁴ refined this model by relaxing the imposed restrictive assumptions and presented a numerical solution of the heat balance equations. While using these equations to describe the growth of steam zone, Mandl and Volek²⁵ discovered that the equations become inconsistent with the physical model of the steam drive process after a certain critical time which is dependent on the reservoir thickness, temperature and steam quality. They also found that the process of heat flow across the condensation front changes from purely conductive in nature to increasingly convective after the critical time. As a result of their findings they modified the existing equations and presented a method to determine the saturation at the downstream side of the condensation front. Gottfried²⁶ presented a theory of thermal recovery processes in linear systems and developed a sophisticated mathematical model that explicitly accounted for the conduction-convection heat transfer with convective external heat loss, aqueous phase change and hydrodynamics

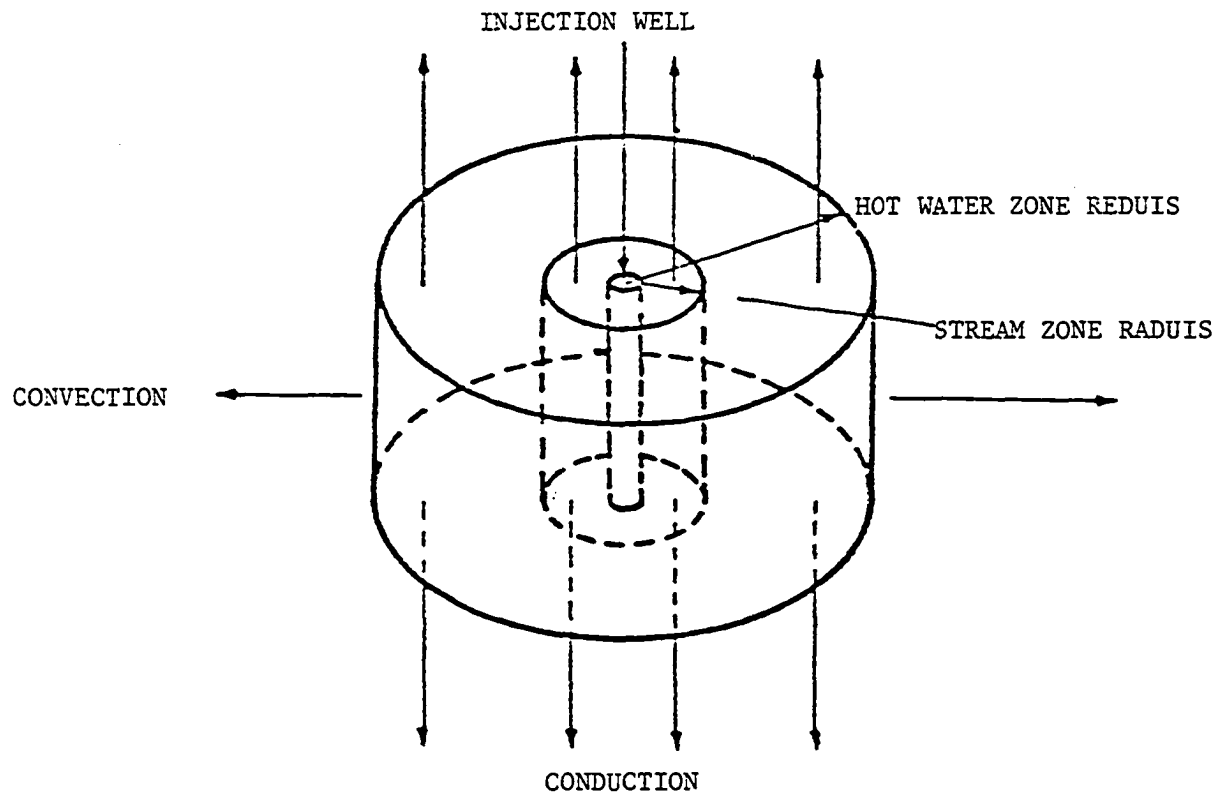


Figure 2.1: Willman et al.²⁰ Steam Drive Model

of three phase flow. Although considerable computer time is required to obtain solutions of the system of equations to predict the temperature, pressure and saturation profiles in space and time, the model represented a major advance in ability to simulate the physical & chemical phenomena observed in thermal recovery experiments.

Farouq Ali²⁷ used the Marx and Langenheim approach to determine the effects of changes in the thermal properties of the overburden and underburden on steam flood performance and presented estimates of the error caused by the usual assumption of identical properties for overlying and underlying formations. In another related investigation²⁸ he studied the effects of variable rates of steam injection on the extent of heated area of the reservoir.

Closmann²⁹ using the same approach studied the growth of steam zones as a function of time due to steam injection into stratified formation consisting of highly permeable paths of equal steam injectivity separated by impermeable layers of equal thicknesses. He found that the presence of more permeable stringers is beneficial to overall heating of the reservoir.

Baker^{30,31} conducted laboratory steam flood experiments using a radial flow model (see Fig. 2.2) that comprised of disc shaped sand-pack reservoir, and an overburden and underburden consisting of water saturated sand. He observed, among other things, significant gravity override at all injection rates and found that:

1. The heat lost to the overburden and underburden when expressed as a fraction of total heat injected, is independent of injection rate and is solely a function

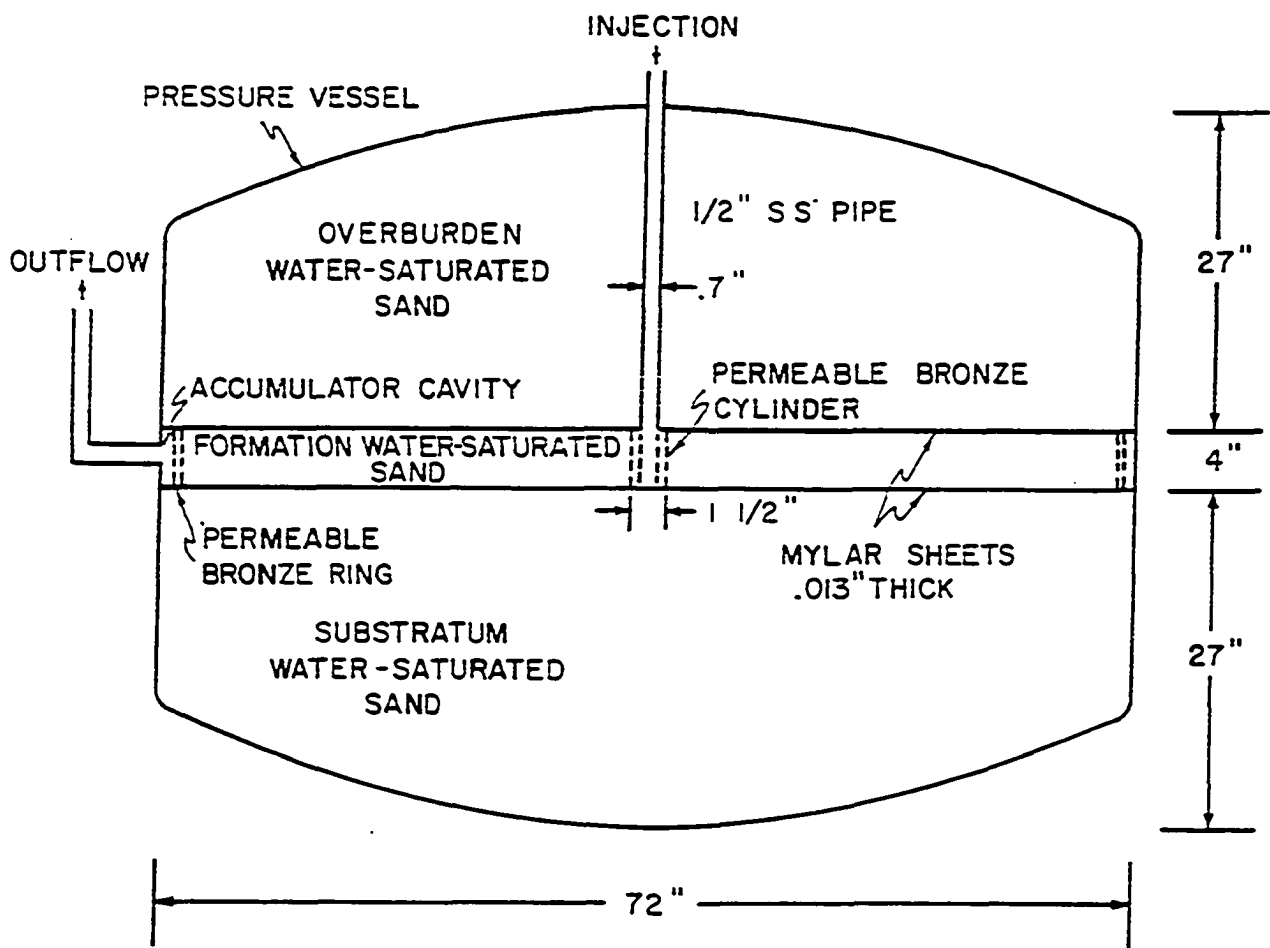


Figure 2.2: Schematic Drawing of Baker's³⁰ Flow Model.

of time for a given formation thickness.

2. The division of heat between the steam and hot water zones is dependent on mass injection rate.
3. Gravity override is a strong function of injection rate and has minimal dependence on pressure and time.

Gravity override has also been noticed by Blevins, Aseltine and Kirk³² while analysing a steam flood field project.

Shutler^{33,34} presented three phase steam flooding models for both linear and two dimensional fluid flow for the first time. The models allowed for interphase mass transfer between water and gas phases but assumed the oil to be non volatile and the hydrocarbon gas insoluble in liquid phases, thereby excluding the effects of miscibility from the steam drive process. Abdalla and coats³⁵ also derived a three phase, two dimensional steam flooding model and used an implicit pressure explicit saturation numerical technique to solve the system of equations. Shutler and Boberg³⁶ developed an analytic technique to calculate the size of the steam zone and to predict oil recoveries in one dimensional reservoirs using buckley Leverette method. The method is restricted to be used only for thin reservoirs.

Vinsome,³⁷ Coats et al³⁸, Coats³⁹ and Weinstein et al⁴⁰ advanced the technology a step further by presenting three phase, three dimensional steam flooding models. The advantages of these models over the previous ones stem from their ability to give simultaneous solution of the mass and energy balance equations; and implicit treatment of capillary pressure, water transmissibility,

and rates. The last two models also account for steam distillation.

Based on observations in Kern River steam drive project, Neuman⁴¹ included the important effects of gravity over-ride in his analytical model to describe the performance of a steam flood process in three dimensional reservoirs. He used Marx and Langenheim²¹ approach to calculate the rate of areal growth by the thermal balance between the net heat injection as steam and that required for steam condensation to sustain vertical growth. He predicted that the oil produced from the heated zone is a function of the net heat injected as steam.

Miller⁴² studied the effect of heat transport near the front and expansion or contraction due to thermodynamic phase change or chemical reaction at the front and showed that both these effects act to stabilize a moving front at which steam condenses and displaces water thus causing significant improvement in oil recovery.

Van Lookeren⁴³ following a different approach than Neuman, based on segregated flow principles and Dupuit⁴⁴ approximation, developed an analytical model to estimate the approximate shape of the steam/liquid interface for linear and radial flow systems. Rhee and Doscher⁴⁵ included the effect of steam distillation and extended this work to develop a method based on Higgen's Leighton's⁴⁶ areal model to determine the shape and growth of steam and hot condensate zones by integrating Van-Looeren's solution according to either Marx-Langenheim or Mandl Volek's approaches. One should not ignore the very interesting study of Myhill and Stegmeier⁴⁷ in the development of a prediction model based on simple energy balance equations to estimate ultimate oil/steam

ratios by assuming no contributions of the condensate zone to the oil recovery. They claimed that the model compared very well with the field and laboratory results. One should also mention the remarkable work of Ferrer et al⁴⁸ in deriving a three phase, three dimensional multicomponent flow model, designed to simulate steam injection processes. The model allows interphase mass and heat transfer to account for changes in oil composition in space and time.

Gomma⁴⁹ reported a novel curve matching model based on parametric studies done with a numerical simulator to predict steam flood performance.

Yortsos and Gavalas⁵⁰ reported analytical models that address the problem of heat transfer in detail in the hot liquid zone. They followed an integral balance approach to obtain upper bounds for one or multi-dimensional reservoirs under constant or variable injection rates and developed approximate asymptotic solutions in one dimensional reservoirs at constant injection rates. During the course of this work, they developed and delineated the range of validity of the existing models of Lauwrier, Marx-Langenheim, Mandl-Volek, Myhill-Stegmeier and Van Lookeren. Yortsos⁵¹ later extended this model to describe the fluid flow and the resulting saturation distributions inside the steam zone in a one dimensional steam injection process.

Based on Van Lookeren and Myhill-Stegmeier Works, Jeff Jones⁵² proposed a steam drive model that can be used on a hand-held programmable calculator. The model comprises two integrated components. The first component calculates an optimal steam rate for

a given set of steam and reservoir parameters, while the second component calculates the oil production history by using the data obtained in the first component. He claimed that the results obtained by using this model matched well with the field results.

Moughamian et al⁵³ studied the effects of selected reservoir and operating parameters on oil recovery. They found among other things, that reservoir dip, steam quality, and steam injection rate are among the most important parameters affecting recovery efficiency (see Figures 2.3 through 2.7).

Krueger⁵⁴ extended Miller's theory to include injection of Nitrogen, a non condensing gas, together with the steam to study the stability of a flat condensation front displacing water. He concluded among other things that:

1. Injection of Nitrogen together with steam increases the possibility of having fingers compared with no Nitrogen case.
2. Cooling fingers and surface tension have a stabilizing effect.
3. Increasing temperature has a destabilizing effect.

Closmann and Seba⁵⁵ conducted an experimental study to determine oil recovery by steam injection in linear systems and to investigate the effects of core length, saturation variations, pore size, and injection rates on residual oil saturations. They found among other things that:

1. The breakthrough oil saturation is dependent on oil/water viscosity ratio evaluated at steam temperature and is not influenced by core length.

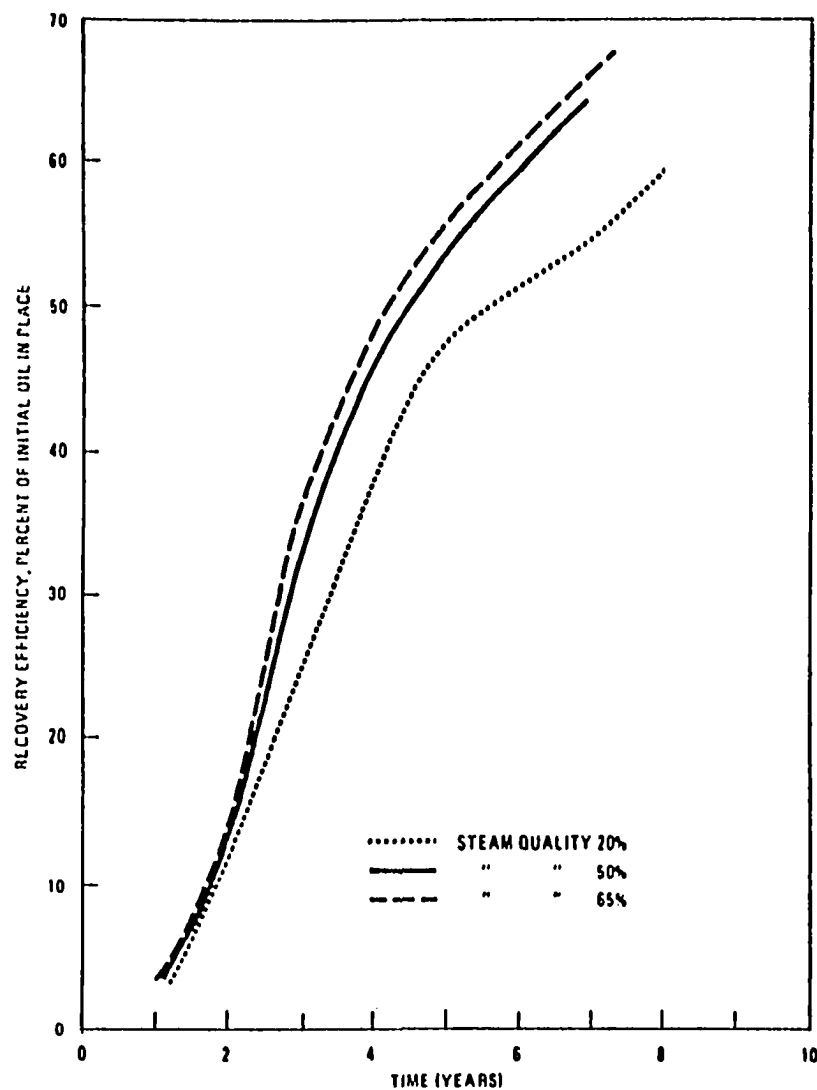


Fig. 2.3: Effect of steam quality on oil recovery (after Ref. 53).

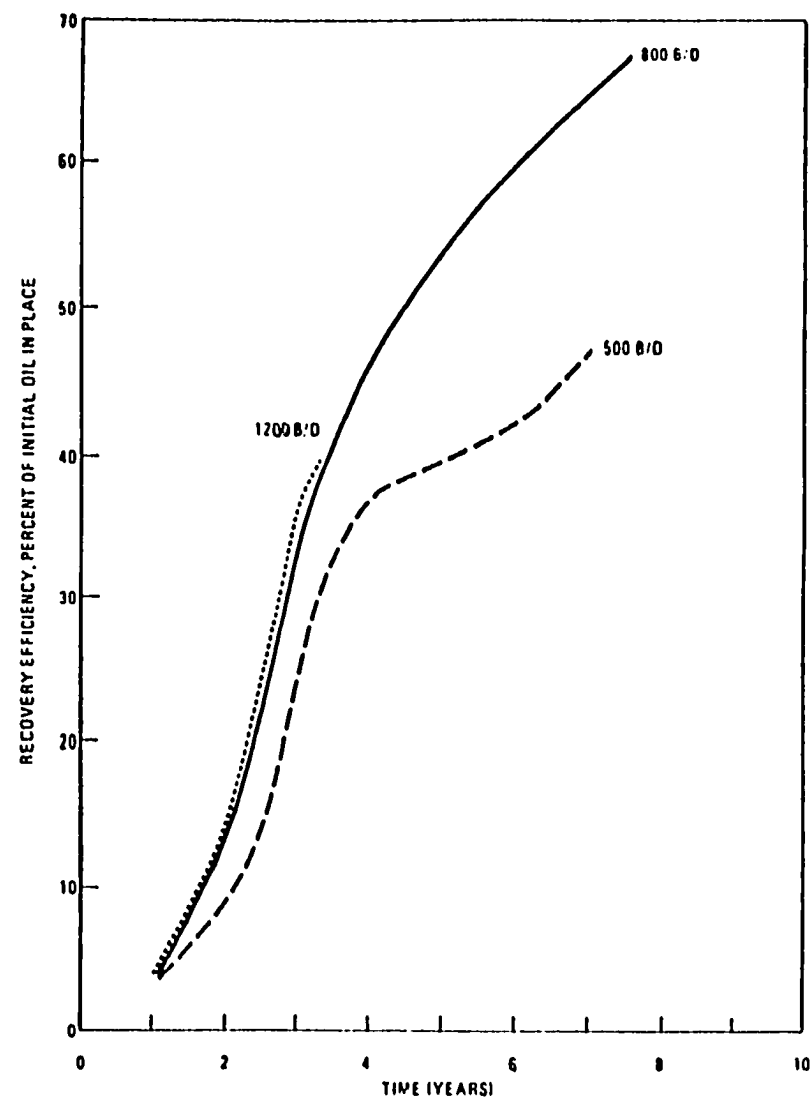


Fig. 2.4: Effect of steam injection rate on oil recovery (after Ref. 53).

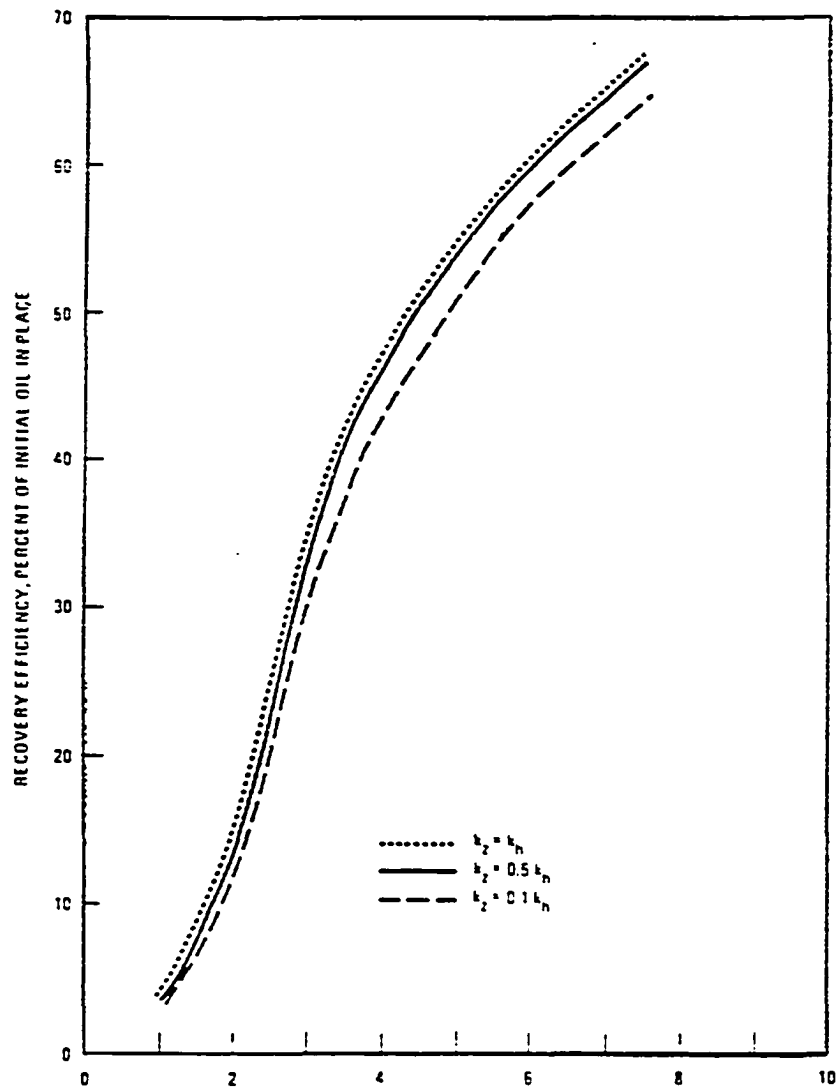


Fig. 2.5: Effect of permeability on oil recovery (after Ref. 53).

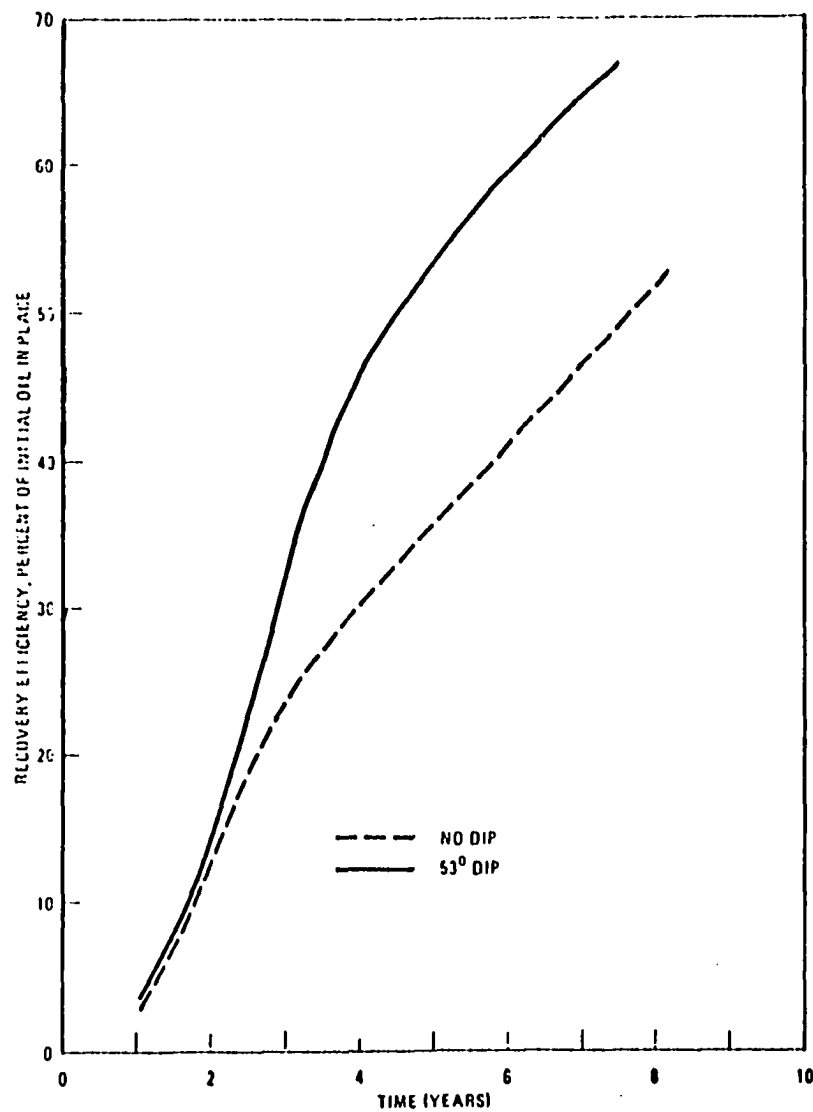


Fig. 2.6: Effect of dip on oil recovery (after Ref. 53).

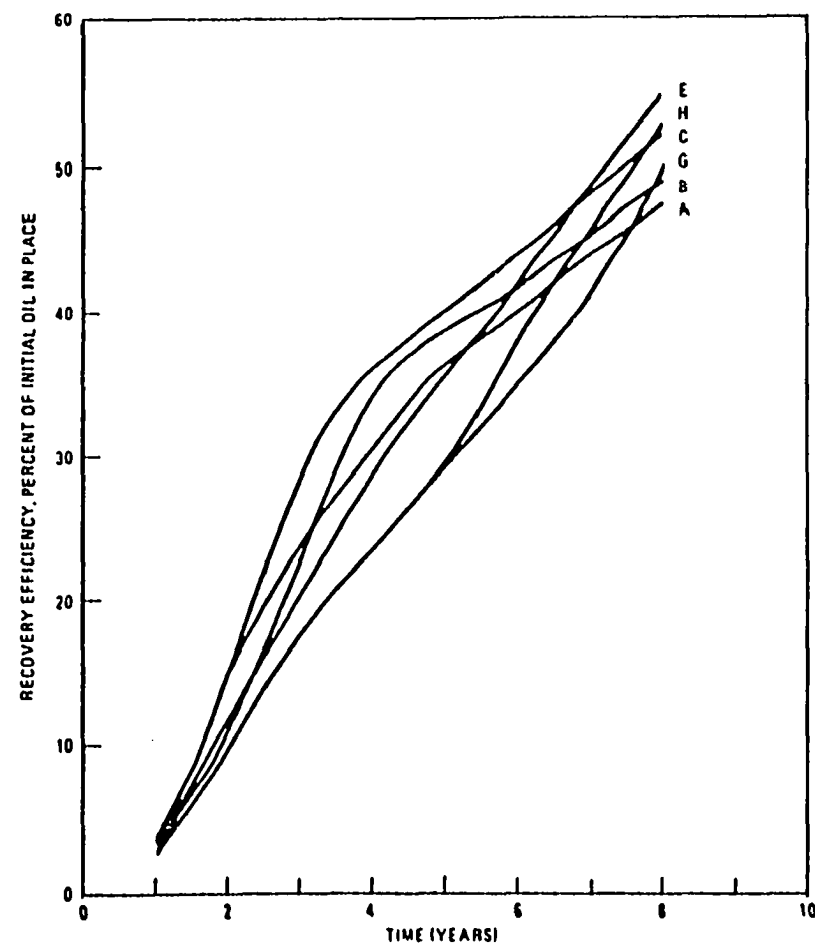


Fig. 2.7: Effect of well location on oil recovery (after Ref. 53).

2. The oil produced after steam breakthrough is also a function of oil/water viscosity ratio at steam temperature.

Steam injection technology has advanced significantly since its inception by the continuous research and analysis of laboratory and field results thus providing greater understanding of the process and its mechanisms. Several investigators have tried to improve the already good performance of the steamflooding process by the use of additives such as alkalis, polymers, solvents, surfactants etc. with steam but no systematic evaluation was either presented or published. In this connection Leung⁵⁶ applied numerical techniques to evaluate the effect of simultaneous steam and carbon dioxide injection on the recovery of heavy oil and found that the addition of carbon dioxide to injected steam improves the ultimate recovery slightly but enhances the oil production rate significantly before the steam breakthrough.

Mechanisms:

Steam flooding is a complex oil displacement process that defies an exact description. As soon as steam enters the formation, it starts rapidly migrating upward due to strong gravitational gradients while advancing into the originally cool reservoir. As the steam zone grows, gravity overlay occurs, and this overlay increases as steam injection progresses. Simultaneously, part of the steam condenses forming a bank of water and displaced oil. The reservoir may then be divided into two distinct zones separated by a moving boundary: 1.) steam zone 2.) a hot

liquid zone which also includes initial cold region (see Fig.2.8).

The principal mechanisms responsible for the enhanced oil recovery are identified as:

1. Steam drive
2. In Situ Solvent drive
3. Viscosity reduction
4. Thermal permeability and capillary pressure variations
5. Thermal expansion
6. Gravity Segregation
7. Solution gas drive
8. Emulsification

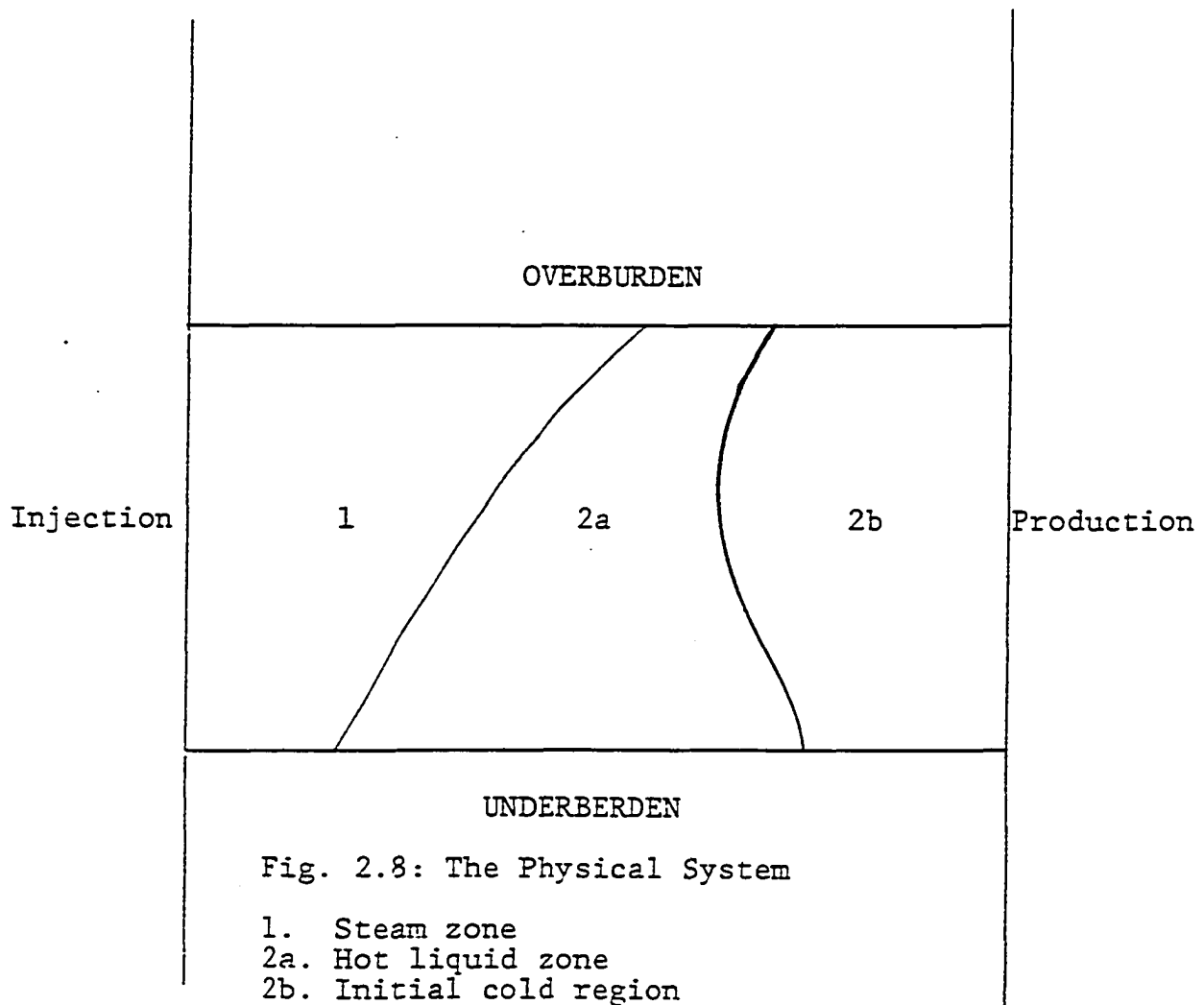
WU⁵⁷ discussed these mechanisms in detail.

STEAM DRIVE AND IN-SITU SOLVENT DRIVE

Steam distillation and steam displacement are the two important mechanisms known to exist in the steam zone. A fraction of the crude oil in the steam zone vaporizes and is carried forward through the advancing steam. These hydrocarbon vapors condense along with steam, mixing with the original crude at the condensation front to form a hot water zone and a hydrocarbon distillate or solvent bank. The distillate bank drives the oil miscibly ahead of the front followed by the steam drive which eventually establishes a low residual oil saturation in the steam zone.

VISCOSITY REDUCTION AND THERMAL EXPANSION

In addition to the solvent dilution, the most important mechanisms in the hot condensate zone responsible for enhanced



oil production rate, are viscosity reduction and thermal expansion. Fast heating by condensing steam raises the temperature resulting in thermal expansion or swelling of the oil and a significant reduction in its viscosity. The viscosity reduces to such an extent that the condensed hot water is able to displace the heated oil relatively efficiently. Thermal expansion increases the oil saturation and decreases its density thus resulting in an increased relative permeability to oil.

THERMAL PERMEABILITY AND CAPILLARY PRESSURE VARIATIONS

Several investigators^{58,59,60,61} have published results showing variations in relative permeability and capillary pressure due to changes in temperature. All these workers found that with an increase in temperature:

1. The irreducible water saturation increased while the residual oil saturation decreased significantly.
2. The relative permeability curve shifted in the direction of increasing water saturation suggesting an increase in relative permeability to oil for a given water saturation.
3. The relative permeability ratio decreases.

They attributed these changes to the changes in rock-fluid inter-action or wettability. Since wettability is characterized by contact angle, they investigated the effect of temperature and found that the contact angle decreased with an increase in temperature, indicating that the system becomes more water wet with increasing temperature.

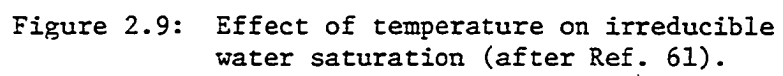
Davidson⁶¹ presented data showing a decrease in oil-water interfacial tension with increasing temperature. Figures 2.9 through 2.12 show these results. The overwhelming evidence suggests that variations in relative permeability and capillary pressure with increasing temperature are important recovery mechanisms in steam drive.

GRAVITY SEGREGATION AND EMULSIFICATION

As steam is injected, it channels through the reservoir and because of gravity its fingers rise to the top of the permeable sand. The fingers then spread out and after the overlay has occurred, the principal forces causing the oil flow are the gravity head and steam drag. Steam sweeps or drags the underlying oil towards the producing well. Hot water falls out of the steam zone due to gravity as it condenses, and establishes a hot water displacement below the interface. Thus gravity override and the underderrunning of hot water play an important role as the displacement mechanisms in the hot condensate zone.

It has also been suggested by a number of investigators and there is significant evidence that emulsification of the oil by the condensing high velocity steam is an important factor contributing to the mobilization of the heated oil.

K.C. Hong and J.W. Ault⁶⁶ studied the effects of non-condensable gas injection on oil recovery by steamflooding and reported among other things that the injection of a noncondensable gas with steam significantly accelerates oil production.



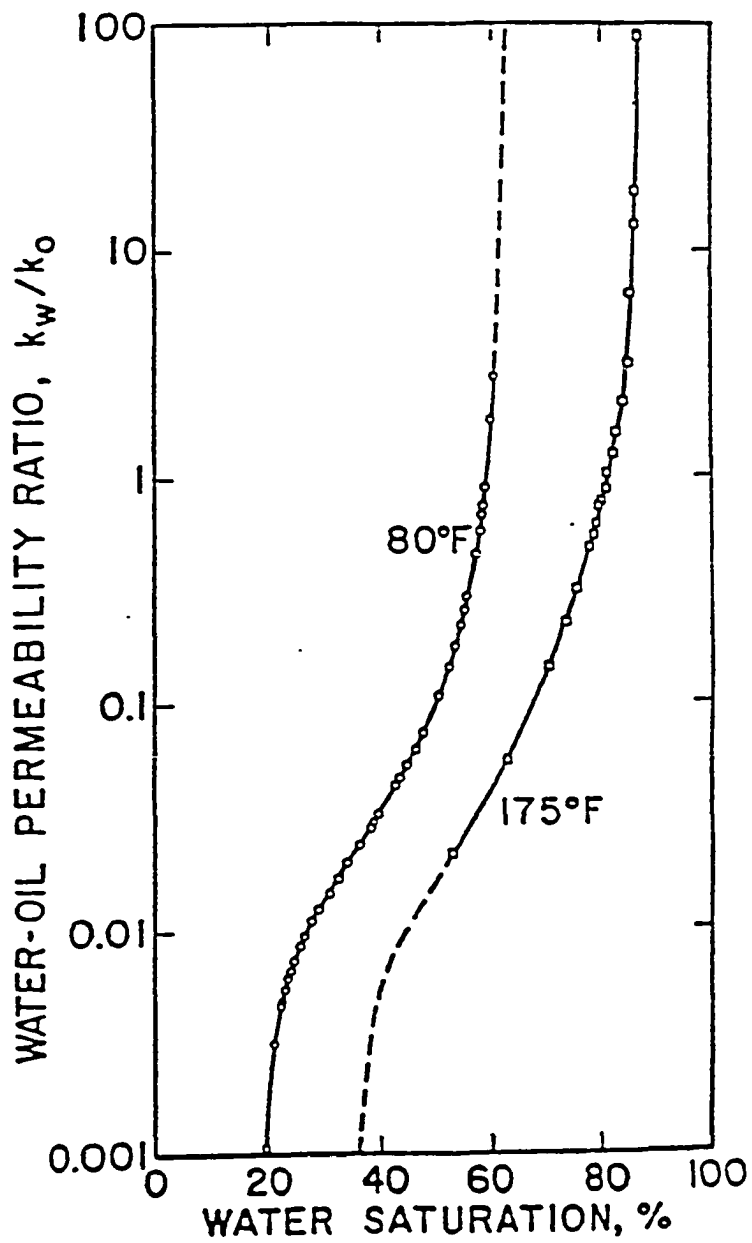


Fig. 2.10: Effect of temperature on relative permeability ratio (after Ref. 61).

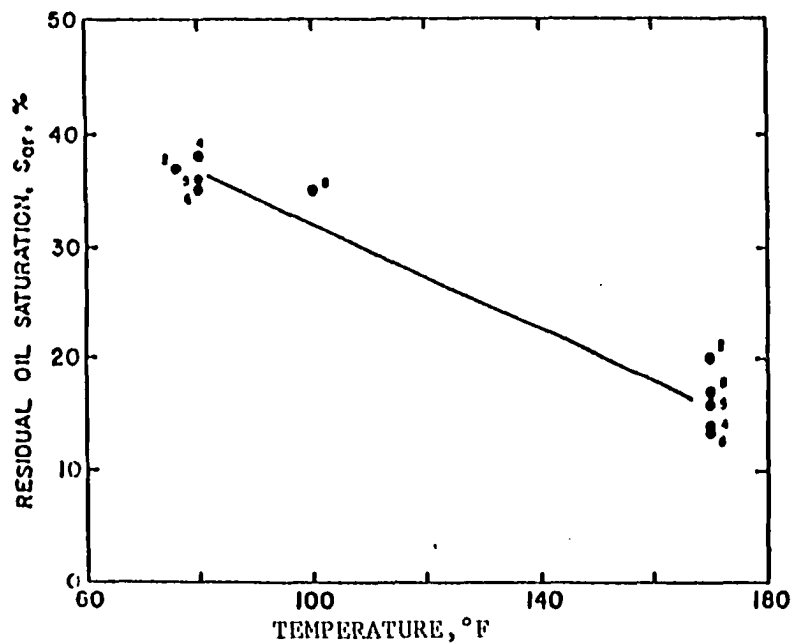


Fig. 2.11: Effect of temperature on residual oil saturation (after Ref. 61).

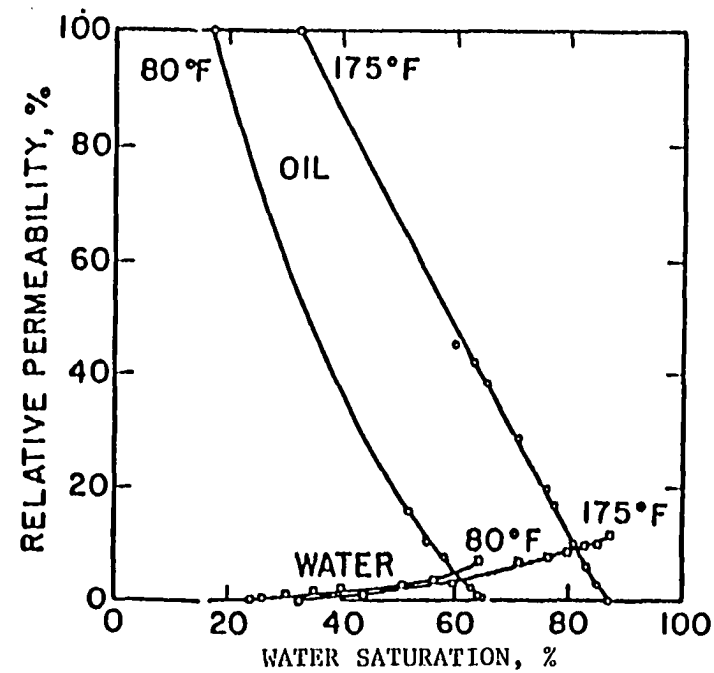


Fig. 2.12: Individual relative permeability as a function of temperature (after Ref. 61).

CHAPTER III
MATHEMATICAL FORMULATION

A mathematical model is nothing but a set of equations describing certain physical processes occurring in the reservoir. These equations express conservation of some quantity flowing through the reservoir. This model consists of equations expressing conservation of energy; conservation of mass for each component, phase equilibrium relationships and algebraic constraints. A general energy balance equation can be derived expressing conservation of the flowing quantity of interest.

Consider a small element of reservoir space $\Delta X \Delta Y \Delta Z$, shown in figure 3-1. The element is a rock containing fluids in the pore space.

A balance about the element, expressing conservation of the flowing thermal energy over a small time increment Δt , is given as:

$$\begin{aligned} (\text{Energy in} - \text{Energy out} + \text{Energy input from source} \\ = \text{Gain in internal energy} \dots (3.1) \end{aligned}$$

Where

Energy in = Amount of the energy flowing into the element during time Δt .

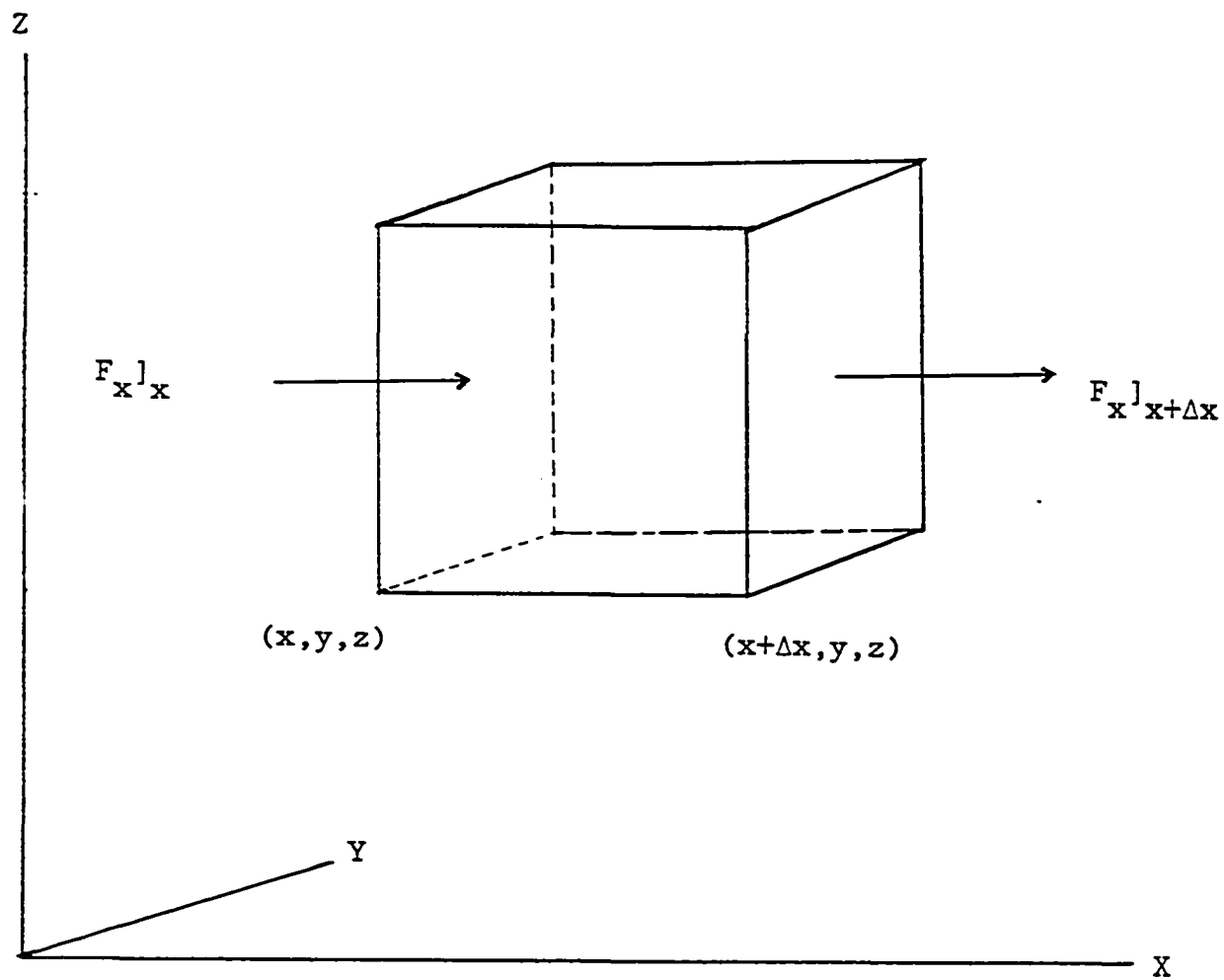


Fig. 3.1 SYSTEM FOR MASS OR HEAT BALANCE

Energy out = Amount of energy flowing out of the element during
time Δt .

Gain in internal energy = Amount of energy in the element at time
"t+ Δt " - Amount present at time "t".

The total energy flux due to flow of a fluid in the x-direction
is the sum of the conductive and convective components (radiation
neglected).

$$(F_{e,x}) = F_{k,x} + F_{c,x} \dots\dots\dots(3.2)$$

Where

$(F_{e,x})$ = Total energy flux in the x-direction

$F_{k,x}$ = Conductive heat flux in the x-direction i.e;
the rate of heat transfer by conduction in
the positive x-direction per unit cross-sec-
tional area normal to the x-direction.

$F_{c,x}$ = Convective heat flux in the x-direction.

$$F_{k,x} = -k_h \frac{\partial T}{\partial X} \dots\dots\dots(3.3)$$

$$F_{c,x} = U_x \rho_f h_f \dots\dots\dots(3.4)$$

Where

k = Thermal Conductivity

U_x = x-component of the volumetric flux.

h_f = Heat content of the fluid

Referring to figure 3.1, flow into the element takes place at three faces of areas:

$\Delta Y \Delta Z$	at	position X
$\Delta X \Delta Z$	at	position Y
$\Delta X \Delta Y$	at	position Z

Therefore

$$\text{Energy in} = [(F_x)_x \Delta Y \Delta Z + (F_y)_y \Delta x \Delta Z + (F_z)_z \Delta x \Delta Y] \Delta t \dots (3.5)$$

Where

F_x, F_y, F_z are fluxes at the three faces mentioned earlier.

Similarly flow out of the element takes place at three faces of areas

$\Delta Y \Delta Z$	at	position	$x + \Delta x$
$\Delta X \Delta Z$	at	position	$Y + \Delta Y$
$\Delta X \Delta Y$	at	position	$Z + \Delta Z$

Therefore

$$\text{Energy out} = [(F_x)_{x+\Delta x} \Delta y \Delta z + (F_y)_{y+\Delta y} \Delta x \Delta z + (F_z)_{z+\Delta z} \Delta x \Delta y] \Delta t \dots 3.6$$

$$\text{Energy input from sources} = \dot{Q} \Delta x \Delta y \Delta z \Delta t \dots 3.7$$

Where

$$\dot{Q} = \text{Rate of energy input per unit volume of the element.}$$

And finally "gain" during time Δt

$$\text{Gain in internal energy} = [(\rho e)_{t+\Delta t} - (\rho e)_t] \Delta x \Delta y \Delta z \dots 3.8$$

Where

$$\rho e = (1-\phi) M_c \Delta T + \phi \sum_{i=1}^{n_p} S_i \rho_i e_i$$

substitution of equations 3.5 through 3.8 in 3.1 yields:

$$\begin{aligned} & -[(F_x)_{x+\Delta x} - (F_x)_x] \Delta y \Delta z \Delta t - [(F_y)_{y+\Delta y} - (F_y)_y] \Delta x \Delta z \Delta t - [(F_z)_{z+\Delta z} - (F_z)_z] \Delta x \Delta y \Delta t \\ & + \dot{Q} \Delta x \Delta y \Delta z \Delta t = [(\rho e)_{t+\Delta t} - (\rho e)_t] \Delta x \Delta y \Delta z \dots 3.9 \end{aligned}$$

Dividing each term in equation 3.9 by $\Delta x \Delta y \Delta z \Delta t$, gives

$$\begin{aligned}
& - \frac{(F_x)_{x+\Delta x} - (F_x)_x}{\Delta x} - \frac{(F_y)_{y+\Delta y} - (F_y)_y}{\Delta y} - \frac{(F_z)_{z+\Delta z} - (F_z)_z}{\Delta z} + \dot{Q} \\
& = \frac{(\rho e)_{t+\Delta t} - (\rho e)_t}{\Delta t}
\end{aligned}$$

Taking limits, when $\Delta x, \Delta y, \Delta z$, and Δt tend to zero

$$- \frac{\partial F_x}{\partial x} - \frac{\partial F_y}{\partial y} - \frac{\partial F_z}{\partial z} + \dot{Q} = \frac{\partial (\rho e)}{\partial t} \quad \dots\dots\dots 3.10$$

Continuity Equation:

Applying law of conservation of mass for each component——
oil, water, steam, hydrocarbon gas and CO_2 :

mass in — mass out + mass input from sources

$$= \text{Mass accumulation} \quad \dots\dots\dots 3.11$$

Let the mole fraction of any component j in the gas, oil and water phases be denoted by y_j , x_{oj} , and x_{wj} respectively:

At equilibrium conditions

$$y_j = x_{oj} k_{oj} \quad \dots\dots\dots 3.12$$

$$y_j = x_{wj} k_{wj} \quad \dots\dots\dots 3.13$$

From equations 3.12 & 3.13

$$x_{oj} = \frac{k_{wj}}{k_{oj}} \quad \dots\dots\dots 3.14$$

Also from Daltons law:

$$y_w = \frac{p_s(T)}{p_g} \dots\dots\dots 3.15$$

Where

p_s = Saturation pressure of steam which is also partial pressure of steam

p_g = Pressure of the gas phase

Also

$$y_w = x_{ow} k_{ow} \dots\dots\dots 3.16$$

Total mass flux of component j in the x-direction:

$(F_{m,x})_j$ = Mass flux of component j in gas phase + mass flux of component j in oil phase + mass flux of component j in water phase + Diffusive mass flux of component j

$$(F_{m,x})_j = M_j \left[\frac{U_{g,x} \rho_g y_j}{M_g} + \frac{U_{o,x} \rho_o x_{oj}}{M_o} + \frac{U_{w,x} \rho_w x_{wj}}{M_w} - D_j \frac{\partial}{\partial x} \left(\frac{\rho_g y_j}{M_g} \right) \right] \dots\dots\dots 3.17$$

Where

$$c_j = \text{concentration of component } j \text{ in terms of } y_j \\ = \frac{M_j \rho_g y_j}{M_g}$$

An approach similar to the one used for deriving energy balance equation, yields:

$$(\text{Mass in} - \text{Mass out}) = - \left[\frac{\partial}{\partial x} (F_{m,x})_j + \frac{\partial}{\partial y} (F_{m,y})_j + \frac{\partial}{\partial z} (F_{m,z})_j \right] \\ \dots\dots\dots 3.18$$

Mass input of component j

$$\begin{array}{l} \text{from sources per unit} \\ \text{volume of the element} \end{array} = m_j \dots\dots\dots 3.19$$

Accumulation of component j

$$= \frac{\partial}{\partial t} \left[M_j \phi \left(\frac{\rho_g S_g y_j}{M_g} + \frac{\rho_o S_o x_{oj}}{M_o} + \frac{\rho_w S_w x_{wj}}{M_w} \right) \right] \\ \dots\dots\dots 3.20$$

Also from Darcy's law:

$$U_{i,x} = \frac{-k_i}{\mu_i} \frac{\partial P_i}{\partial x} \dots\dots\dots 3.21$$

$$U_{i,y} = \frac{-k_i}{\mu_i} \frac{\partial P_i}{\partial y} \dots\dots\dots 3.22$$

$$U_{i,z} = \frac{-k_i}{\mu_i} \left(\frac{\partial P_i}{\partial z} + \rho_i \frac{g}{g_c} \right) \dots\dots\dots 3.23$$

Substitution of equations 3.18 through 3.23 in equation 3.11 yields the differential equations describing the law of conservation of mass for each component j.

$$\begin{aligned} & - \left[\frac{\partial}{\partial x} (F_{m,x})_j + \frac{\partial}{\partial y} (F_{m,y})_j + \frac{\partial}{\partial z} (F_{m,z})_j \right] + \dot{m}_j \\ & = - \frac{\partial}{\partial t} \left[M_j \phi \left(\frac{\rho_g S_g y_j}{M_g} + \frac{\rho_o S_o x_{oj}}{M_o} + \frac{\rho_w S_w x_{wj}}{M_w} \right) \right] \dots\dots 3.24 \end{aligned}$$

or

$$\begin{aligned} & - \frac{\partial}{\partial x} M_j \left(\frac{x_{oj} \rho_o}{M_o} U_{o,x} + y_j \frac{\rho_g}{M_g} U_{g,x} + x_{wj} \frac{\rho_w}{M_w} U_{w,x} \right. \\ & \left. - D_j \frac{\partial}{\partial x} \frac{\rho_g y_j}{M_g} \right) \\ & - \frac{\partial}{\partial y} M_j \left[x_{oj} \frac{\rho_o}{M_o} U_{o,y} + y_j \frac{\rho_g}{M_g} U_{g,y} + x_{wj} \frac{\rho_w}{M_w} U_{w,y} - D_j \frac{\partial}{\partial y} \frac{\rho_g y_j}{M_g} \right. \\ & \left. - \frac{\partial}{\partial z} M_j \left[x_{oj} \frac{\rho_o}{M_o} U_{o,z} + y_j \frac{\rho_g}{M_g} U_{g,z} + x_{wj} \frac{\rho_w}{M_w} U_{w,z} - D_j \frac{\partial}{\partial z} \frac{\rho_g y_j}{M_g} \right] \right. \\ & \left. + \dot{m}_j = - \frac{\partial}{\partial t} \left[M_j \phi \left(x_{oj} \frac{\rho_o}{M_o} S_o + y_j \frac{\rho_g}{M_g} S_g + x_{wj} \frac{\rho_w}{M_w} S_w \right) \right] \dots\dots 3.25 \end{aligned}$$

or

$$\frac{\partial}{\partial x} \left[x_{oj} \frac{\rho_o}{M_o} \cdot \frac{k_o}{\mu_o} \frac{\partial P_o}{\partial x} + y_j \frac{\rho_g}{M_g} \frac{k_g}{\mu_g} \frac{\partial P_g}{\partial x} + x_{wj} \frac{\rho_w}{M_w} \frac{k_w}{\mu_w} \cdot \right.$$

$$\left. \frac{\partial P_w}{\partial x} + D_j \frac{\partial}{\partial x} \left[\frac{\rho_g}{M_g} y_j \right] \right]$$

$$\frac{\partial}{\partial y} \left[x_{o,j} \frac{\rho_o}{M_o} \cdot \frac{k_o}{\mu_o} \frac{\partial P_o}{\partial y} + y_j \frac{\rho_g}{M_g} \frac{k_g}{\mu_g} \frac{\partial P_g}{\partial y} + x_{wj} \frac{\rho_w}{M_w} \cdot \frac{k_w}{\mu_w} \frac{\partial P_w}{\partial y} \right.$$

$$\left. + D_j \frac{\partial}{\partial y} \left[\frac{\rho_g}{M_g} \cdot y_j \right] \right]$$

$$\frac{\partial}{\partial z} \left[x_o j \frac{\rho_o}{M_o} \cdot \frac{k_o}{\mu_o} \left(\frac{\partial P_o}{\partial z} + \frac{g \rho_o}{g_c} \right) + y_j \frac{\rho_g}{M_g} \frac{k_g}{\mu_g} \left(\frac{\partial P_g}{\partial z} + \frac{g \rho_g}{g_c} \right) \right.$$

$$\left. + x_{wj} \frac{\rho_w}{M_w} \frac{k_w}{\mu_w} \left(\frac{\partial P_w}{\partial z} + \frac{g \rho_w}{g_c} \right) \right]$$

$$+ D_j \frac{\partial}{\partial z} \left[\frac{\rho_g}{M_g} y_j \right] = \frac{\partial}{\partial t} \left[\left(x_{oj} \frac{\rho_o}{M_o} S_o + y_j \frac{\rho_g}{M_g} S_g + x_{wj} \frac{\rho_w}{M_w} S_w \right) \right]$$

$$- \frac{m_j}{M_j} \dots \dots \dots 3.26$$

For a reservoir with n_c components, there will be n_c differential equations similar to equation 3.26 (one for each component), one energy balance equation (3.10) and $2 n_c$ equilibrium equations such as equations (3.12 through 3.14).

Therefore:

$$\text{Total number of equation available} = 3 n_c + 1$$

$$\text{Total number of unknowns} = 3 n_c + 7$$

- i. $3 n_c$ — (y_j, x_{oj} and x_{wj}) in each continuity equation
- ii. Temperature
- iii. Pressures of each phase (p_w, p_g, p_o)
- iv. Saturations of each phase (S_w, S_g, S_o)

Therefore six additional equations are required to determine all the unknowns and these are:

$$S_o + S_g + S_w = 1 \quad \dots\dots\dots 3.27$$

$$P_{c,wo} = P_o - P_w \quad \dots\dots\dots 3.28$$

$$P_{c,og} = P_g - P_o \quad \dots\dots\dots 3.29$$

$$\sum_{j=1}^{n_c} y_j = 1 \quad \dots\dots\dots 3.30$$

$$\sum_{j=1}^{n_c} x_{oj} = 1 \quad \dots\dots\dots 3.31$$

$$\sum_{j=1}^{n_c} s_{wj} = 1 \dots\dots\dots 3.32$$

We have:

number of phases $n_p = 3$ (Gas, Water, & Oil)

number of component $n_c = 3$ (CO_2 that can exist in both the gas phase and the oil phase, water, oil).

PHASE

<u>Componenets</u>	<u>i = g (gas)</u>	<u>i = o (oil)</u>	<u>i = w (water)</u>
J=1 (CO_2)	y_1	x_{o1}	$x_{w1} = 0$
J=2 (water)	$y_2 \frac{p_s}{p_g}$	$x_{ow} = 0$	$x_{ww} = 1$
J=3 (oil)	$y_3 = 0$	x_{o3}	$x_{w3} = 0$
$\sum_{j=1}^3$	1	1	1

$$y_1 = x_{o1} k_{o1} (p_g, T) \dots\dots\dots 3.33$$

$$y_2 = \frac{p_s (T)}{p_g} \dots\dots\dots 3.34$$

$$x_{o1} + x_{o2} + x_{o3} = 1 \dots\dots\dots 3.35$$

$$y_1 + y_2 + y_3 = 1 \dots\dots\dots 3.36$$

$$S_o + S_g + S_w = 1 \dots\dots\dots 3.37$$

For dead oil, there is no partitioning into or out of the oil phase. Therefore, the equation expressing conservation of mass applied to the oil phase, as obtained from equation 3.25, is given by

$$\begin{aligned}
 & - \frac{\partial}{\partial x} \left[M_o \frac{x_{oo} \rho_o}{M_o} \cdot U_{o,x} \right] - \frac{\partial}{\partial y} \left[M_o \frac{x_{oo} \rho_o}{M_o} U_{o,y} \right] - \frac{\partial}{\partial z} \left[M_o \frac{x_{oo} \rho_o}{M_o} U_{o,z} \right] \\
 & = \frac{\partial}{\partial t} \left[M_o \phi(x_{oo} \frac{\rho_o}{M_o} S_o) \right]
 \end{aligned}$$

or

$$- \frac{\partial}{\partial x} (\rho_o U_{o,x}) - \frac{\partial}{\partial y} (\rho_o U_{o,y}) - \frac{\partial}{\partial z} (\rho_o U_{o,z}) = \phi \frac{\partial}{\partial t} (\rho_o S_o)$$

$$\text{or } \frac{\partial}{\partial t} (\rho_o S_o) + \nabla \cdot (\rho_o U_o) = 0 \dots\dots\dots 3.38$$

Similarly the continuity equation for water, in both the liquid and gaseous phases, is given by

$$\phi \frac{\partial}{\partial t} (\rho_w S_w) + \nabla \cdot (\rho_w U_w) + \phi \frac{\partial}{\partial t} (\rho_s S_s) + \nabla \cdot (\rho_s U_s) = 0$$

.....3.39

where the subscripts o, w, and s denote oil, water and steam respectively.

Conservation of energy for the reservoir containing dead oil is given by equation 3.10, which can also be written as:

$$-\frac{\partial}{\partial x} \left[-k_h \frac{\partial T}{\partial x} + U_x \rho_f h_f \right] - \frac{\partial}{\partial y} \left[-k_h \frac{\partial T}{\partial y} + U_y \rho_f h_f \right]$$

$$- \frac{\partial}{\partial z} \left[k_h \frac{\partial T}{\partial z} + U_z \rho_f h_f \right] = \frac{\partial}{\partial t} [(1-\phi) \rho_r C_r T + \phi \sum S_i \rho_i e_i]$$

or

$$[(1-\phi) \rho_r C_r + \phi (\rho_o C_o S_o + \rho_w C_w S_w)] \frac{\partial T}{\partial t} + L_v \left[\phi \frac{\partial (\rho_s S_s)}{\partial t} + \nabla \cdot \rho_s U_s \right]$$

$$+ (\rho_o C_o U_o + \rho_w C_w U_w) \cdot \nabla T + \rho_s U_s \cdot \nabla h_s + \nabla \cdot (-k_h \nabla T) = 0 \dots \dots \dots 3.40$$

For only steam injection, the saturation identity becomes

$$S_o + S_s + S_w = 0 \dots\dots\dots 3.41$$

At saturated condition,

$$P_{sat} = P_{sat} (T_{sat}.) \dots \text{Clausius-Clapeyron relationship} \dots 3.42$$

The following equations, expressed in the functional form, describe the dependence of material properties on the thermodynamic state variables:

$$\phi = \phi(x, y, z) \dots\dots\dots 3.43$$

$$u_j = u_j (T) \dots\dots\dots 3.44$$

$$k = k (x,y,z) \dots\dots\dots 3.45$$

$$k_{rj} = k_{rj} (S) \dots\dots\dots 3.46$$

$$\rho_j = \rho_j (P,T) \dots\dots\dots 3.47$$

$$h_s = h_s (T) \dots\dots\dots 3.48$$

$$L_v = L_v (T) \dots\dots\dots 3.49$$

$$k_h = k_h (x,y,z) \dots\dots\dots 3.50$$

$$\rho_r = \rho_r (x,y,z) \dots\dots\dots 3.51$$

For the cap and base rock, the energy equation can be written as:

$$\rho_c C_c \frac{\partial T}{\partial t} + \nabla \cdot (-k_h \nabla T) = 0 \dots\dots\dots 3.52$$

The Initial and Boundary Conditions:

The initial condition for the system are given by:

$$S_j (i, x, y, z) = S_{ji} (x, y, z) \dots\dots\dots 3.53$$

$$P (i, x, y, z) = P_i (x, y, z) \dots\dots\dots 3.54$$

$$T (i, x, y, z) = T_i = \text{constant} \dots\dots\dots 3.55$$

Where the subscript i stands for the initial value.

The mass flux is zero at all the boundaries with the exception of the wells, thus:

$$[\rho_j U_{jn}]^{lb} = [\rho_j U_{jn}]^{ub} = 0 \dots\dots\dots 3.56$$

where

lb = lateral boundary

ub = upper and lower boundary.

subscript n refers to the flow in a direction normal to the boundary.

Similarly, the convective heat flux is zero at all the lateral boundaries with the exception of the wells; thus

$$[k_h \frac{\partial T}{\partial n}]^{lb} = 0 \dots\dots\dots 3.57$$

At the upper and lower boundaries

$$[k_{hr} \frac{\partial T}{\partial n}]_r^{ub} = [k_{hc} \frac{\partial T}{\partial n}]_c^{up} \dots\dots\dots 3.58$$

Mass injection rate of wet steam at the injection well is given by:

$$W = \pi d \int_0^{Z_t} (\rho_w U_{wn} + \rho_s U_{sn}) \frac{dz}{\cos \theta} \dots\dots\dots 3.59$$

At the production well, the bottom hole pressure is given by:

$$P = P_p(t) \dots\dots\dots 3.60$$

The rate of energy injection at the injection well :

$$\dot{E} = \pi d \int_0^{Z_t} (\rho_w U_{wn} C_w \Delta T + \rho_s U_{sn} h_s) \frac{dz}{\cos \theta} = W(f_s L_v + C_w \Delta T) \dots\dots\dots 3.61$$

Where

f_s = quality of the steam

$\Delta T = T_s - T_i$

DIMENSIONAL ANALYSIS:

This study was devoted to an experimental determination of oil recovery by simultaneous injection of carbon dioxide and steam in linear systems. The main objective was in obtaining an overall view of the important variables that affected recovery. But for the sake of completeness dimensional analysis are performed to assess the practical value of scaling laws. The principal advantage of using dimensionless groupings is to reduce the number of independent variables in a problem.

Greetsma et al⁶² and Van Daalen and Domselaar⁶³ presented dimensionally scaled models of oil reservoirs under isothermal and nonisothermal conditions of water flooding, while Niko and Troost⁶⁴ developed a partial list of dimensionless parameters and appropriate set of scaling rules in the steam injection area.

The first step in deriving the important groups of parameters that are related to the steam injection processes is the development of scaling parameters which are obtained by either using Buckingham's π theorem or by inspectional analysis. Generally, when two physical systems are identical and are behaving similarly, known parameters of the one can be used to calculate the unknown parameters of the other. The details of these methods and a compilation of the most important dimensionless groups

and an example illustrating the procedure of converting prototype values to model values and vice versa are presented.

Buckingham's π theorem:

This theorem states that the number of independent dimensionless groups is equal to the difference between the number of physical variables and the number of basic dimensions used to express them. Dimensional constants are also included as variables. Designating dimensionless groups by the letters $\pi_1, \pi_2, \pi_3, \dots$, the complete physical statement can be expressed in a functional form as

$$f(\pi_1, \pi_2, \pi_3, \dots) = 0$$

Let us consider the following seven variables

U_c = Convective heat transfer coefficient $[M t^{-3} T^{-1}]$

k_h = thermal conductivity $[M L t^{-3} T^{-1}]$

L = characteristic length $[L]$

ρ = density $[M L^{-3}]$

u = velocity $[L t^{-1}]$

μ = viscosity $[M L^{-1} t^{-1}]$

C_p = specific heat $[L^2 t^{-2} T^{-1}]$

These have four basic dimensions of mass, length, time, and temperature denoted by M, L, t and T respectively.

Therefore, the number
of independent dimensionless groups = $\frac{\text{[number of physical variables]}}{\text{[number of basic dimensions]}}$
= 7 - 4 = 3

Determination of dimensionless groups:

The dimensionless groups may be determined by using the following procedure:

- i. List all the variables involved and their dimensions.
- ii. Find the basic dimensions
- iii. Select a number of repeating variables equal to the number of basic dimensions from the list of the variables.
- iv. Determine the dimensionless groups by solving the dimensional equations set up by combining the variables selected in step (iii) and each of the other remaining variables in turn.

If actual relationship among different variables of a problem is not known, a relation of the following form can be assumed to determine the pertinent dimensionless groups.

$$q_1^a q_2^b q_3^c q_4^d q_5^e = \pi, \quad \text{a dimensionless quantity} \dots\dots\dots 3.62$$

Where

- (i) q_1, q_2, q_3, q_4, q_5 , are pertinent variables in the problem
- (ii) a, b, c, d, e , are unknown exponents

On substitution of the basic dimensions in terms of M, L, t, and T for each of the variables in equation 3.62, the sum of the

exponents of each of these basic dimensions must result in zero; thus leading to a set of four simultaneous equations containing a , b , c , d and e as the unknowns. Any four of these five exponents can be solved in terms of the remaining one. Then, back-substitution in equation 3.62 will result in one independent dimensionless group.

The aforementioned procedure will now be illustrated. Consider a problem where the variables are velocity, V , characteristic length L_c , and gravitational acceleration, g . Then

$$V^a L_c^b g^c = \pi_1, \text{ a dimensionless quantity substitution of dimensions for } V, L, \text{ and } g, \text{ yields}$$

$$[Lt^{-1}]^a [L]^b [Lt^{-2}]^c = \pi_1$$

The basic dimensions are L and t , since M and T are not present in the variables.

$$\text{Exponent of } L: a + b + c = 0$$

$$\text{Exponent of } t: -a - 2c = 0$$

From the above two equations, we have

$$a = -2c$$

$$b = c$$

Back substitution for a and b , yields

$$V^{-2c} L_c^c g^c = \pi_1$$

or

$$\frac{V^2}{L_c g} = \pi_1$$

In the above example, there were three variables and two basic dimensions, thus giving rise to one dimensionless group.

Inspectional analysis: A more straight forward and reliable way to derive the dimensionless groups is by inspectional analysis. The first step towards this end is the development of scaling parameters which are obtained by making the available governing equations, describing fluid flow and heat transfer, dimensionless; followed by determining the similarity parameters by inspectional analysis. The similarity parameters thus determined are combined or modified to obtain the desired scaling parameters.

Dimensionless form: The governing equations of the steam injection processes contain a number of physical variables. Each of these variables is replaced by the product of a dimensionless variable and a reference value of the variable. For instance, a variable U , is divided by its reference value, U_R , to obtain the dimensionless ratio of the variable, U_D , such as

$$U_D = \frac{U}{U_R} \quad \text{or } U = U_R U_D \quad \dots\dots\dots 3.63$$

To make equation 3.38 (conservation of mass equation) dimensionless:

Let

$$\phi = \phi_R \phi_D, \quad \rho_o = \rho_{oR} \rho_{oD}, \quad S_o = S_R S_{omD}$$

$$U_o = U_R U_{oD}, \quad \tau = \tau_R \tau_D$$

$$dt = \tau_R d\tau_D, \quad dx = L_R dx_D$$

$$\nabla = \frac{1}{L_R} \nabla_D$$

Substituting the above in equation 3.38, we have

$$\phi_R \phi_D \frac{\rho_{oR} S_R}{\tau_R} \cdot \frac{\partial (\rho_{oD} S_{omD})}{\partial \tau_D} + \frac{1}{L_R} \nabla_D \cdot (\rho_{oR} \rho_{oD} U_R U_{oD}) = 0$$

or

$$\phi_R \phi_D \frac{\rho_{oR} S_R}{\tau_R} \cdot \frac{\partial (\rho_{oD} S_{omD})}{\partial \tau_D} + \frac{\rho_{oR} U_R}{L_R} \nabla_D \cdot (\rho_{oD} U_{oD}) = 0$$

Multiplication of the above equation by $(\frac{L_R}{U_R \rho_{oR}})$ yields

$$(\frac{\phi_R S_R L_R}{U_R \tau_R}) \phi_D \frac{\partial (\rho_{oD} S_{omD})}{\partial \tau_D} + \nabla_D \cdot (\rho_{oD} U_{oD}) = 0 \dots 3.64$$

Where

S_{omD} = dimensionless movable oil saturation

Movable oil saturation is used to improve the match of the relative permeabilities, since the residual oil saturation and interstitial water saturation generally are not the same between model and the prototype.

Similarly, the conservation of mass equation for water (equation 3.39) in the dimensionless form is,

$$\left(\frac{\phi_R S_R L_R}{U_R t_R} \right) \phi_D \frac{\partial (\rho_{wD} S_{wMD} + \rho_D S_{sD})}{t_D} + \nabla_D \cdot (\rho_{wD} U_{wD} + \rho_{sD} U_s) = 0$$

..... 3.65

The dimensionless form of the Darcy's equation is obtained by making proper substitutions in equation (3.21) and is given by

$$U_R U_{jD} = - \frac{k_R k_D k_{rj}}{\mu_R \mu_{jD}} \cdot \frac{P_R}{L_R} \nabla_D P_D$$

Or

$$\left(\frac{\mu_R U_R L_R}{k_R P_R} \right) U_{jD} = \frac{k_D k_{rj}}{\mu_{jD}} \nabla_D P_D \dots\dots\dots 3.66$$

The energy equation (equation 3.40) is made dimensionless as follows:

To make the first set of brackets dimensionless, let

$$\frac{S_o - S_{ors}}{S_R} + \frac{S_w - S_{wc}}{S_R} + \frac{S_s}{S_R} = S_{omD} + S_{sD} = \frac{1 - S_{ors} - S_{wc}}{S_R}$$

.....3.67

Then

$$\{(1-\phi) \rho_r C_r + \phi[\rho_o C_o (S_R S_{omD} + S_{ors}) + \rho_w C_w (S_R S_{wmD} + S_{wc})]\} \frac{\partial T}{\partial t}$$

or

$$[(1-\phi) \rho_r C_r + \phi(\rho_o C_o S_{ors} + \rho_w C_w S_{wc})] \frac{\partial T}{\partial t} + \phi(\rho_o C_o S_R S_{omD} + \rho_w C_w S_R S_{wmD}) \frac{\partial T}{\partial t}$$

or

$$\rho_{cR} C_{cR} [(1-\phi) \rho_r C_r + \phi(\rho_o C_o S_{ors} + \rho_w C_w S_{wc})]_D \frac{T_R}{\tau_R} - \frac{\partial T_D}{\partial \tau_D}$$

$$+ \phi_R \phi_D \cdot S_R \cdot \rho_R \cdot C_R (\rho_{oD} C_{oD} S_{omD} + \rho_{wD} C_{wD} S_{wmD}) \frac{T_R}{\tau_R} - \frac{\partial T_D}{\partial \tau_D}$$

or

$$\left(\frac{\rho_{cR} C_{cR} T_R}{t_R}\right) [(1-\phi) \rho_r C_r + \phi (\rho_o C_o S_{ors} + \rho_w C_w S_{wc})] \frac{\partial T_D}{\partial t_D} \\ + \left(\frac{\phi_R S_R \rho_r C_R T_R}{t_R}\right) \phi_D (\rho_{oD} C_{oD} S_{omD} + \rho_{wD} C_{wD} S_{wmD}) \frac{\partial T_D}{\partial t_D} \dots 3.68$$

The second set of brackets in the energy equation (equation 3.40) is made dimensionless as follows:

$$L_{vR} L_{vD} [\phi_R \phi_D \frac{\rho_R S_R}{t_R} \frac{\partial (\rho_{sD} S_{sD})}{\partial t_D} + \frac{\rho_R U_R}{L_R} \nabla_D \cdot \rho_{sD} U_{sD}]$$

or

$$\left(\frac{\phi_R S_R \rho_R L_{vR}}{t_R}\right) L_{vD} \cdot \phi_D \frac{\partial (\rho_{sD} S_{sD})}{\partial t_D} + \left(\frac{\rho_R U_R L_{vR}}{L_R}\right) \cdot L_{vD} \nabla_D \cdot \rho_{sD} U_{sD} \\ \dots 3.69$$

The third set of brackets in equation 3.40 is made dimensionless as follows:

$$(\rho_R \rho_{oD} \cdot C_R C_{oD} \cdot U_R U_{oD} + \rho_R \rho_{wD} \cdot C_R C_{wD} \cdot U_R U_{wD}) \frac{T_R}{L_R} \nabla_D \cdot T_D$$

or

$$\frac{\rho_R C_R U_R T_R}{L_R} (\rho_{oD} C_{oD} U_{oD} + \rho_{wD} C_{wD} U_{wD}) \cdot \nabla_D T_D \dots \dots \dots 3.70$$

The fourth and fifth sets of brackets in the energy equation (equation 3.40) are now made dimensionless as follows:

$$\rho_s U_s \nabla (L + C_w T) - k_h \nabla^2 T$$

or

$$\rho_R \rho_{sD} U_R U_{sD} \frac{1}{L_R} \nabla_D (L_{vR} L_{vD} + C_R C_{wD} \cdot T_R T_D) \\ - k_{hR} k_{hD} \frac{1}{L_R^2} \nabla_D^2 T_R T_D$$

or

$$(\frac{\rho_R U_R L_{vR}}{L_R}) \rho_{sD} U_{sD} \nabla_D L_{vD} + (\frac{\rho_R U_R C_R T_R}{L_R}) \rho_{sD} U_{sD} \nabla_D C_{wD} T_D \\ - (\frac{k_{hR} T_R}{L_R^2}) k_{hD} \nabla_D^2 T_D \dots \dots \dots 3.71$$

Equations 3.68, 3.69, 3.70, and 3.71 are now combined and multiplied by $(\frac{t_R}{\phi_R \rho_R S_R C_R T_R})$ to obtain the final dimensionless form of the

energy equation as follows:

$$\begin{aligned}
& \left(\frac{\rho_{cR} C_{cR}}{\phi_R \rho_R S_R C_R} \right) [(1-\phi) \rho_r C_r + \phi (\rho_o C_o S_{oRS} + \rho_w C_w S_{wc})]_D \frac{\partial T_D}{\partial \tau_D} \\
& + \phi_D (\rho_{oD} C_{oD} S_{omD} + \rho_{wD} C_{wD} S_{wmD}) \frac{\partial T_D}{\partial \tau_D} \\
& + \left(\frac{L_{vR}}{C_R T_R} \right) L_{vD} \cdot \left[\phi_D \frac{\partial (\rho_{sD} S_{sD})}{\partial \tau_D} + \frac{U_R t_R}{\phi_R S_R L_R} \nabla_D \cdot \rho_{sD} U_{sD} \right] \\
& + \left[\frac{U_R t_R}{\phi_R S_R L_R} \left(\frac{L_{vR}}{C_R T_R} + 1 \right) \rho_{sD} U_{sD} \cdot \nabla_D (L_{vD} + C_{wD} T_D) \right] \\
& + \left(\frac{U_R t_R}{\phi_R S_R L_R} \right) [\rho_{oD} C_{oD} U_{oD} + \rho_{wD} C_{wD} U_{wD}] \cdot \nabla_D T_D \\
& - \left(\frac{k_{hr} t_R}{\phi_R \rho_R S_R C_R L_R^2} \right) k_{hD} \nabla_D^2 T_D = 0 \dots\dots\dots 3.72
\end{aligned}$$

The dimensionless form of the movable saturations becomes:

$$\frac{S_o - S_{ors}}{S_R} + \frac{S_w - S_{wc}}{S_R} + \frac{S_s}{S_R} = S_{omD} + S_{wmD} + S_{sD}$$

$$= \frac{1 - S_{or} - S_{wc}}{S_R} \dots\dots\dots 3.73$$

Where

Subscript m represents movable.

Equations 3.42 through 3.51 are already in the dimensionless form.

The dimensionless form of the energy equation for the cap and base rock (equation 3.52) is given by:

$$\rho_{cR} \rho_{cD} C_{cR} C_{cD} \frac{T_R}{t_R} \frac{\partial T_D}{\partial t_D} = k_{hR} k_{hcD} \cdot \frac{1}{L_R^2} \nabla_D^2 T_R T_D$$

or

$$\rho_{cD} C_{cD} \frac{\partial T_D}{\partial t_D} = \left(\frac{k_{hR} t_R}{\rho_{cR} C_{cR} L_R^2} \right) k_{hcD} \nabla_D^2 T_D$$

\dots\dots\dots 3.74

Equations 3.53 through 3.55 representing initial conditions are already in the dimensionless form.

The boundary conditions given by equations 3.56 and 3.57 are also dimensionless, but equation 3.58 is made dimensionless as follows:

$$[k_{hr} k_{hrD} \frac{T_R}{n_R} \frac{\partial T_D}{\partial n_D}]_r^{ub} = [k_{hr} k_{hcD} \frac{T_R}{n_R} \frac{\partial T_D}{\partial n_D}]_c^{ub}$$

or

$$[k_{hrD} \frac{\partial T_D}{\partial n_D}]_r^{ub} = [k_{hcD} \frac{\partial T_D}{\partial n_D}]_c^{ub} \dots\dots\dots 3.75$$

The equation giving mass injection rate of wet steam at the injection well (equation 3.59), becomes in the dimensionless form as:

$$w_R w_D = \pi L_R d_D \int_0^{z_{tD}} (\rho_R \rho_{wD} \cdot U_R U_{wnD} + \rho_R \rho_{sD} U_R U_{snD}) L_R \frac{dz_D}{\cos \theta}$$

or

$$\left(\frac{w_R}{\rho_R U_R L_R^2} \right) w_D = \pi d_D \int_0^{z_{tD}} (\rho_{wD} U_{wnD} + \rho_{sD} U_{snD}) \frac{dz_D}{\cos \theta} \dots\dots\dots 3.76$$

Equation 3.60, giving bottom hole pressure at the production well remains unaffected in form and is dimensionless.

The equation for the energy injection (equation 3.61) in the dimensionless form becomes:

$$\begin{aligned}
 & W_R W_D (f_{sR} f_{sD} L_{vR} L_{vD} + C_R C_{wD} T_R \Delta T_D) \\
 = & \pi L_R d_D \int_0^{z_{tD}} [\rho_R \rho_{wD} U_R U_{wD} C_R C_{wD} T_R \Delta T_D + \rho_R \rho_{sD} U_R U_{sD} h_R h_{sD}] \\
 & \cdot L_R \frac{dz_D}{\cos \theta}
 \end{aligned}$$

or

$$\begin{aligned}
 & W_R W_D [(f_{sR} L_{vR}) f_{sD} L_{vD} + (C_R T_R) C_{wD} \Delta T_D] \\
 = & \pi L_R d_D \int_0^{z_{tD}} [(\rho_R U_R C_R T_R) \rho_{wD} U_{wD} C_{wD} \Delta T_D + (\rho_R U_R h_R) \rho_{sD} U_{sD} h_{sD}] \\
 & \cdot \frac{dz_D}{\cos \theta}
 \end{aligned}$$

or

$$\begin{aligned}
& \left(\frac{w_R}{\rho_R U_R L_R^2} \right) w_D \left[\left(\frac{f_{sR} L_{vR}}{C_R T_R} \right) f_{sD} L_{vD} + C_{wD} \Delta T_D \right] \\
& = \pi d_D \int_0^{z_{tD}} \left[\rho_{wD} U_{wnD} C_{wD} \Delta T_D + \left(\frac{h_R}{C_R T_R} \right) \rho_{sD} U_{snD} h_{sD} \right] \frac{dz_D}{\cos \theta} \\
& \dots\dots\dots 3.77
\end{aligned}$$

Determination of Independent Dimensionless Groups:

The dimensionless groups are simply the co-efficients of the individual terms of the governing equations, written in the dimensionless form, describing fluid flow and heat transfer. The independent dimensionless groups are, then, determined either by observation or by using Buckingham Pi theorem. Stegemeirs et al discussed this subject in detail and derived these groups listed in tables 3-1 and 3-2.

TABLE 3-1

Similarity Parameters For Steam Processes (after Ref.65)

Parameters	Source Equation
$\frac{k_R P_R t_R}{R S_R M_R L_R^2}$	3.64 and 3.66
$\frac{P_R}{P_R S_R L_R}$	3.66
$\frac{L_{vR}}{C_R T_R}$	3.72
$\frac{k_{hR} t_R}{R S_R R C_R L_R^2}$	3.72
$\frac{k_{hR} t_R}{c_R C_{cR} L_R^2}$	3.74
$\frac{R k_R P_R L_R}{w_R R}$	3.66 and 3.76
$\frac{f_{sR} L_{vR}}{C_R T_R}$	3.77

TABLE 3-2

Scaling Parameters For Steam Processes (after Ref. 65)

<u>Parameter</u>	<u>Number</u>
$\frac{P_R}{\rho_R g_R L_R}$	I
$(\frac{f_{sR} L_{vR}}{C_R T_R} + 1) A^*$	II
$\frac{f_{sR} \mu_{sR} \rho_R}{\mu_R \rho_{sR}}$	III
$\frac{k_{hR} t_R}{\phi_R \rho_R S_R C_R L_R^2} \cdot A^*$	IV
$\frac{\phi_R s_R \mu_R L_R}{k_R \rho_R S_R t_R}$	V
$\frac{w_R t_R}{\rho_R \phi_R S_R L_R^3}$	VI

* When $\phi \Delta s$ is not matched, A takes on a value between unity and

$$\rho_R s_R \left(\frac{\rho_R C_R}{\rho_{cR} C_{cR}} \right).$$

If reservoir heating or heat production predominates, use unity, if cap and base rock heating predominates, use $\phi_R s_R$

$$\left(\frac{\rho_R C_R}{\rho_{cR} C_{cR}} \right).$$

Selection of the characteristic quantities:

The characteristic quantities are chosen in such a way that the system does not change when the scale is changed from the model to the prototype. For example the reference saturation, S_R , is chosen as

$$S_R = 1 - S_{ors} - S_{wc} \dots\dots\dots 3.78$$

The saturation identity, given by equation 3.67, then becomes:

$$S_{omD} + S_{wmD} + S_{sD} = 1 \dots\dots\dots 3.79$$

Equation 3.79 is equally good for both model and prototype if S_{ors} and S_{wc} are constant. Thus equation 3.53, for the initial condition on oil saturation, becomes:

$$\frac{S_o(i, x, y, z) - S_{ors}}{1 - S_{ors} - S_{wc}} = \frac{S_{oi}(x, y, z) - S_{ors}}{1 - S_{ors} - S_{wc}} \dots\dots\dots 3.80$$

and for the model and the prototype to be similar

$$\frac{\left[\frac{S_{oi}(x, y, z) - S_{ors}}{1 - S_{ors} - S_{wc}} \right]_{\text{prototype}}}{\left[\frac{S_{oi}(x, y, z) - S_{ors}}{1 - S_{ors} - S_{wc}} \right]_{\text{model}}} = 1 \dots\dots\dots 3.81$$

reference pressure is chosen

$$P_R = P_{\max} - P_{\min} = \Delta P_{\max} \dots\dots\dots 3.82$$

Thus equation 3.54, the initial condition on pressure, becomes:

$$\frac{p(i, x, y, z) - P_{\min}}{P_{\max} - P_{\min}} = \frac{P_i(x, y, z) - P_{\min}}{P_{\max} - P_{\min}} \dots\dots\dots 3.83$$

and for the model and prototype to be similar

$$\left[\frac{P_i(x, y, z) - P_{\min}}{P_{\max} - P_{\min}} \right]_{\text{prototype}} = \left[\frac{P_i(x, y, z) - P_{\min}}{P_{\max} - P_{\min}} \right]_{\text{model}} = 1$$

\dots\dots\dots 3.84

Example of Scaling Procedure:

Scaling of pressure:

Given:

Prototype well head pressure, $(P_p)_p = 100 \text{ Psia}$

Model well production pressure, $(P_p)_M = 61 \text{ Psia}$

Prototype to model length ratio $[\frac{L_P}{L_M}] = \gamma(L) = 200$

Prototype to model density ratio $[\frac{(\rho_o)_P}{(\rho_o)_M}] = \gamma(\rho) = 1$

Using scaling parameter 1 in table F2, we have

$$(\frac{\Delta P}{\rho g L})_P = (\frac{\Delta P}{\rho g L})_M$$

$$[\frac{P - P_P}{\rho g L}]_P = [\frac{P - P_P}{\rho g L}]_M$$

$$(P - P_P)_P = \frac{(\rho g L)_P}{(\rho g L)_M} (P - P_P)_M$$

$$P_P = 200 (P - P_P)_M + (P_P)_P$$

$$P_P = 200 (P - 61)_M + 100 \dots\dots\dots 3.85$$

$$= 200 P_M - 12200 + 100$$

$$= 200 P_M - 12100$$

Where

P_M = model pressure

P_P = prototype pressure

If

Model steam pressure = 67 Psia

Then

Prototype steam pressure = 200 (67) - 12100
 ≈ 1300 Psia

Scaling of temperature:

Given:

Initial prototype reservoir temperature, $(T_r)_p$ = 105°F

Initial model reservoir temperature, $(T_r)_M$ = 105°F

Prototype steam temperature at 1300 Psia $(T_s)_p$ = 577°F

Model steam temperature = 300°F

$$\text{Temperature ratio} = \frac{(\Delta T)_p}{(\Delta T)_M} = \frac{577 - 105}{300 - 105} = \frac{472}{195} = 2.42$$

Therefore for any model temperature, the prototype temperature is given by:

$$\frac{(T - T_r)_p}{(T - T_r)_M} = 2.42$$

$$\begin{aligned} T_p &= 2.42 (T - T_r)_M + (T_r)_p \\ &= 2.42 T_M - 254.1 + 105 \end{aligned}$$

Or

$$T_P = 2.42 T_M - 149.1 \dots \dots \dots 3.86$$

Where

T_M = any model temperature

T_P = prototype temperature °F

Therefore for a model temperature of 300°F the prototype temperature, T_P is given by

$$\begin{aligned} T_P &= 2.42 (300) - 149.1 \\ &\approx 577^\circ\text{F} \end{aligned}$$

....

Scaling of time:

Scaling parameter IV in table 3.63 is used to convert the prototype time to model time and vice versa, illustrated as follows:

$$\left(\frac{k_{hR} \tau_R}{\phi_R S_R \rho_R C_R L_R^2} \right)_P = \left(\frac{k_{hR} \tau_R}{\phi_R S_R \rho_R C_R L_R^2} \right)_M$$

$$\frac{\tau_M}{\tau_P} = \left(\frac{k_{hp}}{k_{hM}} \right) \left(\frac{\rho_{cM}}{\rho_{cp}} \right) \left(\frac{C_{cM}}{C_{cp}} \right) \left(\frac{L_M}{L_P} \right)^2 \dots \dots \dots 3.87$$

Given:

$$k_{hp} = 1.2 \text{ Btu/hr-ft-}^\circ\text{F}$$

$$k_{hM} = 0.5 \text{ Btu/hr-ft-}^\circ\text{F}$$

$$(\rho_r C_r)_M = (\rho_r C_r)_P$$

Substituting these values, we have

$$\frac{t_M}{t_p} = \left(\frac{1.2}{0.5}\right)(1)\left(\frac{1}{200}\right)^2 = 6.00 \times 10^{-5}$$

or

$$\frac{t_M}{t_p} = (6.00 \times 10^{-5}) \left(365.25 \frac{\text{days}}{\text{years}}\right) \left(\frac{24 \text{ hrs}}{\text{day}}\right) \left(\frac{60 \text{ min.}}{\text{hr.}}\right)$$

$$= 31.55 \text{ minutes/year}$$

This means that 31.55 minutes in the model are equivalent to one year in the field.

Scaling of permeability:

Scaling parameters V in table 3.63 is used to convert prototype permeability to model permeability and vice versa, as illustrated below:

$$\left[\frac{\phi_R S_R \mu_R L_R}{k_R \rho_R g_R t_R}\right]_P = \left[\frac{\phi_R S_R \mu_R L_R}{k_R \rho_R g_R t_R}\right]_M$$

or

$$\frac{k_M}{k_p} = \frac{\phi_M}{\phi_p} \cdot \frac{\Delta S_M}{\Delta S_p} \cdot \frac{L_M}{L_p} \cdot \frac{\mu_M}{\mu_p} \cdot \frac{\rho_{op}}{\rho_{oM}} \cdot \frac{t_p}{t_M} \dots \dots \dots 3.88$$

$$\text{If } k_M = 4 \text{ darcies}$$

Then for a prototype pressure of 100 Psia, substitution of previously calculated values in equation 3.88 yields:

$$k_p = 4 \left(\frac{.24}{.29} \right) \left(\frac{.7}{.85} \right) \left(\frac{200}{1} \right) (1) (1) (6 \times 10^{-5})$$

$$= .0327 \text{ darcies}$$

Scaling of injection and production rates:

Scaling parameter VI in table 3.63 is used to convert prototype injection and production rates to model rates and vice versa, as given below:

$$\left(\frac{w_R t_R}{\rho_R \phi_R S_R L_R^3} \right)_P = \left(\frac{w_R t_R}{\rho_R \phi_R S_R L_R^3} \right)_M$$

or

$$\frac{w_M}{w_P} = \frac{\rho_{oM}}{\rho_{oP}} \cdot \frac{L_M^3}{L_P^3} \cdot \frac{\phi_M \cdot \Delta S_M}{\phi_P \cdot \Delta S_P} \cdot \frac{t_P}{t_M} \dots\dots\dots 3.89$$

Substitution of previously known values in equation 3.89, gives

$$\frac{w_M}{w_P} = \left(\frac{1}{200} \right)^3 \left(\frac{.29}{.24} \right) \left(\frac{.85}{.70} \right) \left(\frac{1}{600 \times 10^{-5}} \right)$$

$$= 3.057 \times 10^{-3}$$

Or

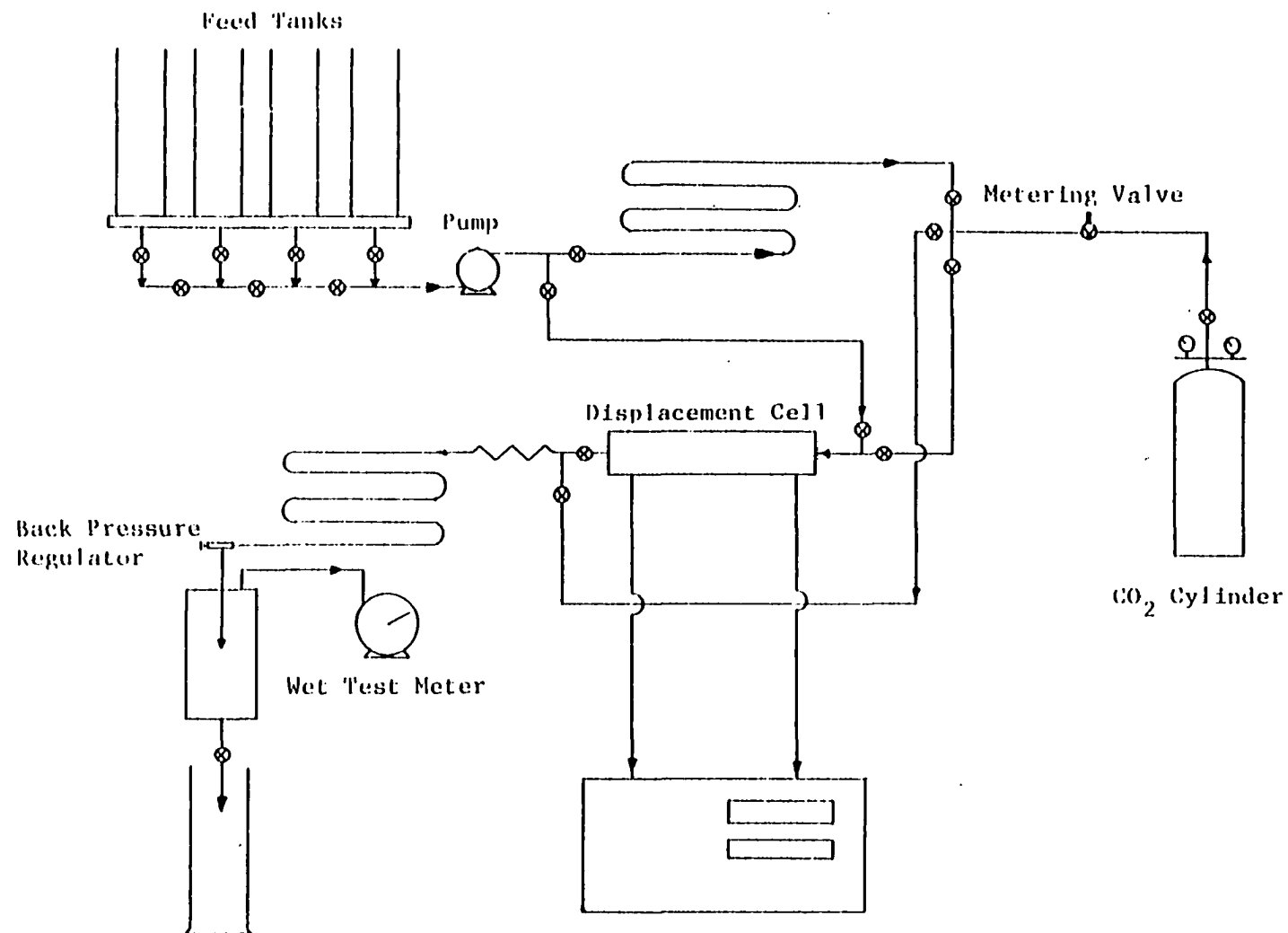
$$\frac{w_M}{w_p} = (3.057 \times 10^{-3}) \left(\frac{110.4 \text{ cm}^3/\text{min.}}{\text{bbl/day}} \right)$$
$$= 0.336 \frac{\text{cm}^3/\text{min.}}{\text{bbl/day}}$$

CHAPTER IV
EXPERIMENTAL EQUIPMENT AND MATERIALS

An extensive experimental facility was constructed for investigating the effects of simultaneous injection of steam and CO₂ on the recovery of heavy oils. The laboratory equipment used in the displacement tests, as shown in figure 4.1, includes a linear displacement cell, feed tanks, a positive displacement metering pump, heating tapes, high pressure CO₂ cylinders along with measuring, recording and controlling devices. The important components of the facility, designed with enough flexibility to allow for varying degrees of complexity in the experimental process, are described as follows:

1. Linear Displacement Cell:

The experiments were conducted in a stainless steel cell equipped with Hassler-type Core holders and one thermocouple at each end to measure the temperature of the flowing fluid. The cell was 24 inches in length, 3 inches in internal diameter and 0.25 inches in wall thickness with end caps screwed on the cell and sealed with high pressure, high temperature corrosion resistant O-rings. There was one swagelock quick disconnect at each end to maintain pressure inside the cell when it was taken out from the assembly for weighing. The cell was wrapped with an



Data Acquisition and Controlling System

FIG. 4.1: SCHEMATIC OF EXPERIMENTAL SETUP.

asbestos insulating tape to reduce heat losses. The system is shown in figure 4.2.

2. Porous medium:

It consisted of 20-40 mesh Halliburton frac sand. The sand pack was prepared by pouring sand in the core holder while it was constantly shaken to provide almost a tight, homogeneous and consistent reservoir. While packing sand acetone was periodically added to facilitate its settling. The sand was held in place by a metal screen followed by an O-ring and an end cap on each side of the core holder.

3. Feed tank:

Four feed tanks made of plexi-glass served as reservoirs for oil, water, solvent and brine. All the tanks were connected to the inlet side of the positive displacement metering pump through a system of valves and the feed line as shown in fig. 4.1.

4. Positive displacement metering pump:

A positive displacement metering pump was used to inject fluids at the desired rate into the displacement cell. The outlet of the pump was connected to two lines through a T connection. One of the lines was wrapped with heating tapes and properly insulated to generate steam and was connected to the displacement cell through a system of valves and a flexible disconnect. The other line was connected directly to the displacement cell and was used to saturate the core with oil. The system is shown in figure. 4.1

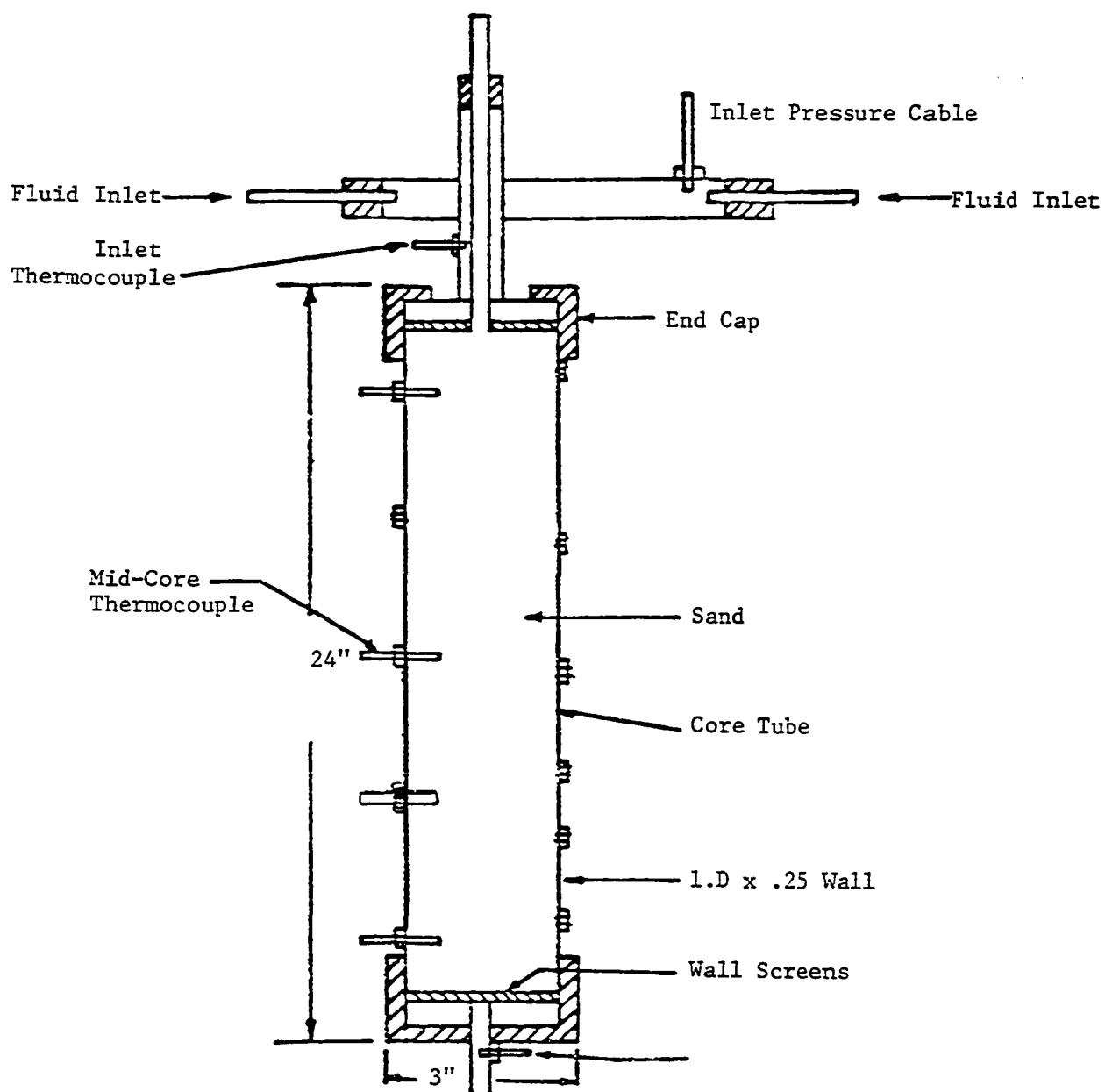


FIGURE 4.2: SCHEMATIC OF THE DISPLACEMENT CELL

5. CO₂ cylinder:

A high pressure CO₂ cylinder, equipped with forward pressure regulator, was connected to the steam generating line through a metering valve used to control the flow rate of CO₂ to the system.

6. Pressure monitoring:

The fluid pressure in the flow system was monitored by pressure gauges and pressure transducers. The pressure transducers were connected to a validyne digital transducer indicator equipped with digital display and analog DC output proportional to the input pressure signal.

7. Temperature monitoring:

The fluid temperature in the flow system was monitored by an array of five thermocouples. Two of them were connected to two zone temperature controllers through their respective heating tapes to control the temperature of the generated steam and to regulate heat to the displacement cell to set it at initial reservoir temperature. The remaining four were connected at 3, 7, 11, and 19 inches from the inlet of the displacement cell to monitor temperature at these points.

8. Production system:

The produced fluids passed through a pressure gauge into the production facilities consisting of a heat exchanger, a back pressure regulator, a sealed tubing to allow separation of CO₂ and liquids produced, a wet test meter and several valves and graduated cylinders.

The heat exchanger was built by placing about 4 ft. of the production line inside a tank full of water cooled by a

refrigeration system.

Fluids out of the heat exchanger passed through the back pressure regulator into the sealed tubing fitted with a rubber stopper at the top and a valve at the bottom. The liquids collected at the bottom were produced into the graduated cylinders through the valve while CO_2 escaping through a top line in the rubber stopper passed through a wet test meter and to the atmosphere.

The backpressure regulator and the wet test meter were used to control the pressure of the system and to measure the amount of CO_2 produced respectively.

CHAPTER V
EXPERIMENTAL PROCEDURE

The gravity and viscosity of the crude oil samples used in this experimental investigation were 15°, 20° and 26°API at 75°F respectively.

All the tests were carried out in a stainless steel core-holder of 24 inches in length and 3 inches in diameter equipped with 3 thermocouples, one at each end and one at the center, and packed with unconsolidated 20-40 mesh Halliburton frac. Sand of specific gravity 2.65. Total or absolute porosity of the sand was determined by using a pycnometer and the following equation.

$$\phi_{abs} = 1 - \frac{V_{sg}}{V_b} \dots\dots\dots 5.1$$

Where

ϕ_{abs} = Absolute porosity

V_{sg} = Sand grain volume

V_b = Bulk volume

1. Before The Run:

The following steps were taken before the commencement of each run :

- i. The displacement cell was packed with sand. This was done by shaking and tapping the cell with mallet continuously, while the sand was being poured in, to provide a tight, homogeneous and consistent reservoir. After packing the excess sand was removed, the end plates of the cell were screwed inplace and the weight of the cell recorded.
- ii. The cell was connected to the flow lines after flushing them with water and then it was pressure tested for leakes. This was done by closing the inlet valve and pulling a vaccum on the cell followed by closing the outlet valve. A stable pressure in the cell indicated no leaks.
- iii. All thermocouples were connected to the recorder and checked to be in good condition.
- iv. The inlet valve was, now, opened and water was injected at the minimum possible rate to avoid the creation of flow channels. After breakthrough water was allowed to flow for some time when the flow rate was measured and the corresponding differential pressure across the cell recorded. By using Darcy's law and this data, the absolute permeability was determined that ranged between 3 and 4.5 darcies.
- v. The cell was disconnected from the assembly and weighed to calculate the pore volume and effective porosity as follows:

$$P.V = \frac{W_2 - W_1}{\rho_w}$$

$$\phi_{eff} = \frac{P.V}{V_b}$$

Where

W_1 = Weight of cell + sand

W_2 = Weight of cell + sand + water

ρ_w = Density of water

P.V.= Pore volume

V_b = Bulk volume of sand pack

- vi. The cell was mounted back and heated by turning on the thermal tapes wrapped around it and setting the temperature controller at the initial reservoir temperature of 105°F. The oil, heated by thermal tapes to reduce its viscosity and facilitate injection, was now allowed to flow through the cell to irreducible water saturation. The core was allowed to cool, disconnected from the assembly and weighed again to determine the initial oil and irreducible water saturations as follows:

$$(1-S_{wi}) \cdot \rho_o \cdot (P.V) + S_{wi} \cdot \rho_w \cdot (P.V) = W_{firr}$$

Where

S_{wi} = Initial or irreducible water saturation

ρ_o = Density of oil

ρ_w = Density of water

W_{firr} = Weight of fluids in the cell at the irreducible water saturation.

- vii. The injection and production lines were cleaned by flowing solvent through them and then flushing them with distilled water. The cell was connected back to the assembly and isolated from the flow lines by closing the inlet valve and opening the by-pass valve.
- viii. The pump and the thermal tapes on the injection lines were turned on to generate steam and the temperature controller was set at the desired steam temperature. The flow rate and pressure were adjusted to required values by regulating the stroke of the pump and the back pressure valve.

2. During The Run:

a. Steam Drive Only:

As the pressure, temperature and the flow rate of the generated steam stabilized at the pre-set values, the by-pass valve was closed and the steam was flowed into the displacement cell by opening the inlet valve. The temperature and pressure recordings were made by the data acquisition system. The producing line was heated when the produced fluids were

cold to facilitate their flow and cooled when they became hot after steam breakthrough. The produced fluids were collected in graduated cylinders and the time of production for each cylinder recorded. The run was continued until the oil/water ratio dropped to a value that could not be measured.

b. Injection Of Steam In Combination With CO₂:

CO₂ was mixed with steam in the injection line and its rate and pressure were controlled by the metering valve and the forward pressure regulator mounted on the CO₂ cylinder respectively to obtain a mixture of steam and CO₂ of required proportions at the required pressure. This was confirmed by measuring the volume of the condensed water collected at the production end and the volume of CO₂ produced as indicated by the wet test meter in a given time. As the pressure, temperature, and injection rates stabilized at the desired values, the bypass valve was closed and the mixture allowed to flow through the displacement cell by opening the inlet valve. The rest of the procedure was the same as described in the steam drive process except that the produced CO₂ was flowed through the wet test meter into the atmosphere as illustrated in figure 4.1.

3. After The Run:

The system was turned off and the rates and volumes of the produced fluids recorded. The produced fluids were in the form of milky brown emulsions, and some of them were very

hard to break. A little Amoco surfactant was added to facilitate separation of oil & water. The cell was unpacked, cleaned and re-packed for the next run.

CHAPTER VI
RESULTS AND INTERPRETATIONS

The primary objective of this study was to investigate the use of CO_2 , when injected simultaneously with steam in varying proportions, as a means of improving oil recovery. With this end in view a total of 39 experiments were conducted to establish an optimum range of CO_2 /steam ratio and to determine the effects of injection pressure (temperature), rate, viscosity and pH on the oil recovery.

The experiments were carried out in five phases as follows:

In phase 1 only steam, at temperatures of 300,350,400,450, 500, & 550°F, was used to displace a 20°API oil. The data obtained from this phase is recorded in tables B-11 through B-17 Appendix B.

In Phase 2 a mixture of steam and CO_2 adjusted to a predetermined temperature and CO_2 /steam ratio was injected continuously into the core and the corresponding recoveries of the 20°API oil were recorded. The results of the runs conducted in this phase are given in tables B-21 through B-47. The data of tables B-11 through B-17 and B-21 through B-47 was integrated together and plotted as shown in figures 6.1 and G1 through G5 appendix G to evaluate the effects of CO_2 , when injected along with steam, on the oil recovery.

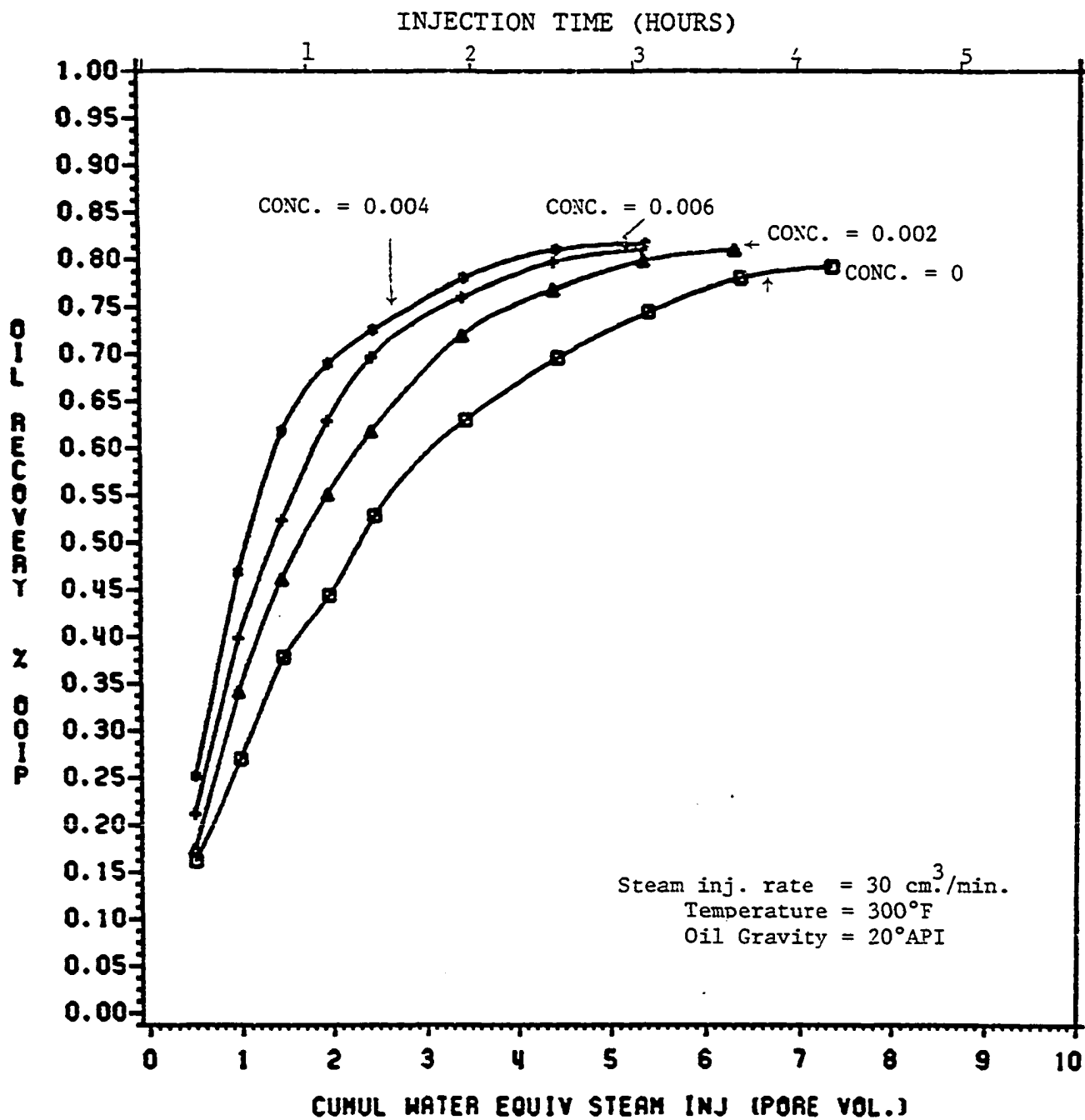


FIGURE 6.1: EFFECT OF CO₂ ON STEAM DRIVE RECOVERY

CONC. = CO₂/STEAM RATIO (SCF CO₂/CM³ STEAM INJ.)

In phase 3 the injection rate of steam, at a fixed temperature of 400°F and optimal CO₂/steam ratio, was varied and the corresponding recoveries of the 20°API oil were recorded in tables C-11 through C-14. The data obtained so far was used to determine the effect of injection rate on oil recovery as illustrated in figure 6.2.

In phase 4, 15° and 26°API oils were used and the tests were run as in phases 1 and 2. The results obtained from this series of experiments are given in tables D-11 through D-19 and plotted as shown in figures 6.3 and G6 through G7 appendix G to evaluate the effect of viscosity of the oil, at the steam temperature, on oil recovery.

In phase 5 alkaline water of pH 12 was used for the steam generation and the experiments were conducted similar to the ones described in phases 1 and 2. The results obtained are given in tables E-11 through E-15 and plotted in figures G8 through G11 appendix G to evaluate the effect of high pH on oil recovery from the core when subjected to simultaneous injection of CO₂ and steam.

6.1 PHASE 1: Determination of recovery by conventional steam flooding.

The results obtained from this series of experiments, as summarized in tables B-11 through B-17 and plotted in figures 6.1 and G1 through G5 appendix G are used as a criteria of comparison with the results of all other experiments conducted in the subsequent phases to find out if the addition of CO₂ in steam improves recovery. A total recovery of 79.2% of the original oil in place was obtained when steam was injected at 300°F.

The total recoveries at injection temperatures of 350, 400, 450, and 550°F were 76.8, 73.0, 67.8, 65.3, and 63.0% respectively. The purpose of making the runs at different temperatures was to evaluate the effect of pressure and temperature on oil recoveries which will be discussed later in this chapter.

6.2 PHASE 2: Determination of CO₂ concentration in the injected steam to maximize recovery.

Results from this study are summarized in tables B-21 through B-47 and plotted in figures 6.1 and G1 through G5 appendix G. The examination of these figures indicates that at a CO₂/steam ratio of .004 SCF CO₂/cm.³ steam, the oil recovery is maximized at all temperatures. The total recovery at 300°F is 81.6% which is only 2.4% higher over the conventional steam flooding process. However, it may be noted that the injection of CO₂ increases the rate of recovery significantly as illustrated in figure 6.1. An overall recovery of 79.2% is obtained in about 4.2 hours with conventional steam flooding, while only about 2.15 hours are needed to realize the same amount of recovery when a mixture of CO₂ and steam (.004 SCF CO₂/cm.³ steam) is injected.

The additional recovery obtained by carbon dioxide injection with steam is attributed to the:

1. High solubility of carbon dioxide in oil which results in swelling of the oil ahead of the steam front thus decreasing its viscosity and increasing its permeability, both favoring a more efficient displacement.

2. Solubility of carbon dioxide in water increases its viscosity and improves water-oil mobility ratio.
3. Improved miscibility at the condensation front due to enhanced steam distillation behind the heat front.
4. Lowering of interfacial tension and promotion of miscibility effects that promotes pistonlike displacement.
5. Better heat distribution and additional volumetric sweep provided by the injected gas.
6. Trapped gas effect.
7. Solution gas drive effects.

Generally carbon dioxide is not miscible on first contact with reservoir oils, but may develop miscibility through multiple contacts at sufficiently high pressure depending upon the reservoir temperature and oil characteristics. Holm and Josendal reported that miscibility may be achieved in case of light oils at pressures of the order of 2000-3000 psig, but with very viscous oils the miscibility pressure can never be reached as shown in figures G12 and G13 appendix G. The examination of these figures also indicates the dependence of minimum miscibility pressure on temperature. The miscibility pressure requirement increases with increasing temperature.

This experimental study was conducted at such pressures and temperatures that carbon dioxide miscibility requirements with oil are not met. However, even without miscibility the swelling caused by the dissolution of carbon dioxide in the oil decreases its viscosity and increases its permeability, both of which favor a more efficient displacement.

As soon as the mixture of steam and carbon dioxide enters the experimental cell, it starts rapidly migrating upward due to strong gravitational gradients while advancing into the originally cool reservoir. The injected steam heats the formation and a fraction of crude oil in the steam zone vaporizes. The vaporization process is further enhanced by the presence of carbon dioxide in the injected steam. The hydrocarbon vapor is carried forward through the advancing mixture of steam and carbon dioxide. The steam and the hydrocarbon vapor condense and mix with the original crude at the condensation front to form a hot water zone and a hydrocarbon distillate or solvent bank; whereas the noncondensable carbon dioxide, some of which gets dissolved in the water and oil phases, creates a permanent gas phase along the top of the reservoir. All these processes assist in enhancing and improving recovery.

The distillate bank drives the oil miscibly ahead of the steam front and the solubility of carbon dioxide in water increases its viscosity and thus improves water-oil mobility ratio. The dissolved carbon dioxide in oil breaks out of solution with decreasing pressure, as the front moves towards the producing end, and consequently provides additional drive energy. The overlying permanent gas phase provides additional sweep and assists in propagation of steam thus resulting in earlier arrival of heat at the producing end. This heats up the formation close to the producing end much sooner than the conventional steam flooding process thus resulting in accelerated oil production due to increased mobilization of oil caused by viscosity

reduction. A schematic diagram of the CO₂/steam injection system is shown in figure G14 appendix G.

The examination of figures 6.1 and G1 through G5 appendix G indicates that oil recovery is also affected by the level of concentration of carbon dioxide in the injected steam. As the carbon dioxide concentration increases from .002 to .004 SCF CO₂/cm.³ steam the recovery also increases, but a further increase in concentration of carbon dioxide from .004 to .006 SCF CO₂/cm.³ steam results in a decreased recovery. The first increase in concentration from .002 to .004 SCF/cm.³ steam, increases the amount of carbon dioxide dissolved in the oil phase, but when the concentration is increased from .004 to .006 SCF/cm.³ steam, very little additional carbon dioxide goes into solution. The dissolved gas helps to decrease the viscosity of oil and provides additional energy to move it towards the producing end. Whereas the undissolved gas simply builds up the gas saturation resulting in increased relative permeability to the gas. With increasing concentration of carbon dioxide, the decreasing oil viscosity contributes towards the improvement in recovery while the increasing relative permeability to gas lowers the ultimate recovery. The counteracting effects of both these parameters result in an optimum concentration of about .004 SCF CO₂/cm.³ steam observed in this study.

6.3 PHASE 3: Determination of the steam injection rate required to maximize recovery.

The results from this study are summarized in tables C-11 through C-14 and plotted in figure 6.2. The examination of this figure indicates that the recovery is maximized at the steam injection rate of 30 cc/min. The probable explanation for the poor

EFFECT OF INJ RATE ON STEAM DRIVE RECOVERY

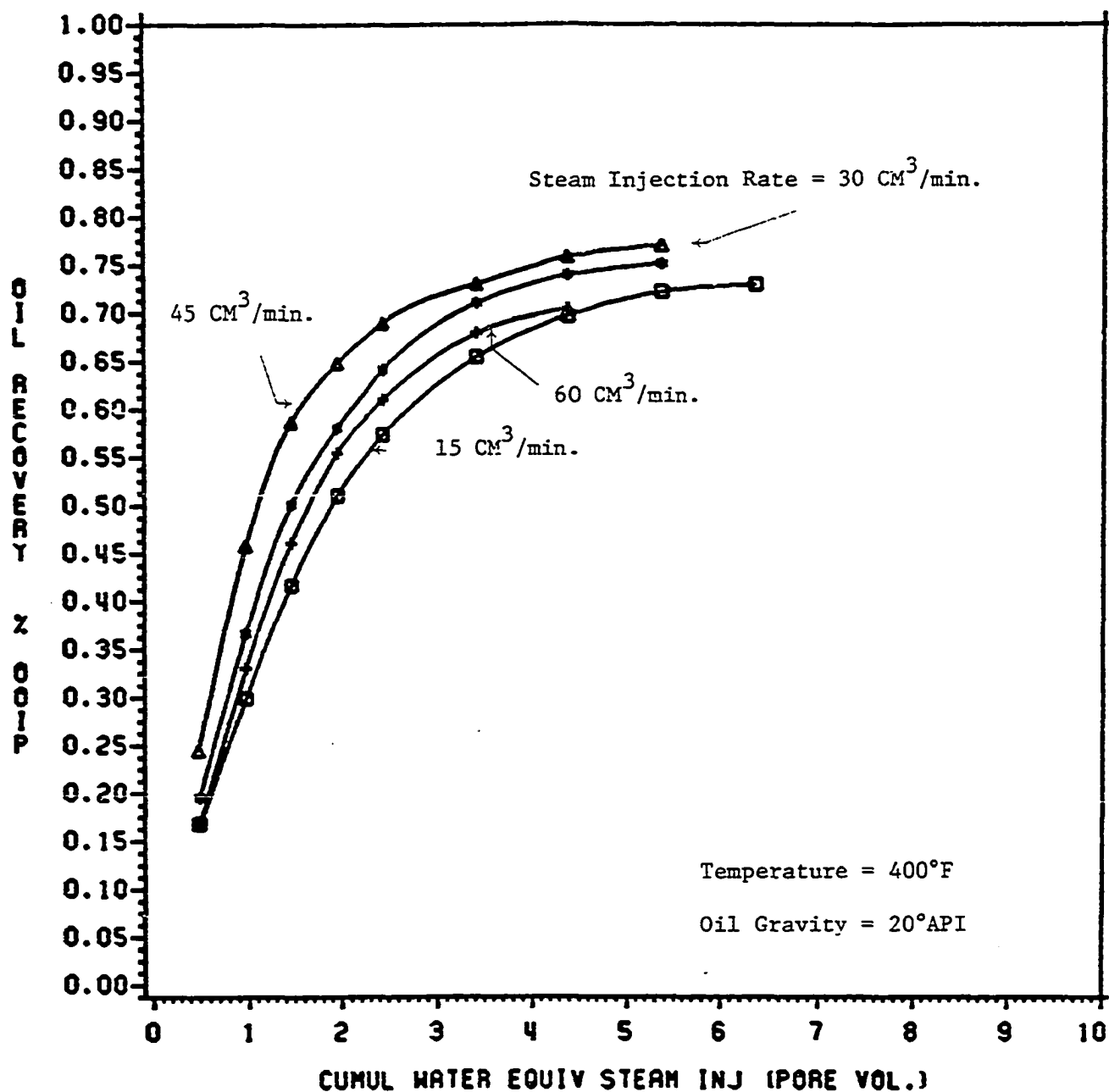


FIGURE 6.2: EFFECT OF INJECTION RATE ON STEAM DRIVE RECOVERY

CO₂/STEAM RATIO = .004 SCF CO₂/CM³ STEAM INJECTION

efficiency exhibited at very low and high rates is as follows:

A very low rate of steam injection implies a very low rate of heat injection into the reservoir which causes the steam zone to develop very slowly thus lowering the possibility of developing a steam drive. In other words the process will be equivalent to a hot water drive with all its accompanying inefficiencies in terms of oil/water ratio.

With continuing increase in the steam injection rate, the steam zone grows accordingly until a steam drive is developed accompanied by its unique efficiency in terms of oil/water ratio. At high injection rates, the steam zone which increases relative permeability to highly mobile steam vapor and promotes steam channeling to the production end, thus lowering the recovery efficiency significantly.

6.4 PHASE 4: Effect of oil Gravity.

Figure G15 appendix G indicates that at any given temperature, the viscosity of an oil is a function of its gravity. A low API gravity oil is more viscous than a higher API gravity oil under similar conditions. Also the examination of figure G16 shows the effect of viscosity on the rate of development and the degree of override. As the steam enters the formation, it starts migrating upwards because of the marked difference in density between the steam and the reservoir fluids. The rate of this upward migration is dependent on oil viscosity at steam temperature in addition to vertical permeability. The higher viscosity

dictates higher rates of upward migration and more pronounced gravity override effects which in turn implies a poor displacement efficiency and poor recovery.

The above discussion points out that the viscosity of oil and hence the API gravity are very important parameters affecting the recovery efficiency that increases with decreasing viscosity.

Carbon dioxide dissolves in crude oil and when it goes into solution, the volume of the oil increases and its viscosity decreases significantly. The amount of swelling and the reduction in viscosity depends on the crude oil gravity as shown in figures G15 and G17 appendix G. Generally speaking, the lower the API gravity of the oil the greater the percentage reduction that takes place in the viscosity on dissolution of carbon dioxide in the oil. Thus, viscosity reduction is significant and more pronounced with medium and heavy oils than with the light oils which leads to higher incremental recovery due to simultaneous injection of carbon dioxide and steam over the conventional steam flooding process under similar conditions of temperature and pressure.

The effect of oil gravity was examined by displacing three oils of gravities 15°, 20°, 26° API with a mixture of carbon dioxide and steam at 400°F. The results thus obtained are given in tables D-11 through D-19 and plotted in figures 6.3 and

EFFECT OF GRAVITY ON STEAM DRIVE RECOVERY

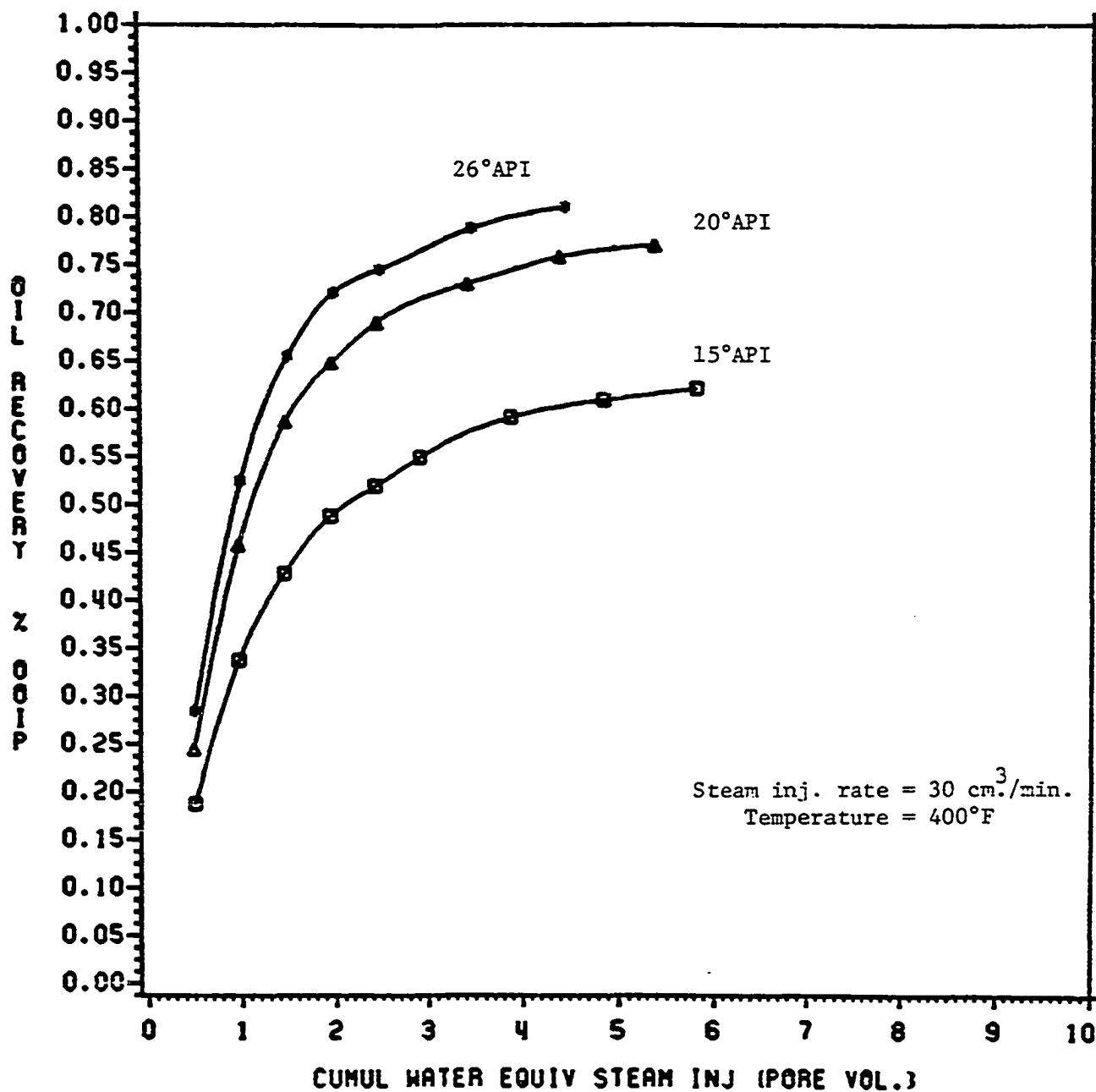


FIGURE 6.3: EFFECT OF GRAVITY ON STEAM DRIVE RECOVERY

CO₂/STEAM RATIO = .004 SCF CO₂/CM³ STEAM INJ.

G6 and G7 appendix G. The examination of these figures indicates that the optimum CO_2 /steam ratio of .004 SCF CO_2 /cm³ steam still prevails, but the total recovery increases with decreasing oil gravity. The total recovery of 15°API oil at the optimum CO_2 /steam ratio is about 8% higher than the case when no carbon dioxide is injected with steam. In case of 20°API oil the improvement in recovery is only 4% while there is no improvement in ultimate recovery in case of 26°API oil. This is, because, the percentage reduction in viscosity due to dissolution of carbon dioxide in oil and even distribution of heat decreases with increasing API gravity, thus giving rise to lower incremental recoveries in case of higher API gravity oils.

6.5 PHASE 5: Effect of pH.

The effect of pH on oil recovery was examined by displacing a 20° API oil first with caustic steam (pH = 12) alone and then with varying levels of carbon dioxide concentrations in the injected steam at 400°F. The results thus obtained are given in tables E-12 through E-15. The results of similar experiments when conventional steam (pH = 8.5) was used as a displacing fluid are given in tables B-14, B-24, B-34, and B-44 respectively. The data of tables E-12 and B-14 is plotted in figure G8 to evaluate the effect of pH on oil recovery when no carbon dioxide is injected with steam. Similarly, data of tables E-13/B-24, E-14/B-34, E-15/B-44 is plotted in figures G9 through G11 respectively to determine the effect of pH on oil recovery

when steam is injected with varying concentrations of carbon dioxide. The examination of these figures indicates that:

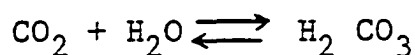
1. Although there is no significant improvement in ultimate recovery, the rate of recovery increases significantly with increasing pH when no carbon dioxide is injected with steam (fig. G8).
2. Neither the rate of recovery nor the ultimate recovery is affected by pH when carbon dioxide is injected in combination with steam (fig. G9 through G11).

The process of caustic flooding has been studied by various investigators who reported that the incremental recovery of caustic flooding over conventional steam flooding results from:

1. Lowering of interfacial tension
2. Reversal of rock wettability
3. Emulsification and entrapment

The results of this study are in agreement with the findings of these investigators when steam is injected alone to recover oil. The probable reasons that the recovery is not affected by pH when carbon dioxide and steam are injected together, are as follows:

1. Carbon dioxide dissolves in water to form carbonic acid according to the following equilibrium relationship



which reduces pH.

2. The displacement mechanisms of carbon dioxide dominate the displacement mechanisms of the caustic flooding.

Although it is not part of this study, the importance of steam injection process to recover heavy oil makes it necessary to understand the effect of high pH and high temperature on the reservoir minerals and fluids. Laboratory studies have indicated that the injection of high pH fluids cause substantial dissolution of reservoir minerals. These minerals are carried forward through the advancing fluids and reprecipitate in the pore spaces as the temperature and pH falls, thus causing significant reduction in permeability of the areas away from the injection end. Incompatibility of the injected and formation water causes chemical reactions between the dissolved salts resulting in the production of precipitates which can reduce permeability too. Generally, clays are more compatible with low pH fluids than with high pH fluids, which cause expansion and dispersion of water-sensitive clays and thus reduce the formation permeability the production of solid particles in the produced fluids, plugging of surface equipment, and deterioration of gravel packs and liners are some of the other problems associated with the injection of high pH fluids. To minimize this kind of damage it is advisable to maintain the pH of the injected fluids as low as possible. The formation of carbonic acid due to carbon dioxide injection may help to reduce pH and moreover because of the neutralization the corrosion problems associated with carbon dioxide injection may be reduced.

6.6 EFFECT OF PRESSURE:

The effect of pressure on oil recovery is examined by studying figure 6.4 plotted by using data obtained in phase 2. These results indicate that the total recovery decreases with increasing pressure. A possible explanation for this is as follows.

Pressure and temperature are inter related in steam flooding. The solubility of carbon dioxide in crude oil is affected both by temperature and pressure. It increases with increasing pressure while decreases with increasing temperature, both parameters counteracting the effects of each other. For a given quality of steam, a high pressure is coupled with high temperature with resulting low viscosity of oil and greater driving force for displacement, both mechanisms contributing towards improvement in recovery. But at high pressure, the resulting lower specific volume of steam is coupled with lower flow rate and hence a lower recovery.

The latter effect dominates the former with the result that the total recovery is reduced at high pressures. But in case of very viscous oils, a greater driving force for displacement is necessary to ensure the desired oil mobility which can only be developed by high pressure steam injection. Therefore, it is recommended that all steam flood operations should be conducted at the lowest possible pressure to insure the efficient use of steam vapor.

EFFECT OF PRESSURE ON STEAM DRIVE RECOVERY

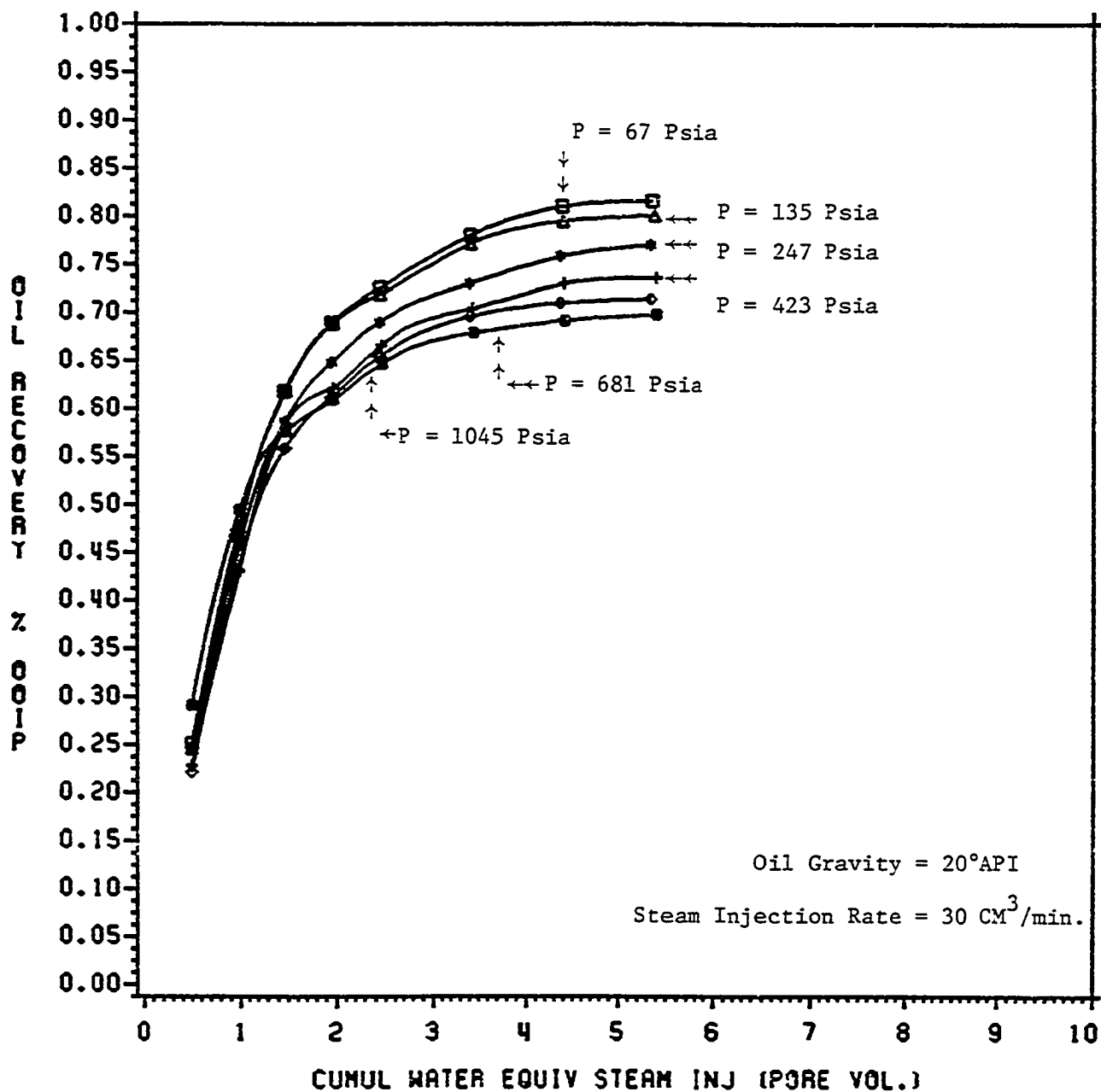


FIGURE 6.4 : EFFECT OF PRESSURE ON STEAM DRIVE RECOVERY

CO₂/STEAM RATIO = .004 SCF CO₂/CM³ STEAM
INJECTED.

6.7 COMPARISON WITH THEORY:

In figure 6.5, the oil recoveries calculated by using the Myhill and Stegemeier⁴⁷ prediction model are compared with those obtained experimentally for run 3 and given in table B-14 Appendix B. Sample calculations and results for the run are presented later in this section illustrating the use of the prediction model. Generally good agreement exists between the observed and calculated values. The difference however, is insignificant and is probably due to the assumptions made in the derivation of the prediction model. Also, qualitatively similar reservoir simulation results were obtained by K.C. Hong and J.W. Ault⁶⁶. A quantitative comparison can not be made because of the different reservoir and fluid properties. However, both studies appear to follow the same general trend, thus supporting the results of this study.

In figures 6.6 and G18 through G22 the temperature distributions calculated by using the Lauwerier²² model are compared with those obtained experimentally for runs 1 through 6 and given in tables F-1 and F-2, Appendix F. Since the Lauwerier model describes the temperature distribution in a linear system with hot water injection, the deviations between the observed and calculated values are as expected indicating the development of a steam zone which makes the thermal profile steeper. A knowledge of the temperature profile helps in predicting the location and rate of advance of the steam zone. A computer programme and the computed results, based on the Lauwerier model, are given in Appendix F for runs 1 through 6.

SAMPLE CALCULATIONS USING MYHILL AND STEGEMEIER⁴⁷

PREDICTION MODEL FOR RUN 3.

DATA:

$$T_s = 400^{\circ}\text{F} ; T_r = 105^{\circ}\text{F}$$

$$P_v = 1035 \text{ cc} = .0365 \text{ ft}^3$$

$$S_{oi} = 0.805$$

$$S_{wi} = 0.195$$

$$S_{or} = 0.208$$

$$L_v = 825.9 \text{ Btu/lb}_m \text{ (steam tables)}$$

$$\text{Oil gravity} = 20^{\circ}\text{API}$$

Heat capacity of oil

$$C_o = (0.388 + 0.00045 T) / \gamma_o$$

$$\gamma_o = \frac{141.5}{131.5 + \text{API}}$$

$$= \frac{141.5}{131.5 + 20} = 0.934$$

$$C_o = (0.388 + .00045 \frac{105 + 400}{2}) / 0.934$$

$$= 0.537 \text{ Btu/lb}_m - ^{\circ}\text{F}$$

$$C_w = \frac{h_w(400) - h_w(105)}{400 - 105}$$

$$= \frac{375.1 - 72.991}{295} = 1.0241 \text{ Btu/lb}_m - ^\circ\text{F}$$

$$\rho_o(400) = 62.4 (0.81) = 50.54 \text{ lb}_m/\text{ft}^3$$

$$\rho_w(400) = \frac{1}{.01864} = 53.648 \text{ lb}_m/\text{ft}^3$$

$$M_w = C_w \rho_w$$

$$= (1.0241) (53.648) = 54.941 \text{ Btu/ft}^3 - ^\circ\text{F}$$

$$M_o = C_o \rho_o$$

$$= 0.537 * 50.54 = 27.14 \text{ Btu/ft}^3 - ^\circ\text{F}$$

$$\rho_s = 0.5368 \text{ lb}_m/\text{ft}^3$$

$$M_s = \left(\frac{\lambda}{\alpha}\right) = 56.13 \text{ Btu/ft}^3 - ^\circ\text{F}$$

$$M_\sigma = 42.3 \text{ Btu/ft}^3 - ^\circ\text{F}$$

$$M_R = (1-\phi) M_\sigma + (S_o)(M_o) + \phi S_w M_w$$

$$+ S_g \left[f M_g + (1-f) \left(\frac{\rho_s L_v}{\Delta T} + \rho_s C_w \right) \right]$$

$$= (1 - .3723) 42.3 + .3723 (.208)(27.14)$$

$$+ (.3723)(.195)(54.941) + .3723 (.597).$$

$$\left[\frac{.5368 * 825.9}{295} + .5368 * 1.0241 \right]$$

$$= 33.098 \text{ Btu/ft}^3 - ^\circ\text{F}$$

$$\begin{aligned}
 f_{hv} &= \left[1 + \frac{C_w \Delta T}{f_{sdh} L_{vdh}} \right]^{-1} \\
 &= \left[1 + \frac{1.0241 (295)}{(1.) (825.9)} \right]^{-1} \\
 &= 0.7322
 \end{aligned}$$

$$\begin{aligned}
 e^{t_{cd}} \operatorname{erfc} t_{cd} &= 1 - .7322 \\
 &= 0.2678 \\
 t_{cd} &= 3.672
 \end{aligned}$$

$$\begin{aligned}
 t &= \frac{1}{4} \left(\frac{M_R}{M_S} \right)^2 \left(\frac{\pi r^2}{\alpha_S} \right) t_D \\
 &= .001033 t_D \dots\dots\dots \text{days}
 \end{aligned}$$

or

$$t = 1.487 t_D \text{ minutes}$$

$$w_f = 30 \frac{\text{cm}^3}{\text{min.}} \quad \text{or} \quad 95.2 \text{ lb}_m/\text{day}$$

$$\begin{aligned}
 \dot{Q}_i &= 95.2 [1.0241 (295) + 825.9] \\
 &= 107386 \text{ Btu/D}
 \end{aligned}$$

$$Q_i = 107386 * t$$

$$V_s = \frac{Q_i}{M_R} \cdot \frac{E_{h,s}}{T}$$

$$= \frac{107386 \frac{\text{Btu}}{\text{D}} \cdot \frac{\text{D}}{24 \text{ hr.}} \cdot \frac{1 \text{ hr.}}{60 \text{ min.}}}{33.098 \frac{\text{Btu}}{\text{ft}^3 \cdot ^\circ\text{F}} * 295 ^\circ\text{F}} t \text{ (minutes)}$$

$$= .007638 E_{h,s} t$$

$$N_p = (S_{oi} - S_{or}) E_c V_s$$

$$= 0.3723 (.805 - .208) .7 V_s$$

$$= 0.155584 V_s \text{ ft}^3$$

or

$$N_p = 4405.6 V_s \text{ cm}^3$$

t_D	$t=1.487t_D$	* $E_{h,s}$	Q_i Btu	V_s ft ³	N_p cc	R
5	7.435	.346	554.4	.1965	86.6	.104
10	14.87	.275	1109.0	.03123	137.6	.165
15	22.305	.235	1663.4	.04004	176.4	.212
20	29.74	.205	2217.8	.04656	205.1	.246
30	44.61	.179	3326.7	.06099	268.7	.322
40	59.48	.160	4435.6	.07269	320.2	.384
50	74.35	.14	5544.5	.07951	350.3	.420
60	89.22	.132	6653.4	.08995	396.3	.476
80	118.96	.118	8871.3	.10722	472.4	.566
100	148.7	.115	11089.1	.13062	575.5	.691
120	178.44	.1	13306.9	.13629	600.4	.721
150	223.05	.08	16633.6	.13629	600.4	.721

*Values of $E_{h,s}$ are obtained from figure G23.

EFFECT OF CO2 ON STEAM DRIVE RECOVERY

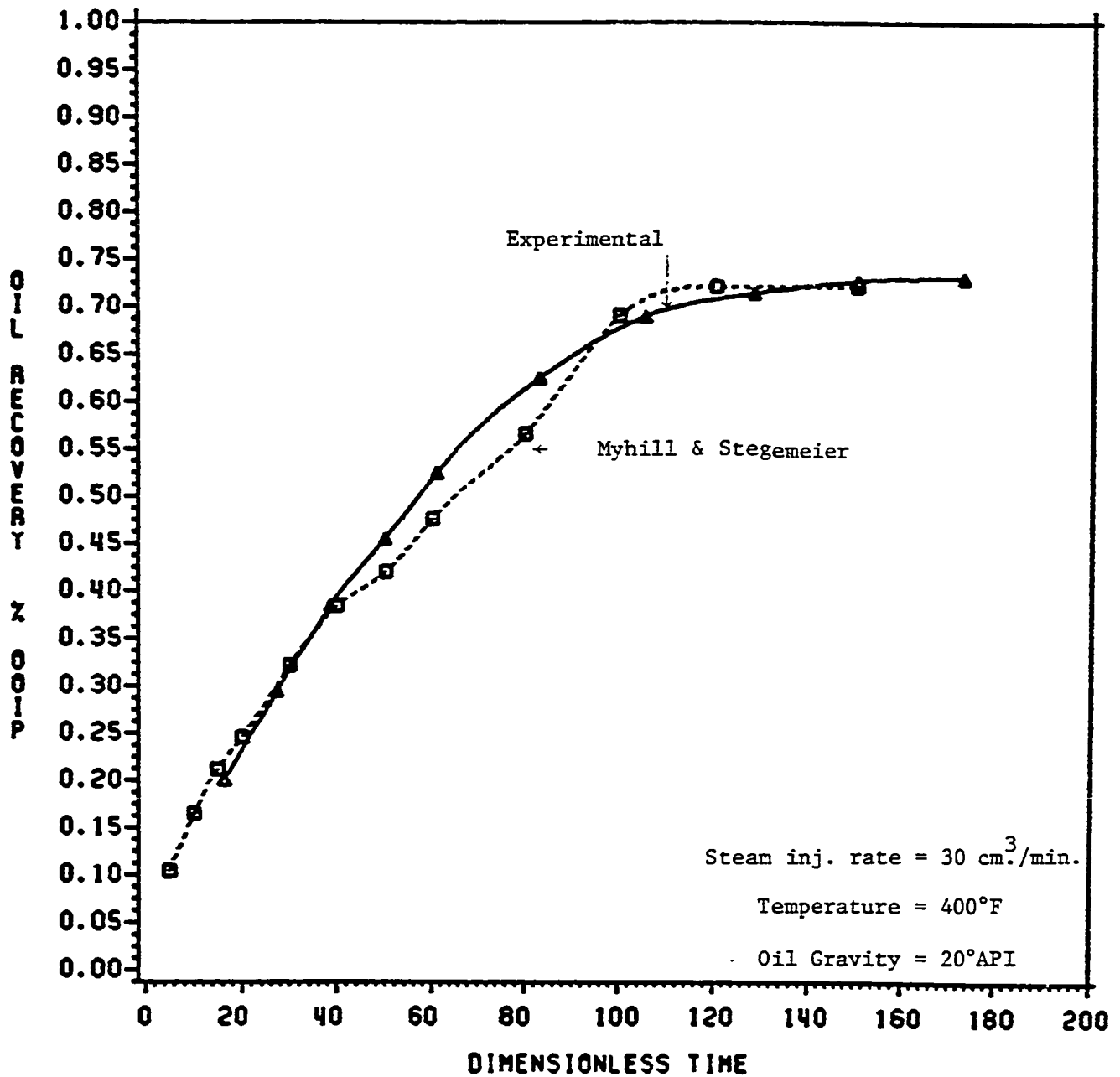


FIGURE 6.5: COMPARISON OF EXPERIMENTAL RESULTS WITH
THOSE OBTAINED BY USING MYHILL
STEGMEIER THEORY

CO₂/STEAM RATIO = .00 (SCF CO₂/CM³ STEAM INJ.)

TEMPERATURE DISTRIBUTION

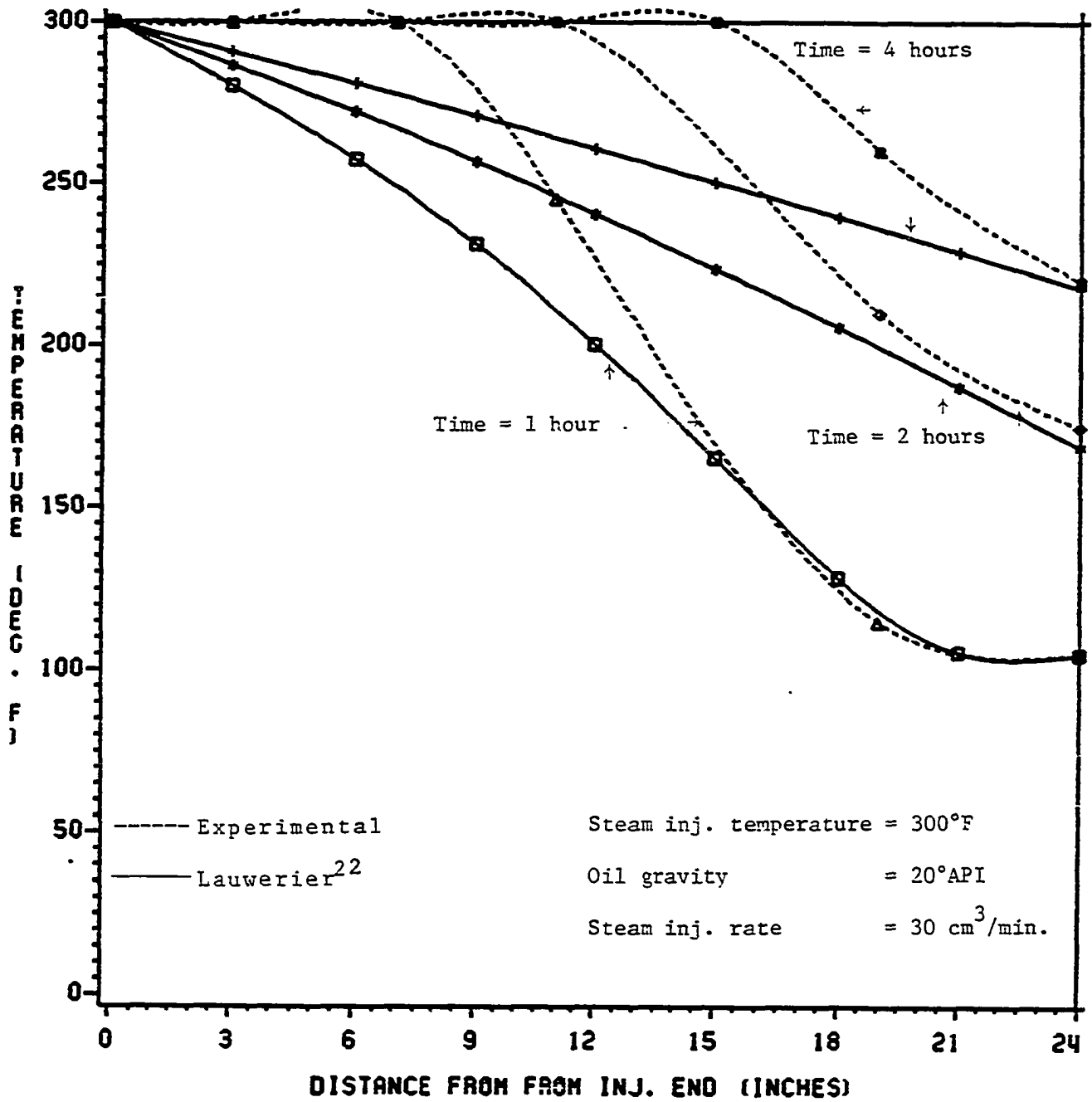


FIGURE 6.6: TEMPERATURE DISTRIBUTION WITH DISTANCE FOR RUN NO. 1

CHAPTER VII

SUMMARY AND CONCLUSIONS

Summary and Field Applications:

The injection of carbon dioxide with steam results in significantly increased production rates. This is due to (a) additional sweep and oil viscosity reduction and (b) better heat distribution provided by the injected gas.

Simultaneous injection of carbon dioxide and steam also results in the improvement of ultimate recovery of heavy oil which may be as high as eight percent over the conventional steam flooding process. This increase in the ultimate recovery is attributed to:

- a. The swelling of the crude oil with the dissolved carbon dioxide ahead of the heat front, thus resulting in decreased oil viscosity and increased oil permeability, both favoring a more efficient displacement of the oil.
- b. Improved oil mobilization due to better heat distribution and additional volumetric sweep provided by the injected gas.
- c. Enhanced steam distillation behind the heat front.
- d. Reduced interfacial tension.

e. Trapped gas effect.

f. Solution gas drive.

The results show that recovery is affected by carbon dioxide concentration in the injected steam. Increasing its concentration from .002 to .004 SCF CO₂/cc steam, increases the amount of CO₂ dissolved in oil, but when the concentration is increased from .004 to .006 SCF CO₂/cc steam, very little additional CO₂ goes into solution. The dissolved gas helps to decrease the viscosity of oil and provides additional energy to move it towards the producing end, while the undissolved gas simply builds up the gas saturation resulting in increased relative permeability to gas. The decreasing oil viscosity contributes towards improvement in recovery and the increasing relative permeability to gas lowers the ultimate recovery. The counteracting effects of both these parameters results in an optimum concentration of CO₂ which is about .004 SCF CO₂/cc steam observed in this study. The results obtained show the importance of the steam injection rate. At very low injection rates, the recovery is low due to very low rates of heat injection into the reservoir, which causes the steam zone to develop very slowly thus lowering the possibility of a steam drive. At very high injection rates the recovery is low due to very rapid growth of steam zone which increases the relative permeability to highly mobile steam. The study suggests the existence of an optimal steam injection rate at which the recovery is maximized. This was found to be around 30 cc/min.

The experimental results indicated the importance of the viscosity and gravity of the crude oils at steam temperature in affecting ultimate recovery. Generally, a low gravity oil is more viscous than a high gravity oil. It was observed that the ultimate recovery decreased with increasing viscosity of the crude. This was because of the displacement efficiency, which decreases with increasing viscosity due to more pronounced gravity override. But the incremental recovery due to simultaneous injection of CO_2 and steam over the conventional steam flooding process, under similar conditions of temperature and pressure, was higher for more viscous oils because of the fact that the percentage reduction in viscosity resulting from the carboration of these oils is greater and more pronounced than for the less viscous oils.

A change in pH has no effect on recovery when CO_2 is added to the injected steam. However, when steam is injected alone the rate of recovery is slightly increased with increasing pH, but there is no significant improvement in ultimate recovery.

The ultimate recovery decreases with increasing pressure and hence the temperature for a given quality of steam due to the competing effects of viscosity reduction and reduced volumetric sweep, in which the latter effects dominate the former. The solubility of CO_2 in crude oil increases with increasing pressure but decreases with increasing temperature, both parameters counteracting the effects of each other.

For a given quality of steam a high pressure is coupled with high temperature with resulting low viscosity of oil and a greater driving force for displacement, both mechanisms contributing towards improvement in recovery. But at high pressures the volumetric sweep is reduced due to lower specific volume of steam coupled with lower flow rate thus resulting in lower recovery. The latter effect dominates the former and hence the total recovery is reduced at high pressures.

In case of very viscous oils, a greater driving force for displacement is necessary to ensure the desired oil mobility which can only be developed by high pressure steam injection. Therefore it is recommended that all steam flood operations should be conducted at the lowest possible pressure to ensure the efficient use of steam vapor. In this connection it is suggested to start a steam flood at a high pressure necessary for the mobilization of oil and should be gradually reduced to the full realization of the process. The requirement for high pressure CO₂/steam injection can be greatly reduced if it is preceded by cyclic steam stimulation process which reduces resistance to flow near the producing end and thus facilitates communication between the injection and producing end.

It should be pointed out that recovery is affected by the boundary of the reservoir. These effects can be minimized by using longer laboratory cells if space limitations allow. Closmann et al⁵⁵ reported a higher recovery factor for longer

sand packs than for shorter ones. This is due to the lengths of the mixing zones which are a much longer fraction of the model lengths in case of shorter sand packs. This suggests that the results obtained in this study are pessimistic and therefore a higher recovery in the field may be expected.

The reservoir characteristics suitable for the simultaneous injection of CO_2 and steam should be such that maximum contact between the injected fluids and the resident oil could be established in order to maximize the effects of viscosity reduction, oil swelling and miscible displacement. Therefore, reservoirs with fractures, thin pay zones underlain by large aquifers or reservoirs with large free gas caps will not be suitable for this process.

Economically it is not feasible to use downhole steam generators in very shallow heavy oil reservoirs. Therefore, the cost of external injection of CO_2 must be justified by the additional or accelerated oil recovery. But where downhole steam generators are used, the CO_2 available as flue gas can be utilized and injected along with steam.

Reservoirs containing highly asphaltic crudes and having a low permeability are not suitable for simultaneous injection of CO_2 and steam, since permeability may be damaged due to the deposition of asphaltenes resulting from the contact of crude oil by CO_2 .

Conclusions:

The following conclusions were made on the present experimental investigation.

1. The injection of carbon dioxide with steam increases the rate of recovery significantly.
2. The recovery is affected by the concentration of CO_2 in the injected steam and is maximized at a concentration of about .004 standard cubic feet of CO_2 per cubic centimeter of cold water equivalent steam.
3. The overall recovery is dependent on oil viscosity and hence the API gravity. It improves by 8% in case of 15°API oil, 4% in case of 20°API oil, whereas no significant improvement in ultimate recovery, over the conventional steamflooding process, was observed in case of 26°API oil.
4. The recovery decreases with increasing pressure and hence the temperature.
5. The recovery is rate dependent and is maximized at a steam injection rate of $30\text{cm}^3/\text{minute}$.
6. The recovery is not affected by pH, when steam and CO_2 are injected simultaneously. However, when steam is injected alone the rate of recovery is slightly increased with increasing pH, but there is no significant improvement in ultimate recovery.

Recommendations for further research:

It is recommended that further work in this area should be directed to find:

1. The effect of cyclic steam injection prior to CO₂/steam injection process on oil recovery.
2. The effect of gradual reduction of pressure after steam breakthrough on oil recovery.
3. The effect of gradual reduction of steam injection rate after steam breakthrough on oil recovery.
4. The effect of injection of CO₂ in an alternate fashion with steam.
5. The effect of any other noncondensable inert gas such as nitrogen and the result compared with this study.
6. The effect of pH on oil recovery when heavy oils of varying acidity are displaced by a mixture of CO₂ and steam.

REFERENCES

1. Konopnicki, D. T., Traversen E. F., Brown, A., Deibert, A.D. Design and evaluation of the shiells canyon field steam distillation drive pilot project. J.P.T., May, 1979, pp. 546-552.
2. Welker, J.R. and Dunlop, D.D. Physical properties of carbonated oils. J.P.T., Aug. 1963, pp. 873-876.
3. Pursley, S.A. Experimental study of thermal recovery processes. Paper presented at Heavy Oil Symposium, Univ. of Zulia, Maracaibo, Vanezuela, July 1974.
4. Weinstein, H.G. Mathematical models for thermal recovery processes. Paper presented at Heavy Oil Symposium, Univ. of Zulia, Marcaibo, Venezuela, July 1974.
5. Redford, D.A. The use of solvents and gases with steam in the recovery of bitumen from oil sands. J. Cdn. Pet. Tech. Jan. 1982, pp. 45-53.
6. Lo H.Y. and Mungan N. Effect of temperature on water-oil relative permeabilities in oil-wet and water-wet systems. Annual Fall meeting of Soc. of Petroleum Engineers. SPE, paper 4505, Oct. 1973.
7. Poston, S.M. et al. The effect of temperature on irreducible water saturation and relative permeability of unconsolidated sands. Trans., AIME 1970, 249, pp. 171-180.
8. Weinbrandt, R.M. and Ramey, H.J. Jr. The effect of temperature on relative permeability of consolidated rocks. Annual fall meeting of Soc. Petroleum Engrs., SPE paper 4142, Oct. 1972.
9. Bucher, C.E. and Parkhurst, I.P. Effect of dissolved gas upon the viscosity and surface tension of crude oil. Trans., AIME(1926) G 26, pp. 51-69.
10. Russell, W.J. Art of Extracting Hydrocarbons from oil-bearing strata. U.S. Patent no. 1, 658,305 (1928).

11. Clark, N.J. et al. Miscible Drive - Its theory and application. J. Pet. Tech. June (1958), pp.11-23.
12. Holm, L.W. and O'Brien, L.J. Carbon Dioxide test at the Mead-Strawn Field. J. Pet. Tech. April (1971), pp. 431-42.
13. Holm, L.W. CO₂ slug and carbonated water oil recovery process. Prod. monthly Sept. (1963) p. 6.
14. Holm L.W. and Josendal, V.A. Mechanisms of oil displacement by Carbon Dioxide. J.P.T. Dec. (1974), pp. 1427-1436.
15. Cronquist, C. Carbon Dioxide dynamic miscibility with light reservoir oils. Proc. 4th annual DOE Symposium, Tulsa (1978), IB, C5.
16. Holm, L.W. and Josendal, V.A. Discussion of determination and prediction of the CO₂ minimum miscibility pressures. J.P.T. May (1980) pp. 870-71.
17. Yelling, W.F. and Metcalfe, R.S. Determination and prediction of the CO₂ minimum miscibility pressures. J.P.T. Jan. (1980) pp. 160-68.
18. Holm, L.W. and Josendal, V.A. Effect of oil composition on miscible-type displacement by Carbon Dioxide. Soc. Pet. Eng. Feb. (1982) pp. 87-98.
19. Heller and Taber. Mobility control for CO₂ floods - A literature study, DOE/MC/10689-3. New Mexico Petroleum recovery research center, Oct. (1980).
20. Willman, B. T. et al. Laboratory studies of oil recovery by steam injection. J. Pet. Tech., July (1961) pp. 681-690.
21. Marx, J.W. and Langenheim, R.H. Reservoir heating by hot fluid injection. Trans., AIME (1959) pp. 216-312.
22. Lauwerier, H.A. The Transport of heat in an oil layer caused by the injection of hot fluid. Appl. Sci. Res., A-5 (1955) p. 145.
23. Spillette, A. G. Heat transfer during hot fluid injection into an oil reservoir. J. Cdn. Pet. Tech., Oct. - Dec. (1965) pp. 213-217.
24. Thomas, G.W. Approximate Methods for calculating the temperature distribution during hot fluid injection. J. Cdn. Pet. Tech. Oct. - Dec. (1967), pp. 123-129.

25. Mandl, G. and Volek, C.W. Heat and mass transport in steam-drive processes. Soc. Pet. Eng. J., March (1969) 59-79.
26. Gotfried, B.S. A mathematical model of thermal oil recovery in linear systems. Soc. Pet. Eng. J., Sept. (1965), 196-210.
27. Farouq Ali, S.M. Effects of differences in the overburden and underburden on steamflood performance. Prod. Mon. Dec. (1966).
28. Farouq Ali, S.M. Oil recovery by steam injection. Producers publishing company, Inc., Pennsylvania (1970) 46-50.
29. Closmann, P.J. Steam zone growth during multiple layer steam injection. Soc. Pet. Eng. J., March (1967), pp. 1-10.
30. Baker, P.E. An experimental study of heat flow in steam flooding. Soc. Pet. Eng. J., March (1969), pp. 89-99.
31. Baker, P.E. Effect of pressure and rate on steam zone development in steamflooding. Soc. Pet. Eng. J., Oct. (1973) pp. 274-284.
32. Belvins, T.R. et al. Analysis of a steam drive project. Inglewood Field, California. J. Pet. Tech., Sept. (1969) 1141-50.
33. Shutler N.D. Numerical Three-phase simulation of the linear steamflood process. Soc. Pet. Eng. J., June (1969), pp. 232-46.
34. Shutler, N.D. Numerical Three-phase model of the Two-dimensional steamflood process. Soc. Pet. Eng. J. Dec. (1970) pp. 405-17.
35. Abdalla, A. and Coats, K.H. Three-phase experimental and numerical simulation study of the steamflood process. SPE paper No. 3600, presented at the 46th annual fall meeting of the Society of Petroleum Engineers, held in New Orleans, Louisiana, October 3-6, 1971.
36. Shutler, N.D. and Boberg, T.C. A One-dimensional analytical technique for predicting oil recovery by steamflooding. Soc. Pet. Eng. J. Dec. (1972), pp. 489-98.
37. Vinsome, P.K.W. A numerical description of hot water and steam drive by the finite difference method. SPE paper no. 5248, presented at the 49th annual fall meeting of the Society of Petroleum Engineers, held in Houston, Texas, Oct. 6-9, 1974.

38. Coats, K.H. et al. Three-dimensional simulation of steamflooding. Soc. Pet. Eng. J. Dec. 1974, pp. 573-92.
39. Coats, K.H. Simulation of steamflooding with distillation and solution gas. SPE paper no. 5015 presented at the 49th annual fall meeting of the Society of Petroleum Engineers, held in Houston, Texas, October 6-9, 1974.
40. Weinstein, H.G. et al. Numerical model for thermal processes. Soc. Pet. Eng. J. Feb., 1977, pp. 65-75.
41. Neuman, C.H. A mathematical model of the steam drive process-applications. SPE paper no. 4757, presented at the 45th annual California, regional meeting, held in Ventura, California, April 2-4, 1975.
42. Miller, C.A. Stability of moving surfaces in fluid systems with heat and mass transport. AIChE journal May, 1975, pp. 474-78.
43. Van Looeren, J. Calculation methods for linear radial steam flow in oil reservoirs. SPE paper no. 6788, presented at the 52nd annual fall technical conference and exhibition of the Society of Petroleum Engineers, held in Denver, Colorado, Oct. 9-12, 1977.
44. Dupuit, J. Etudes theoriques et pretiques sur le mouvement des eaux. Dumod, Paris, 1963.
45. Rhee, S.W. and Doscher, T. M. A method for predicting oil recovery by steamflooding including the effects of distillation and gravity override. Soc. Pet. Eng. J., Aug. 1980, pp. 249-66.
46. Higgins, R.B. and Leighton, A. J. Waterflood performance in stratified reservoirs. R 15618, USBM (1960).
47. Myhill, N.A. and Stegemeier, G.L. Steam Drive Correlation and prediction. J. Pet. Tech., Feb. (1978), pp. 173-82.
48. Ferrer, J. and Farouq Ali, S.M. A Three-phase, Two-dimensional computational thermal simulator for steam injection processes. J. Cdn. Pet. Tech., Jan. (1977), pp. 78-90.
49. Gomaa, Ezzat E. Correlations for predicting oil recovery by steamflood. J.P.T., Feb. (1980), pp. 325-332.
50. Yortsos, Y.C. and Gavalas, G.R. Analytical modeling of oil recovery by steam injection. Soc. Pet. Eng. J. April (1981), pp. 162-90.

51. Yortosos, Y. C. Distribution of fluid phases within the steam zone in steam-injection processes. J. Pet. Tech. Aug. (1984), pp. 458-466.
52. Jeff Jones. Steam Drive model for hand-held programmable calculators. J. Pet. Tech., Sept. (1981) pp. 1583-1598.
53. Moughamian, J. M., Woo, P. T., Dakessian, B. A. & Fitzgerald, J. G. Simulation and design of steam drive in a vertical reservoir. J. Pet. Tech., July (1982), pp. 1546-1554.
54. Krueger, D. A. Stability of piston-like displacements of water by steam and Nitrogen in porous media. SPEJ Oct. (1982), pp. 625-634.
55. Closmann, P. J. and Seba, R. D. Laboratory tests on heavy recovery by steam injection. SPEJ, June (1983), pp. 417-426.
56. Leung, Louis C. Numerical evaluation of the effect of simultaneous steam and Carbon Dioxide injection on the recovery of heavy oil. JPT, Sept. (1983), pp. 1591-1599.
57. Wu, Ching H. A critical review of steamflood mechanisms. Paper SPE 6550 presented at the 47th annual California regional meeting, Bakerfield, April, 13-15, 1977.
58. Poston et al. The effect of temperature on irreducible water saturation and relative permeability of unconsolidated sands. SPEJ, June (1970), pp. 171-180.
59. Edmondson, J. A. Effect of temperature on waterflooding. J. Cdn. Pet. Tech. (1965), Vol. 4, 236.
60. Weinbrandt et al. The effect of temperature on relative and absolute permeability of sandstones. SPEJ, Oct. (1975), pp. 376-384.
61. Davidson, L. B. The effect of temperature on the permeability ratio of different fluid pairs in two phase system. JPT, Aug. (1969), pp. 1037-1046.
62. Geertsma, J., Croes, G.A. and Schwarz, N. Theory of dimensionally scaled models of petroleum reservoirs. Trans., AIME (1956), pp. 207, 118-127.
63. Van Daalen, F. and Van Domselaar, H.R. Scaled fluid flow models with geometry differing from that of prototype. Soc. Pet. Eng. J., June (1972), pp. 220-28.
64. Niko, H. and Troost, P.J.P.M. Experimental investigation of steam soaking in a depletion-type reservoir. J. Pet. Tech., Aug. (1971), pp. 1006-1014.

65. Stegemeier et al. Representing Steam Processes with Vacuum Models. Soc. Pet. Eng. J., June (1980), pp. 151-174.
66. K.c. Hong and J.W. Ault. Effects of Noncondensable Gas Injection on Oil Recovery by Steamflooding. J. Pet. Tech. Dec. (1984) pp. 2160-2170.
67. Holm, L.W. and Josendal, V.A. Effect of Oil Composition on Miscible-Type Displacement by Carbon Dioxide. Soc. Pet. Eng. J., Feb. (1982), pp. 87-98.
68. Mungan, N. Carbon Dioxide Flooding-Fundamentals. J. Cdn. Pet. Tech. Jan.-March (1981), pp. 87-92.
69. NRL Chart for Temperature Variation of Crude Oil Viscosity. Feb. 9, 1959, McGraw-Hill, Inc.
70. Todd M. Doscher et al. Steam Drive Definition and Enhancement. J. Pet. Tech. July (1982), pp. 1543-1545.
71. John S. Miller and Ray A. Jones. A Laboratory Study to Determine Physical Characteristics of Heavy Oil After CO₂ Saturation. U.S. Dept. of Energy January (1984) p. 44.

NOMENCLATURE

Symbol	Description	Units
A	Area.....	ft^2
C	Compressibility	psi^{-1}
C	Concentration.....	lb_m/ft^3
C_{CO_2}	Carbon dioxide concentration.....	$\frac{\text{lb}_m \text{ mole}}{\text{lb}_m \text{ mole}}$
C	Isobaric specific heat	$\text{Btu}/\text{lb}_m\text{-}^\circ\text{F}$
C_o	Isobaric specific heat of oil	$\text{Btu}/\text{lb}_m\text{-}^\circ\text{F}$
C_w	Isobaric specific heat of water	$\text{Btu}/\text{lb}_m\text{-}^\circ\text{F}$
C_v	Heat capacity at constant volume	$\text{Btu}/\text{lb}_m\text{-}^\circ\text{F}$
C_σ	Isobaric specific heat of solids in reservoir matrix.....	$\text{Btu}/\text{lb}_m\text{-}^\circ\text{F}$
d	Grain diameter.....	cm
D	Dispersion co-efficient.....	ft^2/D
D_M	Molecular diffusivity.....	ft^2/D
e	Internal energy per unit mass.....	Btu/lb_m
erfc (x)	Complementary error function	
E_c	Fraction of oil displaced that is produced	dimensionless
E_h	Heat efficiency, the fraction of the injec- ted heat present in the reservoir.....	dimensionless

$E_{h,s}$	Steam zone heat efficiency.....dimensionless
f_{hv}	Fraction of heat injected in vapor form.....dimentionless
f_s	Steam qualitydimensionless
g	Acceleration due to gravityft/sec. ²
h	Enthalpy per unit mass.....Btu/lb _m
h	Reservoir thicknessft.
h_n	Net reservoir thickness.....ft.
h_t	Gross reservoir thickness.....ft.
i	Injection ratebbl/D
k	Permeability.....md
k_h	Thermal conductivity.....Btu/ft-D-°F
k_r	Relative permeabilitydimensionless
k_{oj}	Equilibrium ratios..... $\frac{lb_m \text{ mole}}{lb_m \text{ mole}}$
L	Length of distanceft.
L_v	Latent heat per unit massBtu/lb _m
m	Arbitrary variable.....dimensionless
m	Mass.....lb _m
M	Molecular weight.....lb _m /lb-mole
M	Volumetric isobaric heat capacity (C).....Btu/ft ³ -°F
M_R	Volumetric heat capacity of reservoirBtu/ft ³ -°F
M_s	Volumetric heat capacity of steamBtu/ft ³ -°F
M_S	Volumetric heat capacity of surrounding.....Btu/ft ³ -°F formation.....

n_c	Number of components	
x_n	Distance, direction normal to boundary.....ft.	
N_p	Cumulative oil production.....	bbl
N_{Re}	Reynolds number	dimensionless
p	Pressure	Psi
$\frac{\partial p}{\partial n}$	Pressure gradient normal to displacement.... front.....	$\frac{\text{Psi}}{\text{ft.}}$
$P_{c,og}$	Capillary pressure between oil and gas phase..	Psi
$P_{c,wo}$	Capillary pressure between water and oil..... phase.....	Psi
q	Production rate, flow rate.....	bbl/D
q	Conductive heat flux.....	
Q	Amount of heat in reservoir	Btu
\dot{Q}	Rate of energy input from sources.....	Btu/D
r	radius.....	ft.
R	Recovery.....	%OOIP
R_s	Solution gas oil ratio.....	M_{scf}/bbl
S	Saturation.....	dimensionless
t	time	D
t_{cD}	Dimensionless critical time.....	
T	Temperature.....	$^{\circ}\text{F}$
u	Volumetric flux.....	$\frac{\text{ft}^3}{\text{ft}^2\text{-D}}$
v	Fluid velocity	ft/D
v	Specific volume	$\frac{\text{ft}^3}{\text{lb}_m}$

V	Volume	ft ³
V _s	Steam zone volume.....	ft ³
W	Mass rate of flow.....	lb _m /D
x,y	Co-ordinate distances.....	ft.
Z	Co-ordinate distance normal to bedding plane.	ft.
Z _t	Reservoir thickness normal to bedding plane.	ft.
x	Thermal diffusivity.....	ft ² /D
(m)	Function equal to ratio of values of its argument (m) in the prototype to that in the model.....	dimensionless
γ	Specific gravity.....	dimensionless
Δ()	Increment or decrement in ().....	
μ	Viscosity.....	CP
ρ	Density.....	lb _m /ft ³
φ	Porosity.....	

SUBSCRIPTS

a	Aqueous phase; apparent or effective
b	Bulk; bottom hole
c	Cap or base rock; Critical; Capillary (with pressure)
C	Component
CO ₂	Carbon dioxide
D	Dimensionless
e	Energy
eq	Equivalent
f	Fluid
g	Gas, gas phase, gaseous phase

gr	Grain
i	Initial; Injection
inj	Injection
j	index ($j=1,2,3,\dots$); phase (oil, water or gas)
lb	Lateral boundary
m	Movable saturation
M	Model
n	Normal to boundary
O	Oil
ors	Residual oil saturation
p	Produced
p	prototype; phase
r	Reservoir rock; relative (with k)
R	Reference quantity used to obtain dimensionless number
s	Steam
Sat	Saturation temperature or pressure
Sc	Standard conditions
t	Total interval
ub	Upper or lower boundary
v	Vaporization (with latent heat)
w	Water
Wc	Connate water (irreducible water)

APPENDIX A
PROPERTIES OF OIL AND POROUS MEDIA

TABLE A-1

CRUDE OIL PHYSICAL PROPERTIES

<u>Oil Gravity at 70°F (°API)</u>	<u>Temperature (°F)</u>	<u>Viscosity (CP)</u>
15	70	1950
	150	100
	200	41
<hr/>		
20	70	170
	150	22
	200	11
<hr/>		
26	70	43
	150	10
	200	5.4

TABLE A2

MINERAL CONTENT BY PERCENT WEIGHT OF THE POROUS MEDIA
(HALLIBURTON 20-40 FRAC SAND)

<u>MINERAL</u>	<u>WEIGHT PERCENT</u>
QUARTZ	98.5
FELDSPAR	1.0
CLAYS	0.5
Fe, Mg, Al & Ti	0.2

APPENDIX B1
SUMMARY OF DISPLACEMENT TEST RESULTS
(PHASE 1)

LEGEND FOR TABLES B12 THROUGH B47

Column

- 1 = Volume of steam injected (water eq.) cc.
- 2 = Oil produced cc.
- 3 = Cumulative volume of steam injected
(cum. water eq.) cc.
- 4 = Cumulative oil produced cc.
- 5 = Cumulative oil produced % of OOIP.

TABLE B11

PROPERTIES OF THE SANDPACK AND FLUIDS

Oil gravity = 20°API
 CO₂/Steam ratio = 0
 Steam injection rate = 30 cc./min.

RUN NO.	P.V. cc.	N cc.	SO _i	T _s °F
1	1021	831	.813	300
2	1034	833.4	.806	350
3	1035	833.2	.805	400
4	1019	818.3	.803	450
5	1027	803.0	.782	500
6	1035	833.4	.805	550

TABLE B-12: DISPLACEMENT TEST RESULTS

(RUN 1)

1	2	3		4	5
cc	cc	cc	PV		
500	135	500	0.49	135	0.162
500	90	1000	0.98	225	0.27
500	90	1500	1.47	315	0.378
500	55	2000	1.96	370	0.444
500	70	2500	2.45	440	0.528
1000	85	3500	3.43	525	0.63
1000	55	4500	4.41	580	0.696
1000	40	5500	5.39	620	0.744
1000	30	6500	6.37	650	0.480
1000	10	7500	7.35	660	0.792

TABLE B-13: DISPLACEMENT TEST RESULTS (RUN 2)

	1	2	3		4	5
	cc	cc	cc	PV		
	500	125	500	.48	125	0.15
	500	95	1000	.97	220	0.264
	500	75	1500	1.45	295	0.354
	500	75	2000	1.93	370	0.444
	500	70	2500	2.42	440	0.528
	1000	80	3500	3.38	520	0.624
	1000	55	4500	4.35	575	0.69
	1000	40	5500	5.32	615	0.738
	1000	20	6500	6.29	635	0.762
	1000	5	7500	7.25	640	0.768

TABLE B-14: DISPLACEMENT TEST RESULTS (RUN 3)

	1	2	3		4	5
	cc	cc	cc	PV		
135	720	168	720	.7	168	.201
	500	78	1220	1.18	246	.295
	500	74	1720	1.66	320	.384
	500	60	2220	2.14	380	.455
	500	57	2720	2.63	437	.525
	980	83	3700	3.57	520	.625
	1000	55	4700	4.54	575	.69
	1000	20	5700	5.51	595	.714
	1000	12	6700	6.47	607	.727
	1000	Trace	7700	7.44	Trace	.73

TABLE B-15: DISPLACEMENT TEST RESULTS (RUN 4)

	1	2	3		4	5
	cc	cc	cc	PV		
136	500	125	500	.49	125	.153
	500	90	1000	.98	215	.263
	500	70	1500	1.47	285	.348
	500	65	2000	1.96	350	.428
	500	45	2500	2.45	395	.483
	1000	80	3500	3.43	475	.580
	1000	50	4500	4.42	525	.641
	1000	25	5500	5.4	550	.672
	1000	5	6500	6.38	555	.678
	1000	-	7500	7.36	-	-

TABLE B-16: DISPLACEMENT TEST RESULTS (RUN 5)

1	2	3		4	5
cc	cc	cc	PV		
500	115	500	0.49	115	.143
500	85	1000	0.97	200	.249
500	75	1500	1.46	275	.342
500	55	2000	1.95	330	.41
500	45	2500	2.43	375	.467
1000	80	3500	3.41	455	.567
1000	45	4500	4.38	500	.623
1000	20	5500	5.36	520	.647
1000	5	6500	6.33	525	.653
1000	-	7500	7.3	-	-

TABLE B-17: DISPLACEMENT TEST RESULTS

(RUN 6)

1	2	3		4	5
cc	cc	cc	PV		
500	135	500	0.48	135	0.162
500	80	1000	0.97	215	0.258
500	70	1500	1.45	285	0.342
500	50	2000	1.93	335	0.402
500	50	2500	2.41	385	0.462
1000	75	3500	3.38	460	0.552
1000	40	4500	4.35	500	0.6
1000	20	5500	5.31	520	0.624
1000	5	6500	6.28	525	0.63
1000	-	7500	7.25	-	-

APPENDIX B2
SUMMARY OF DISPLACEMENT TEST RESULTS
(PHASE 2)

TABLE B-21

PROPERTIES OF THE SANDPACK AND FLUIDS

Oil gravity = 20°API
 CO₂/steam ratio = .002 scF/cc steam inj.
 Steam injection rate = 30 cc/min. water eq.

Run no.	P.V.	N	S _{oi}	T _s
	cc.	cc		°F
7	1031	833.36	.8083	300
8	1027	833.3	.8114	350
9	1032	818.4	.793	400
10	1023	818.4	.80	450
11	1019	787.9	.7732	500
12	1030	803.1	.7797	550

TABLE B-22: DISPLACEMENT TEST RESULTS (RUN 7)

	1	2	3		4	5
	cc	cc	cc	PV		
141	500	145	500	0.48	145	0.174
	500	140	1000	0.97	285	0.342
	500	100	1500	1.45	385	0.462
	500	75	2000	1.94	460	0.552
	500	55	2500	2.42	515	0.618
	1000	85	3500	3.39	600	0.72
	1000	40	4500	4.36	640	0.768
	1000	25	5500	5.33	665	0.798
	1000	10	6500	6.3	675	0.81
	1000	-	7500	7.27	-	-

TABLE B-23: DISPLACEMENT TEST RESULTS

(RUN 8)

1	2	3		4	5
cc	cc	cc	PV		
500	140	500	0.49	140	0.168
500	130	1000	0.97	270	0.324
500	105	1500	1.46	375	0.45
500	65	2000	1.95	440	0.528
500	70	2500	2.43	510	0.612
1000	70	3500	3.41	580	0.696
1000	45	4500	4.38	625	0.75
1000	25	5500	5.36	650	0.78
1000	5	6500	6.33	655	0.786
1000	-	7500	7.3	-	-

142

TABLE B-24: DISPLACEMENT TEST RESULTS (RUN 9)

	1	2	3		4	5
	cc	cc	cc	PV		
143	500	120	500	0.48	120	0.145
	500	105	1000	0.97	225	0.275
	480	110	1480	1.43	335	0.41
	500	90	1980	1.92	425	0.52
	1000	98	2980	2.89	523	0.64
	1000	48	3980	3.86	571	0.7
	990	33	4970	4.82	604	0.74
	1000	10	5970	5.78	614	0.75
	1000	-	6970	6.75	-	-
	1000	-	7970	7.72	-	-

TABLE B-25: DISPLACEMENT TEST RESULTS

(RUN 10)

	1	2	3		4	5
	cc	cc	cc	PV		
144 771	500	127	500	0.49	127	0.155
	500	120	1000	0.98	247	0.3
	500	105	1500	1.47	352	0.43
	500	60	2000	1.96	412	0.5
	500	60	2500	2.44	472	0.577
	1000	50	3500	3.42	522	0.638
	1000	35	4500	4.4	557	0.68
	1000	15	5500	5.38	572	0.699
	1000	5	6500	6.35	577	0.705
	1000	-	7500	7.33	-	-

TABLE B-26: DISPLACEMENT TEST RESULTS (RUN 11)

	1	2	3		4	5
	cc	cc	cc	PV		
145	500	125	500	0.49	125	0.159
	500	115	1000	0.98	240	0.305
	500	95	1500	1.47	335	0.425
	500	70	2000	1.96	405	0.514
	500	40	2500	2.45	445	0.565
	1000	40	3500	3.43	485	0.616
	1000	35	4500	4.42	520	0.66
	1000	10	5500	5.4	530	0.673
	1000	5	6500	6.38	535	0.679
	1000	-	7500	7.36	-	-

TABLE B-27: DISPLACEMENT TEST RESULTS

(RUN 12)

	1	2	3		4	5
	cc	cc	cc	PV		
146	500	135	500	0.485	135	0.168
	500	135	1000	0.97	270	0.336
	500	80	1500	1.46	350	0.436
	500	65	2000	1.94	415	0.498
	500	45	2500	2.43	460	0.552
	1000	70	3500	3.4	510	0.612
	1000	30	4500	4.37	540	0.648
	1000	15	5500	5.34	555	0.666
	1000	5	6500	6.31	560	0.672
	1000	-	7500	7.28	-	-

TABLE B-31

PROPERTIES OF THE SANDPACK AND FLUIDS

Oil Gravity = 20° API

CO₂/steam ratio = .004 scF/cc. steam injected

Steam injection rate = 30 cc/min. water eq.

Run no.	P.V.	N	S _{oi}	T _s
	cc.	cc.		°F
13	1026	833.3	.8122	300
14	1023	848.5	.8294	350
15	1030	818.2	.7944	400
16	1021	787.9	.7717	450
17	1029	833,4	.81	500
18	1018	787.9	.774	550

TABLE B-32: DISPLACEMENT TEST RESULTS (RUN 13)

	1	2	3		4	5
	cc	cc	cc	PV		
148	500	210	500	0.49	210	.252
	500	180	1000	0.97	390	.468
	500	125	1500	1.46	515	.618
	500	60	2000	1.95	575	.69
	500	30	2500	2.44	605	.726
	1000	45	3500	3.41	650	.78
	1000	25	4500	4.39	675	.81
	1000	5	5500	5.36	680	.816
	1000	-	6500	6.33	-	-
	1000	-	7500	7.31	-	-

TABLE B-33: DISPLACEMENT TEST RESULTS (RUN 14)

1	2	3		4	5
cc	cc	cc	PV		
500	210	500	0.49	210	.247
500	195	1000	0.98	405	.477
500	120	1500	1.47	525	.619
500	60	2000	1.96	585	.689
500	25	2500	2.44	610	.719
1000	45	3500	3.42	655	.772
1000	20	4500	4.4	675	.795
1000	5	5500	5.38	680	.801
1000	-	6500	6.35	-	-

TABLE B-34: DISPLACEMENT TEST RESULTS (RUN 15)

	1	2	3		4	5
	cc	cc	cc	PV		
150	500	200	500	0.485	200	.245
	500	175	1000	0.97	375	.458
	500	105	1500	1.46	480	.587
	500	50	2000	1.94	530	.648
	500	35	2500	2.43	565	.69
	1000	35	3500	3.4	600	.730
	1000	20	4500	4.37	620	.758
	1000	10	5500	5.34	630	.77
	1000	-	6500	6.31	-	-

TABLE B-35: DISPLACEMENT TEST RESULTS

(RUN 16)

1	2	3	4	5
cc	cc	cc	PV	
500	180	500	0.49	180
500	160	1000	0.98	340
500	120	1500	1.47	460
500	30	2000	1.96	490
500	35	2500	2.45	525
1000	30	3500	3.43	555
1000	20	4500	4.41	575
1000	5	5500	5.39	580
1000	-	6500	6.37	-

TABLE B-36: DISPLACEMENT TEST RESULTS (RUN 17)

1	2	3		4	5
cc	cc	cc	PV		
500	185	500	0.49	185	.222
500	175	1000	0.97	360	.432
500	105	1500	1.46	465	.558
500	45	2000	1.94	510	.612
500	35	2500	2.43	545	.654
1000	35	3500	3.4	580	.696
1000	10	4500	4.37	590	.71
1000	5	5500	5.34	595	.714
1000	-	6500	6.32	-	-

TABLE B-37: DISPLACEMENT TEST RESULTS (RUN 18)

	1	2	3		4	5
	cc	cc	cc	PV		
153	500	230	500	0.49	230	.292
	500	160	1000	0.98	390	.495
	500	65	1500	1.47	455	.577
	500	25	2000	1.96	480	.609
	500	30	2500	2.46	510	.647
	1000	25	3500	3.44	535	.679
	1000	10	4500	4.42	545	.692
	1000	5	5500	5.40	550	.698
	1000	-	6500	6.38	-	-

TABLE B-41
PROPERTIES OF THE SANDPACK AND FLUIDS

Oil gravity = 20°API
CO₂/steam ratio = .006 scF/cc. steam injected
Steam injection rate = 30 cc./min. water eq.

Run no.	P.V. cc.	N cc.	S _{oi}	T _s °F
19	1033	803	.7774	300
20	1026	803	.7827	350
21	1033	818.1	.792	400
22	1029	803	.7804	450
23	1031	833.3	.8083	500
24	1022	803	.7858	550

TABLE B-42: DISPLACEMENT TEST RESULTS

(RUN 19)

	1	2	3		4	5
	cc	cc	cc	PV		
155	500	170	500	0.48	170	.212
	500	150	1000	0.97	320	.398
	500	100	1500	1.45	420	.523
	500	85	2000	1.94	505	.629
	500	55	2500	2.42	560	.697
	1000	50	3500	3.39	610	.760
	1000	30	4500	4.36	640	.797
	1000	10	5500	5.32	650	.81
	1000	-	6500	6.29	-	-

TABLE B-43: DISPLACEMENT TEST RESULTS (RUN 20)

	1	2	3		4	5
	cc	cc	cc	PV		
156	500	160	500	0.49	160	.2
	500	155	1000	0.97	315	.392
	500	120	1500	1.46	435	.542
	500	70	2000	1.95	505	.629
	500	45	2500	2.44	550	.685
	1000	50	3500	3.41	600	.747
	1000	25	4500	4.39	625	.778
	1000	10	5500	5.36	635	.79
	1000	-	6500	6.33	-	-

TABLE B-44: DISPLACEMENT TEST RESULTS

(RUN 21)

1	2	3		4	5
cc	cc	cc	PV		
460	135	460	0.445	135	.165
500	150	960	0.93	285	.35
500	125	1460	1.41	410	.5
490	75	1950	1.89	485	.593
500	45	2450	2.37	530	.648
1000	50	3450	3.34	580	.71
1000	35	4450	4.31	615	.751
970	5	5420	5.25	620	.76
1000	-	6420	6.21	-	-

TABLE B-45: DISPLACEMENT TEST RESULTS (RUN '22)

	1	2	3		4	5
	cc	cc	cc	PV		
156	500	160	500	0.49	160	.199
	500	130	1000	0.97	290	.361
	500	115	1500	1.46	405	.504
	500	60	2000	1.94	465	.579
	500	40	2500	2.43	505	.629
	1000	50	3500	3.4	555	.691
	1000	20	4500	4.37	575	.716
	1000	5	5500	5.34	580	.722
	1000	-	6500	6.32	-	-

TABLE B-46: DISPLACEMENT TEST RESULTS

(RUN 23)

1	2	3		4	5
cc	cc	cc	PV		
500	140	500	0.48	140	.168
500	145	1000	0.97	285	.342
500	125	1500	1.45	410	.492
500	80	2000	1.94	490	.588
500	35	2500	2.42	525	.63
1000	40	3500	3.39	565	.678
1000	15	4500	4.36	580	.696
1000	5	5500	5.33	585	.702
1000	-	6500	6.3	-	-

TABLE B-47: DISPLACEMENT TEST RESULTS

(RUN 24)

	1	2	3		4	5
	cc	cc	cc	PV		
160	500	200	500	0.49	200	.249
	500	145	1000	0.98	345	.43
	500	80	1500	1.47	425	.51
	500	40	2000	1.96	465	.579
	500	30	2500	2.45	495	.616
	1000	35	3500	3.43	530	.66
	1000	20	4500	4.40	550	.685
	1000	5	5500	5.38	555	.69
	1000	-	6500	6.36	-	-

APPENDIX C
SUMMARY OF DISPLACEMENT TEST RESULTS
(PHASE 3)

PHASE 3

TABLE C-11

PROPERTIES OF THE SANDPACK AND FLUIDS

Oil Gravity = 20° API

CO₂/steam ratio = .004 scF/cc steam injected

T_s = 400°F

Run no.	steam injection rate water eq. cc/min.	P.V.	N	S _{oi}
25	15	1027	803	.782
26	45	1023	818.4	.786
27	60	1026	803	.783

TABLE C-12 DISPLACEMENT TEST RESULTS (RUN 25)

	1	2	3		4	5
	cc	cc	cc	PV		
	500	150	500	0.49	135	.168
	500	130	1000	0.97	240	.299
	500	95	1500	1.46	335	.417
	500	65	2000	1.95	410	.510
	500	45	2500	2.43	460	.573
	1000	55	3500	3.41	525	.654
	1000	30	4500	4.38	560	.697
	1000	10	5500	5.36	580	.722
	1000	10	6500	6.33	585	.729
	1000	-	7500	7.3	-	-

TABLE C-13 DISPLACEMENT TEST RESULTS (RUN 26)

1	2	3		4	5
cc	cc	cc	PV		
500	160	500	0.49	160	.196
500	140	1000	0.97	300	.367
500	110	1500	1.46	410	.501
500	65	2000	1.95	475	.58
500	50	2500	2.43	525	.641
1000	55	3500	3.41	580	.710
1000	25	4500	4.38	605	.739
1000	10	5500	5.36	615	.751
1000	-	6500	6.35	-	-

TABLE C-14: DISPLACEMENT TEST RESULTS

(RUN 27)

1	2	3		4	5
cc	cc	cc	PV		
500	135	500	0.49	135	.168
500	130	1000	0.97	265	.330
500	105	1500	1.46	370	.461
500	75	2000	1.95	445	.554
500	45	2500	2.43	490	.610
1000	55	3500	3.41	545	.679
1000	20	4500	4.38	565	.704
1000	-	5500	5.36	-	-

APPENSIX D
SUMMARY OF DISPLACENT TEST RESULTS
(PHASE 4)

TABLE D-11
PROPERTIES OF THE SANDPACK AND FLUIDS

Steam injection rate = 30 cc/min. (water eq.)

T_s = 400°F

Run no.	CO ₂ /steam ratio scF/CO ₂ / steam cc.	P.V. cc	N cc	S _{oi}	Oil gravity API
28	0	1030	828.57	.8044	15
29	.002	1025	828.57	.808	15
30	.004	1027	828.57	.807	15
31	.006	1033	828.57	.802	15
32	0	1013	726.32	.717	26
33	.002	1009	708.3	.702	26
34	.004	1013	717.2	.708	26
35	.006	1014	701.7	.692	26

TABLE D-12: DISPLACEMENT TEST RESULTS

(RUN 28)

1	2	3		4	5
cc	cc	cc	PV		
500	80	500	0.48	80	.0965
500	55	1000	0.97	135	.1630
500	50	1500	1.46	185	.2232
500	45	2000	1.94	230	.2776
500	35	2500	2.43	265	.3198
1000	65	3500	3.4	330	.3983
1000	45	4500	4.37	375	.4526
1000	25	5500	5.34	400	.4827
1000	30	6500	6.31	430	.5189
1000	15	7500	7.28	445	.5371
1000	5	8500	8.25	450	.5431

TABLE D-13: DISPLACEMENT TEST RESULTS

(RUN 29)

1	2	3		4	5
cc	cc	cc	PV		
500	100	500	0.49	100	.1207
500	95	1000	0.98	195	.2353
500	75	1500	1.46	270	.3259
500	50	2000	1.95	320	.3862
500	30	2500	2.44	350	.4224
1000	50	3500	3.41	400	.4827
1000	35	4500	4.39	435	.5250
1000	20	5500	5.37	455	.5491
1000	15	6500	6.34	470	.5672
1000	5	7500	7.32	475	.5732
1000	-	8500	8.29	-	-

TABLE D-14: DISPLACEMENT TEST RESULTS (RUN 30)

	1	2	3		4	5
	cc	cc	cc	PV		
170	500	155	500	0.48	155	.1871
	500	125	1000	0.97	280	.3379
	500	75	1500	1.45	355	.4284
	500	50	2000	1.94	405	.4888
	500	25	2500	2.42	430	.519
	500	25	3000	2.90	455	.5491
	1000	35	4000	3.87	490	.591
	1000	15	5000	4.84	505	.609
	1000	10	6000	5.81	515	.621
	1000	-	7000	6.78	-	-

TABLE D-15 DISPLACEMENT TEST RESULTS (RUN 31)

	1	2	3		4	5
	cc	cc	cc	PV		
	500	155	500	0.49	155	.1871
	500	100	1000	0.97	255	.3077
	500	75	1500	1.46	330	.3983
	500	45	2000	1.95	375	.4526
	500	30	2500	2.43	405	.4888
171	1000	50	3500	3.41	455	.5491
	1000	25	4500	4.38	480	.5793
	1000	15	5500	5.35	495	.5974
	1000	5	6500	6.33	500	.6034
	1000	-	7500	7.30	-	-

TABLE D-16: DISPLACEMENT TEST RESULTS

(RUN 32)

1	2	3		4	5
cc	cc	cc	PV		
500	130	500	.495	130	.179
500	110	1000	.987	240	.330
500	95	1500	1.481	335	.461
500	85	2000	1.974	420	.578
500	50	2500	2.468	470	.647
1000	65	3500	3.455	535	.737
1000	35	4500	4.442	570	.785
1000	15	5500	5.429	585	.805
1000	5	6500	6.417	590	.812
1000	-	7500	7.404	-	-

TABLE D-17: DISPLACEMENT TEST RESULTS (RUN 33)

1	2	3		4	5
cc	cc	cc	PV		
500	140	500	0.495	140	.198
500	130	1000	0.991	270	.381
500	105	1500	1.487	375	.529
500	80	2000	1.982	455	.642
500	40	2500	2.478	495	.7
1000	50	3500	3.469	545	.769
1000	25	4500	4.46	570	.805
1000	10	5500	5.451	580	.82
1000	-	6500	6.442	-	-

TABLE D-18: DISPLACEMENT TEST RESULTS (RUN 34)

	1	2	3		4	5
	cc	cc	cc	PV		
174	500	160	500	0.495	160	.223
	500	150	1000	0.987	310	.432
	500	115	1500	1.481	425	.592
	500	65	2000	1.974	490	.683
	500	40	2500	2.468	530	.739
	1000	35	3500	3.455	565	.788
	1000	15	4500	4.442	580	.81
	1000	-	5500	5.429	-	-

TABLE D-19: DISPLACEMENT TEST RESULTS (RUN 35)

	1	2	3		4	5
	cc	cc	cc	PV		
175	500	155	500	0.495	155	.221
	500	130	1000	0.987	285	.406
	500	110	1500	1.481	395	.563
	500	70	2000	1.974	465	.663
	500	40	2500	2.468	505	.720
	1000	40	3500	3.455	545	.777
	1000	15	4500	4.442	560	.798
	1000	5	5500	5.429	565	.805
	1000	-	6500	6.41	-	-

APPENDIX E
SUMMARY OF DISPLACEMENT TEST RESULTS
(PHASE 5)

TABLE E-11
PROPERTIES OF THE SANDPACK AND FLUIDS

Oil Gravity = 20° API
 Steam injection rate = 30 cc/min. (water eq.)
 Steam temperature = 400°F
 pH = 12

Run no.	CO ₂ /steam ratio scF CO ₂ /cc steam	P.V. cc	N cc	S _{oi}
36	0	1023.5	825	.806
37	.002	1026.5	826	.8046
38	.004	1025.5	826	.8052
39	.006	1021.6	814	.797

TABLE E-12: DISPLACEMENT TEST RESULTS

(RUN 36)

1	2	3		4	5
cc	cc	cc	PV		
500	125	500	0.49	125	.151
500	95	1000	0.98	220	.267
500	80	1500	1.47	300	.364
500	70	2000	1.95	370	.448
500	60	2500	2.44	430	.521
1000	90	3500	3.42	520	.630
1000	60	4500	4.4	580	.700
1000	20	5500	5.37	600	.730
1000	10	6500	6.35	610	.740
1000	-	7500	7.31	-	-

TABLE E-13: DISPLACEMENT TEST RESULTS

(RUN 37)

1	2	3		4	5
cc	cc	cc	PV		
500	125	500	0.49	125	.151
500	115	1000	0.98	240	.290
500	90	1500	1.47	330	.400
500	95	2000	1.95	425	.515
500	60	2500	2.44	485	.587
1000	75	3500	3.42	560	.678
1000	45	4500	4.40	605	.732
1000	15	5500	5.37	620	.751
1000	-	6500	6.33	-	-

TABLE E-14: DISPLACEMENT TEST RESULTS (RUN 38)

	1	2	3		4	5
	cc	cc	cc	PV		
189	500	215	500	0.49	215	.260
	500	200	1000	0.98	415	.502
	500	80	1500	1.47	495	.599
	500	45	2000	1.95	540	.654
	500	30	2500	2.44	570	.670
	1000	45	3500	3.42	615	.744
	1000	15	4500	4.4	630	.763
	1000	5	5500	5.37	635	.769
	1000	-	6500	6.34	-	-

TABLE E-15: DISPLACEMENT TEST RESULTS

(RUN 39)

	1	2	3		4	5
	cc	cc	cc	PV		
181	500	205	500	0.49	205	.200
	500	165	1000	0.98	370	.362
	500	150	1500	1.47	520	.509
	500	95	2000	1.95	615	.602
	500	65	2500	2.44	680	.666
	1000	55	3500	3.42	735	.719
	1000	30	4500	4.4	765	.749
	1000	10	5500	5.38	775	.759
	1000	-	6500	6.36	-	-

APPENDIX F
SUMMARY OF TEMPERATURE DISTRIBUTION
RESULTS WITH DISTANCE

TABLE F-1: TEMPERATURE DISTRIBUTION WITH DISTANCE.

RUN #	TIME HOURS	DISTANCE FROM INLET, INCHES				
		0	3	7	11	19
1	1	300	300	300	245	115
	2	300	300	300	300	210
	4	300	300	300	300	260
2	1	350	350	340	270	130
	2	350	350	350	340	230
	4	350	350	350	350	280
3	1	400	400	365	290	140
	2	400	400	400	360	255
	4	400	400	400	400	325

TABLE F-2: TEMPERATURE DISTRIBUTION WITH DISTANCE.

RUN #	TIME HOURS	DISTANCE FROM INLET, INCHES				
		0	3	7	11	19
1	1	300	300	300	245	115
	2	300	300	300	300	210
	4	300	300	300	300	260
2	1	350	350	340	270	130
	2	350	350	350	340	230
	4	350	350	350	350	280
3	1	400	400	365	290	140
	2	400	400	400	360	255
	4	400	400	400	400	325

```

c      This programme calculates the temperature distribution in the
c      porous medium
c      ts=Steam injection temperature
c      rc1=Volumetric heat capacity of porous medium
c      rc2=volumetric heat capacity of surroundings
c      rcf=volumetric heat of fluids
c      rcr=volumetric heat capacity of surroundings
c      k1=Thermal conductivity of porous medium
c      k2=Thermal conductivity of surroundings
c      h=Reservoir thickness
c      t0=Initial reservoir temperature
c      z=vertical distance from center of the reservoir
      read*,rcf,rc1,rcr,k1,k2,t0,ts,rc2,h,v,z,l
      do 50 ts=300,550,50
      print*, '-----'
1-----
      print*, '          Injection Temperature= ',ts,' deg.f'
      print*, '-----'
1-----
      do 10 t=.25,4,.25
      do 20 x=.25,2,.25
      theta=rc1/rcr
      eta=4*k2*x/((h**2)*rcf*v)
      tau=4*k2*t/((h**2)*rc1)
      if((tau-eta).le.0.0) goto 10
      any=2*z/h
      a=(eta+abs(any)-1)/(2*sqrt(theta*(tau-eta)))
      xd=x/l
      temp=t0+erfc(a)*(ts-t0)

      write(6,100) t,x,xd,erfc(a),temp
100  format(3x,f5.2,3x,f10.5,3x,f10.5,3x,f10.5,3x,f10.5)
20   continue
10   continue
50   continue
      stop
      end
      function erfc(x)
      implicit real (a-h,o-z)
      a1=.254825952
      a2=-.284496736
      a3=1.421413741
      a4=-1.453152027
      a5=1.061405429

```

```

s=abs(x)
t=1./('1.+3275911*s)
if (s-1e-30) 1,2,?
1  sa=1.
   goto 3
2  sa=s/x
3  erf=t*(a1+t*(a2+t*(a3+t*(a4+a5*t))))*exp(-x*x)
   erf=sa*(1.-erf)
   erfc=1-erf
   return
end
62.4,42.45,36.3,1.4,1.4,105,400,36.3,.2215567,1.2949,.11078,2

```

t hours	x ft.	x/l	T _D	T°F

Injection Temperature=			.300000000e+03	deg.f

.25	.25000	.12500	.72976	247.30292
.50	.25000	.12500	.84462	269.70114
.50	.50000	.25000	.62518	226.91049
.50	.75000	.37500	.27285	158.20490
.75	.25000	.12500	.87975	276.55038
.75	.50000	.25000	.73317	247.96797
.75	.75000	.37500	.54964	212.17911
.75	1.00000	.50000	.31527	166.47853
.75	1.25000	.62500	.05144	115.03131
1.00	.25000	.12500	.89840	280.18863
1.00	.50000	.25000	.78166	257.42380
1.00	.75000	.37500	.64654	231.07565
1.00	1.00000	.50000	.48965	200.48256
1.00	1.25000	.62500	.30991	165.43236
1.00	1.50000	.75000	.12097	128.58916
1.00	1.75000	.87500	.00335	105.65365
1.25	.25000	.12500	.91042	232.53149
1.25	.50000	.25000	.81071	263.08844
1.25	.75000	.37500	.69962	241.42522
1.25	1.00000	.50000	.57607	217.33453
1.25	1.25000	.62500	.43988	190.77602
1.25	1.50000	.75000	.29353	162.23859
1.25	1.75000	.87500	.14746	133.75406
1.25	2.00000	1.00000	.03298	111.43024
1.50	.25000	.12500	.91893	234.20114
1.50	.50000	.25000	.83059	266.96420
1.50	.75000	.37500	.73428	248.18414
1.50	1.00000	.50000	.62972	227.79623
1.50	1.25000	.62500	.51707	205.82816
1.50	1.50000	.75000	.39749	182.50964
1.50	1.75000	.87500	.27435	158.49828
1.50	2.00000	1.00000	.15556	135.33427
1.75	.25000	.12500	.92548	285.46838
1.75	.50000	.25000	.84528	269.82980
1.75	.75000	.37500	.75918	253.04019
1.75	1.00000	.50000	.66712	235.08905
1.75	1.25000	.62500	.56936	216.02464
1.75	1.50000	.75000	.46666	195.99951
1.75	1.75000	.87500	.36076	175.34869
1.75	2.00000	1.00000	.25498	154.72093
2.00	.25000	.12500	.93063	286.47266
2.00	.50000	.25000	.85671	272.05936
2.00	.75000	.37500	.77818	256.74561
2.00	1.00000	.50000	.69510	240.54358
2.00	1.25000	.62500	.60772	223.50583

2.00	1.50000	.75000	.51656	205.74774
2.00	1.75000	.87500	.42298	187.48204
2.00	2.00000	1.00000	.32856	169.06976
2.25	.25000	.12500	.93484	287.29385
2.25	.50000	.25000	.86594	273.35800
2.25	.75000	.37500	.79330	259.69302
2.25	1.00000	.50000	.71703	244.82094
2.25	1.25000	.62500	.63740	229.29285
2.25	1.50000	.75000	.55488	213.20151
2.25	1.75000	.87500	.47025	196.69893
2.25	2.00000	1.00000	.38472	180.02010
2.50	.25000	.12500	.93837	287.98163
2.50	.50000	.25000	.87358	275.34875
2.50	.75000	.37500	.80569	262.10995
2.50	1.00000	.50000	.73493	248.29124
2.50	1.25000	.62500	.60123	233.94043
2.50	1.50000	.75000	.52531	219.13469
2.50	1.75000	.87500	.50764	203.99049
2.50	2.00000	1.00000	.42911	188.57612
2.75	.25000	.12500	.94138	288.56857
2.75	.50000	.25000	.89005	276.51047
2.75	.75000	.37500	.81609	264.13852
2.75	1.00000	.50000	.74964	251.17995
2.75	1.25000	.62500	.68092	237.77878
2.75	1.50000	.75000	.61026	224.00072
2.75	1.75000	.87500	.53815	209.93918
2.75	2.00000	1.00000	.46524	195.72246
3.00	.25000	.12500	.94399	289.07718
3.00	.50000	.25000	.88562	277.59638
3.00	.75000	.37500	.82499	265.87271
3.00	1.00000	.50000	.76222	253.53316
3.00	1.25000	.62500	.69753	241.01808
3.00	1.50000	.75000	.63120	228.08444
3.00	1.75000	.87500	.56364	214.90952
3.00	2.00000	1.00000	.49536	201.59543
3.25	.25000	.12500	.94627	289.52341
3.25	.50000	.25000	.89048	278.64389
3.25	.75000	.37500	.83270	267.37744
3.25	1.00000	.50000	.77308	255.75031
3.25	1.25000	.62500	.71179	243.79945
3.25	1.50000	.75000	.64910	231.57480
3.25	1.75000	.87500	.58534	219.14191
3.25	2.00000	1.00000	.52095	206.58463
3.50	.25000	.12500	.94830	289.91904
3.50	.50000	.25000	.89477	279.49001
3.50	.75000	.37500	.83948	268.69919
3.50	1.00000	.50000	.78257	257.50172
3.50	1.25000	.62500	.72421	246.22141
3.50	1.50000	.75000	.66463	234.50260
3.50	1.75000	.87500	.60411	222.80133
3.50	2.00000	1.00000	.54302	210.88969
3.75	.25000	.12500	.95012	290.27301

3.75	.50000	.25000	.89859	230.22504
3.75	.75000	.37500	.84550	269.87231
3.75	1.00000	.50000	.79097	259.23863
3.75	1.25000	.62500	.73515	248.35518
3.75	1.50000	.75000	.67826	237.26158
3.75	1.75000	.87500	.62055	226.00731
3.75	2.00000	1.00000	.56232	214.55289
4.00	.25000	.12500	.95175	290.59213
4.00	.50000	.25000	.90202	280.39444

4.00	.75000	.37500	.85089	270.32273
4.00	1.00000	.50000	.79846	260.69958
4.00	1.25000	.62500	.74489	250.25372
4.00	1.50000	.75000	.69036	239.52090
4.00	1.75000	.87500	.63510	228.84494
4.00	2.00000	1.00000	.57938	217.97852

Injection Temperature= .350000000e+03 deg.f

.25	.25000	.12500	.72976	283.79083
.50	.25000	.12500	.84462	311.93219
.50	.50000	.25000	.62518	258.16959
.50	.75000	.37500	.27235	171.84718
.75	.25000	.12500	.87975	320.53766
.75	.50000	.25000	.73317	284.52643
.75	.75000	.37500	.54964	239.66092
.75	1.00000	.50000	.31527	182.24231
.75	1.25000	.62500	.05144	117.60344
1.00	.25000	.12500	.39840	325.10880
1.00	.50000	.25000	.78166	296.50684
1.00	.75000	.37500	.64654	263.40274
1.00	1.00000	.50000	.48965	224.96527
1.00	1.25000	.62500	.30991	180.32783
1.00	1.50000	.75000	.12097	134.63766
1.00	1.75000	.87500	.00335	105.32125
1.25	.25000	.12500	.91042	328.05237
1.25	.50000	.25000	.81071	303.62393
1.25	.75000	.37500	.69962	276.40604
1.25	1.00000	.50000	.57607	246.13826
1.25	1.25000	.62500	.43988	212.76985
1.25	1.50000	.75000	.29353	176.31516
1.25	1.75000	.87500	.14746	141.12689
1.25	2.00000	1.00000	.03298	113.07903
1.50	.25000	.12500	.91898	330.15015
1.50	.50000	.25000	.83059	308.49350
1.50	.75000	.37500	.73428	284.89804
1.50	1.00000	.50000	.62972	259.28244
1.50	1.25000	.62500	.51707	231.63153
1.50	1.50000	.75000	.39749	202.38391
1.50	1.75000	.87500	.27435	172.21579
1.50	2.00000	1.00000	.15556	143.11229

1.75	.25000	.12500	.92548	331.74231
1.75	.50000	.25000	.84528	312.09387
1.75	.75000	.37500	.75918	290.99921
1.75	1.00000	.50000	.66712	268.44522
1.75	1.25000	.62500	.56936	244.49251
1.75	1.50000	.75000	.46666	219.33272
1.75	1.75000	.87500	.36076	193.38683
1.75	2.00000	1.00000	.25498	167.46989
2.00	.25000	.12500	.93063	333.00409
2.00	.50000	.25000	.85671	314.89508
2.00	.75000	.37500	.77818	295.65475
2.00	1.00000	.50000	.69510	275.29834
2.00	1.25000	.62500	.60772	253.89194
2.00	1.50000	.75000	.51666	231.58049
2.00	1.75000	.87500	.42298	208.63129
2.00	2.00000	1.00000	.32856	185.49789
2.25	.25000	.12500	.93484	334.03589
2.25	.50000	.25000	.86594	317.15494
2.25	.75000	.37500	.79330	299.35791
2.25	1.00000	.50000	.71703	280.57245
2.25	1.25000	.62500	.63740	261.16281
2.25	1.50000	.75000	.55488	240.94550
2.25	1.75000	.87500	.47025	220.21147
2.25	2.00000	1.00000	.38472	199.25601
2.50	.25000	.12500	.93837	334.89999
2.50	.50000	.25000	.87358	319.02792
2.50	.75000	.37500	.80569	302.39456
2.50	1.00000	.50000	.73483	285.03259
2.50	1.25000	.62500	.66123	267.00208
2.50	1.50000	.75000	.58531	248.39999
2.50	1.75000	.87500	.50764	229.37268
2.50	2.00000	1.00000	.42511	210.13153
2.75	.25000	.12500	.94138	335.63745
2.75	.50000	.25000	.88005	320.61316
2.75	.75000	.37500	.81609	304.94327
2.75	1.00000	.50000	.74564	288.66199
2.75	1.25000	.62500	.68032	271.32462
2.75	1.50000	.75000	.61026	254.51372
2.75	1.75000	.87500	.53815	236.84666
2.75	2.00000	1.00000	.46524	218.98462
3.00	.25000	.12500	.94399	336.27646
3.00	.50000	.25000	.88562	321.97751
3.00	.75000	.37500	.82499	307.12213
3.00	1.00000	.50000	.76222	291.74423
3.00	1.25000	.62500	.69753	275.89453
3.00	1.50000	.75000	.63120	259.64456
3.00	1.75000	.87500	.56364	243.09143
3.00	2.00000	1.00000	.49536	226.36348
3.25	.25000	.12500	.94627	336.83710

3.25	.50000	.25000	.89048	323.16794
3.25	.75000	.37500	.83270	309.01266
3.25	1.00000	.50000	.77308	294.40424
3.25	1.25000	.62500	.71179	279.38904
3.25	1.50000	.75000	.64910	264.02988
3.25	1.75000	.87500	.58534	248.40906
3.25	2.00000	1.00000	.52095	232.63197
3.50	.25000	.12500	.94830	337.33420
3.50	.50000	.25000	.89477	324.21848
3.50	.75000	.37500	.83948	310.67334
3.50	1.00000	.50000	.78257	296.73038
3.50	1.25000	.62500	.72421	282.43204
3.50	1.50000	.75000	.66463	267.83401
3.50	1.75000	.87500	.60411	253.00743
3.50	2.00000	1.00000	.54302	238.04089
3.75	.25000	.12500	.95012	337.77893
3.75	.50000	.25000	.89859	325.15454
3.75	.75000	.37500	.84550	312.14728
3.75	1.00000	.50000	.79097	298.78705
3.75	1.25000	.62500	.73515	285.11292
3.75	1.50000	.75000	.67826	271.17480
3.75	1.75000	.87500	.62055	257.03482
3.75	2.00000	1.00000	.56232	242.76903
4.00	.25000	.12500	.95175	338.17984
4.00	.50000	.25000	.90202	325.99557
4.00	.75000	.37500	.85089	313.46704
4.00	1.00000	.50000	.79846	300.62256
4.00	1.25000	.62500	.74489	287.49826
4.00	1.50000	.75000	.69036	274.13907
4.00	1.75000	.87500	.63510	260.60007
4.00	2.00000	1.00000	.57938	246.94736

Injection Temperature= .400000000e+03 deg.f

.25	.25000	.12500	.72976	320.27878
.50	.25000	.12500	.84462	354.16327
.50	.50000	.25000	.62518	299.42368
.50	.75000	.37500	.27285	185.48946
.75	.25000	.12500	.87975	364.52496
.75	.50000	.25000	.73317	321.28488
.75	.75000	.37500	.54964	267.14273
.75	1.00000	.50000	.31527	198.00604
.75	1.25000	.62500	.05144	120.17558
1.00	.25000	.12500	.89840	370.02896
1.00	.50000	.25000	.78166	335.58987
1.00	.75000	.37500	.64654	295.72983
1.00	1.00000	.50000	.48965	249.44798
1.00	1.25000	.62500	.30991	196.42331
1.00	1.50000	.75000	.12097	140.68617
1.00	1.75000	.87500	.00335	105.98885

1.25	.25000	.12500	.91042	373.57327
1.25	.50000	.25000	.81071	344.15942
1.25	.75000	.37500	.69962	311.33637
1.25	1.00000	.50000	.57607	274.94199
1.25	1.25000	.62500	.43988	234.76370
1.25	1.50000	.75000	.29353	191.59172
1.25	1.75000	.87500	.14746	148.49973
1.25	2.00000	1.00000	.03298	114.72781
1.50	.25000	.12500	.91898	376.09915
1.50	.50000	.25000	.83059	350.02277
1.50	.75000	.37500	.73428	321.61191
1.50	1.00000	.50000	.62972	290.76865
1.50	1.25000	.62500	.51707	257.53491
1.50	1.50000	.75000	.39749	222.25818
1.50	1.75000	.87500	.27435	185.93330
1.50	2.00000	1.00000	.15556	150.89030
1.75	.25000	.12500	.92548	378.01627
1.75	.50000	.25000	.84528	354.35791
1.75	.75000	.37500	.75918	328.95325
1.75	1.00000	.50000	.66712	301.80139
1.75	1.25000	.62500	.56936	272.96036
1.75	1.50000	.75000	.46666	242.65592
1.75	1.75000	.87500	.36076	211.42494
1.75	2.00000	1.00000	.25498	180.21884
2.00	.25000	.12500	.93063	379.53555
2.00	.50000	.25000	.85671	357.73083
2.00	.75000	.37500	.77818	334.56387
2.00	1.00000	.50000	.69510	310.05310
2.00	1.25000	.62500	.60772	284.27805
2.00	1.50000	.75000	.51666	257.41324
2.00	1.75000	.87500	.42298	229.78053
2.00	2.00000	1.00000	.32856	201.92604
2.25	.25000	.12500	.93434	380.77789
2.25	.50000	.25000	.86594	360.45184
2.25	.75000	.37500	.79330	339.02280
2.25	1.00000	.50000	.71703	316.52399
2.25	1.25000	.62500	.63740	293.03278
2.25	1.50000	.75000	.55438	268.68945
2.25	1.75000	.87500	.47025	243.72401
2.25	2.00000	1.00000	.38472	218.49193
2.50	.25000	.12500	.93837	381.81936
2.50	.50000	.25000	.87358	362.70709
2.50	.75000	.37500	.80569	342.57917
2.50	1.00000	.50000	.73433	321.77396
2.50	1.25000	.62500	.66123	300.06372
2.50	1.50000	.75000	.58531	277.56531
2.50	1.75000	.87500	.50764	254.75485
2.50	2.00000	1.00000	.42911	231.58694
2.75	.25000	.12500	.94138	382.70633
2.75	.50000	.25000	.88005	364.61584

2.75	.75000	.37500	.81609	345.74802
2.75	1.00000	.50000	.74964	326.14401
2.75	1.25000	.62500	.68092	305.87045
2.75	1.50000	.75000	.61026	285.02673
2.75	1.75000	.87500	.53815	263.75415
2.75	2.00000	1.00000	.46524	242.24678
3.00	.25000	.12500	.94399	383.47574
3.00	.50000	.25000	.88562	366.25861
3.00	.75000	.37500	.82499	348.37155
3.00	1.00000	.50000	.76222	329.85529
3.00	1.25000	.62500	.69753	310.77097
3.00	1.50000	.75000	.63120	291.20468
3.00	1.75000	.87500	.56364	271.27335
3.00	2.00000	1.00000	.49536	251.13155
3.25	.25000	.12500	.94627	384.15079
3.25	.50000	.25000	.89048	367.69202
3.25	.75000	.37500	.83270	350.64792
3.25	1.00000	.50000	.77308	333.05817
3.25	1.25000	.62500	.71179	314.97867
3.25	1.50000	.75000	.64910	296.48495
3.25	1.75000	.87500	.58534	277.67621
3.25	2.00000	1.00000	.52095	258.67932
3.50	.25000	.12500	.94830	384.74933
3.50	.50000	.25000	.89477	368.95694
3.50	.75000	.37500	.83948	352.64749
3.50	1.00000	.50000	.78257	335.85901
3.50	1.25000	.62500	.72421	318.64264
3.50	1.50000	.75000	.66463	301.06546
3.50	1.75000	.87500	.60411	283.21304
3.50	2.00000	1.00000	.54302	265.19211
3.75	.25000	.12500	.95012	385.28482
3.75	.50000	.25000	.89859	370.08405
3.75	.75000	.37500	.84550	354.42224
3.75	1.00000	.50000	.79097	338.33542
3.75	1.25000	.62500	.73515	321.87064
3.75	1.50000	.75000	.67826	305.08804
3.75	1.75000	.87500	.62055	288.06232
3.75	2.00000	1.00000	.56232	270.33516
4.00	.25000	.12500	.95175	385.76758
4.00	.50000	.25000	.90202	371.09671
4.00	.75000	.37500	.85089	356.01132
4.00	1.00000	.50000	.79846	340.54553
4.00	1.25000	.62500	.74489	324.74280
4.00	1.50000	.75000	.69036	308.65726
4.00	1.75000	.87500	.63510	292.35516
4.00	2.00000	1.00000	.57938	275.91620

Injection Temperature= .450000000e+03 deg. F

.25	.25000	.12500	.72976	356.76669
.50	.25000	.12500	.84462	396.39432
.50	.50000	.25000	.62518	320.68777
.50	.75000	.37500	.27285	199.13174
.75	.25000	.12500	.87975	408.51224

.75	.50000	.25000	.73317	357.94333
.75	.75000	.37500	.54964	294.62457
.75	1.00000	.50000	.31527	213.76978
.75	1.25000	.62500	.05144	122.74770
1.00	.25000	.12500	.89840	414.94913
1.00	.50000	.25000	.78166	374.67288
1.00	.75000	.37500	.64654	328.05695
1.00	1.00000	.50000	.49965	273.93069
1.00	1.25000	.62500	.30991	211.91879
1.00	1.50000	.75000	.12097	146.73468
1.00	1.75000	.87500	.00335	106.15646
1.25	.25000	.12500	.91042	419.09415
1.25	.50000	.25000	.81071	384.69495
1.25	.75000	.37500	.69962	346.36768
1.25	1.00000	.50000	.57607	303.74573
1.25	1.25000	.62500	.43998	256.75757
1.25	1.50000	.75000	.29353	206.26828
1.25	1.75000	.87500	.14746	155.87256
1.25	2.00000	1.00000	.03298	116.37659
1.50	.25000	.12500	.91898	422.04816
1.50	.50000	.25000	.83059	391.55206
1.50	.75000	.37500	.73423	358.32581
1.50	1.00000	.50000	.62972	322.25488
1.50	1.25000	.62500	.51707	283.38828
1.50	1.50000	.75000	.39749	242.13246
1.50	1.75000	.87500	.27435	199.65080
1.50	2.00000	1.00000	.15556	158.56833
1.75	.25000	.12500	.92543	424.29022
1.75	.50000	.25000	.84523	396.52198
1.75	.75000	.37500	.75918	366.91727
1.75	1.00000	.50000	.66712	335.15753
1.75	1.25000	.62500	.56936	301.42822
1.75	1.50000	.75000	.46656	265.99911
1.75	1.75000	.87500	.36076	229.46307
1.75	2.00000	1.00000	.25498	192.90780
2.00	.25000	.12500	.93063	426.06699
2.00	.50000	.25000	.85671	400.56656
2.00	.75000	.37500	.77818	373.47299
2.00	1.00000	.50000	.69510	344.90789
2.00	1.25000	.62500	.60772	314.66415
2.00	1.50000	.75000	.51656	283.24600
2.00	1.75000	.87500	.42298	250.92976
2.00	2.00000	1.00000	.32856	219.35419
2.25	.25000	.12500	.93484	427.51990
2.25	.50000	.25000	.86594	403.74878
2.25	.75000	.37500	.79330	378.68768
2.25	1.00000	.50000	.71703	352.37552
2.25	1.25000	.62500	.63740	324.90271
2.25	1.50000	.75000	.55488	296.43344
2.25	1.75000	.87500	.47025	267.23657
2.25	2.00000	1.00000	.38472	237.72786

2.50	.25000	.12500	.93837	428.73676
2.50	.50000	.25000	.87358	406.38623
2.50	.75000	.37500	.80569	382.96378
2.50	1.00000	.50000	.73433	358.51529
2.50	1.25000	.62500	.66123	333.12537
2.50	1.50000	.75000	.58531	306.93060
2.50	1.75000	.87500	.50764	280.13702
2.50	2.00000	1.00000	.42911	253.04234
2.75	.25000	.12500	.94139	429.77518
2.75	.50000	.25000	.88005	408.61853
2.75	.75000	.37500	.81609	386.55276
2.75	1.00000	.50000	.74964	363.62607
2.75	1.25000	.62500	.68092	339.91629
2.75	1.50000	.75000	.61026	315.53973
2.75	1.75000	.87500	.53815	290.56162
2.75	2.00000	1.00000	.46524	265.50894
3.00	.25000	.12500	.94399	430.67502
3.00	.50000	.25000	.88562	410.53973
3.00	.75000	.37500	.82499	389.62097
3.00	1.00000	.50000	.76222	367.96637
3.00	1.25000	.62500	.69753	345.64740
3.00	1.50000	.75000	.63120	322.76480
3.00	1.75000	.87500	.56364	299.45529
3.00	2.00000	1.00000	.49536	275.89960
3.25	.25000	.12500	.94627	431.46448
3.25	.50000	.25000	.89048	412.21609
3.25	.75000	.37500	.83270	392.28314
3.25	1.00000	.50000	.77308	371.71210
3.25	1.25000	.62500	.71179	350.56827
3.25	1.50000	.75000	.64910	328.94003
3.25	1.75000	.87500	.58534	306.94339
3.25	2.00000	1.00000	.52095	284.72665
3.50	.25000	.12500	.94830	432.16446
3.50	.50000	.25000	.89477	413.69540
3.50	.75000	.37500	.83948	394.62164
3.50	1.00000	.50000	.78257	374.93767
3.50	1.25000	.62500	.72421	354.85327
3.50	1.50000	.75000	.66463	334.29691
3.50	1.75000	.87500	.60411	313.41864
3.50	2.00000	1.00000	.54302	292.34329
3.75	.25000	.12500	.95012	432.79074
3.75	.50000	.25000	.89859	415.01355
3.75	.75000	.37500	.84550	396.59717
3.75	1.00000	.50000	.79097	377.88379
3.75	1.25000	.62500	.73515	358.52839
3.75	1.50000	.75000	.67826	339.00128
3.75	1.75000	.87500	.62055	319.08994
3.75	2.00000	1.00000	.56232	299.00128
4.00	.25000	.12500	.95175	433.35532
4.00	.50000	.25000	.90202	416.19785

4.00	37500	85049	352.55563
4.00	50000	79846	380.46851
4.00	1.25000	74439	361.98734
4.00	1.50000	69036	343.17545
4.00	1.75000	63510	324.11029
4.00	2.00000	57938	304.88507
2.5	25000	72976	393.25464
.50	12500	84462	438.62540
.50	25000	62518	351.94687
.50	37500	27285	212.77402
.75	12500	87975	452.49951
.75	25000	73317	394.60178
.75	37500	54564	322.10639
.75	50000	31527	229.53351
.75	1.00000	65144	125.31984
.75	1.25000	62500	125.31984
1.00	12500	89840	459.86926
1.00	25000	78166	413.75592
1.00	37500	64654	360.38403
1.00	50000	48965	298.41339
1.00	62500	30591	227.41426
1.00	75000	12097	152.78317
1.00	87500	00335	106.32406
1.25	12500	91042	464.61505
1.25	25000	81071	425.23044
1.25	37500	66962	381.34851
1.25	50000	57607	332.54944
1.25	62500	43988	278.75140
1.25	75000	29353	220.94484
1.25	87500	14746	163.24539
1.25	1.00000	03298	118.02537
1.50	12500	91898	467.99716
1.50	25000	83059	433.08133
1.50	37500	73428	395.03967
1.50	50000	62972	353.74109
1.50	62500	51707	309.24167
1.50	75000	39749	262.00671
1.50	87500	27435	213.36832
1.50	1.00000	15556	166.44635
1.75	12500	92548	470.56415
1.75	25000	84528	436.88602
1.75	37500	75918	404.87628
1.75	50000	66712	368.51370
1.75	62500	56936	329.89609
1.75	75000	46666	289.33234
1.75	87500	36076	247.50121
1.75	1.00000	25498	205.71675
2.00	12500	93063	472.59845

Injection Temperature = .50000000e+03 deg. f

2.00	.50000	.25000	.85671	443.40228
2.00	.75000	.37500	.77813	412.38214
2.00	1.00000	.50000	.69510	379.56265
2.00	1.25000	.62500	.60772	345.05026
2.00	1.50000	.75000	.51666	309.07877
2.00	1.75000	.87500	.42298	272.07901
2.00	2.00000	1.00000	.32856	234.78233
2.25	.25000	.12500	.93434	474.26193
2.25	.50000	.25000	.86594	447.04572
2.25	.75000	.37500	.79330	418.35254
2.25	1.00000	.50000	.71703	388.22702
2.25	1.25000	.62500	.63740	356.77267
2.25	1.50000	.75000	.55488	324.17743
2.25	1.75000	.87500	.47025	290.74911
2.25	2.00000	1.00000	.38472	256.96378
2.50	.25000	.12500	.93837	475.65512
2.50	.50000	.25000	.87358	450.06540
2.50	.75000	.37500	.80559	423.24838
2.50	1.00000	.50000	.73483	395.25662
2.50	1.25000	.62500	.66123	366.18701
2.50	1.50000	.75000	.58531	336.19592
2.50	1.75000	.87500	.50764	305.51923
2.50	2.00000	1.00000	.42911	274.49777
2.75	.25000	.12500	.94138	476.34406
2.75	.50000	.25000	.88005	452.62122
2.75	.75000	.37500	.81609	427.35751
2.75	1.00000	.50000	.74964	401.10809
2.75	1.25000	.62500	.68092	373.46213
2.75	1.50000	.75000	.61026	346.05273
2.75	1.75000	.87500	.53815	317.56912
2.75	2.00000	1.00000	.46524	288.77112
3.00	.25000	.12500	.94399	477.37430
3.00	.50000	.25000	.88562	454.32086
3.00	.75000	.37500	.82499	430.37039
3.00	1.00000	.50000	.76222	406.07742
3.00	1.25000	.62500	.69753	380.52383
3.00	1.50000	.75000	.63120	354.32489
3.00	1.75000	.87500	.56364	327.63721
3.00	2.00000	1.00000	.49536	300.56766
3.25	.25000	.12500	.94627	478.77817
3.25	.50000	.25000	.89048	456.74014
3.25	.75000	.37500	.83270	433.91840
3.25	1.00000	.50000	.77308	410.36600
3.25	1.25000	.62500	.71179	386.15787
3.25	1.50000	.75000	.64910	361.39511
3.25	1.75000	.87500	.58534	336.21054
3.25	2.00000	1.00000	.52095	310.77399
3.50	.25000	.12500	.94830	479.57962
3.50	.50000	.25000	.89477	453.43387
3.50	.75000	.37500	.83948	436.59579

3.50	1.00000	.50000	.75257	+14.11630
3.50	1.25000	.62500	.72421	391.05387
3.50	1.50000	.75000	.66453	367.52332
3.50	1.75000	.87500	.60411	343.62424
3.50	2.00000	1.00000	.54302	319.49451
3.75	.25000	.12500	.95012	480.29663
3.75	.50000	.25000	.86859	459.94302
3.75	.75000	.37500	.84550	438.97214
3.75	1.00000	.50000	.79097	417.43216
3.75	1.25000	.62500	.73515	395.38514
3.75	1.50000	.75000	.67626	372.91449
3.75	1.75000	.87500	.62055	350.11737
3.75	2.00000	1.00000	.56232	327.11740
4.00	.25000	.12500	.95175	480.94302
4.00	.50000	.25000	.90202	461.29398
4.00	.75000	.37500	.85089	441.09991
4.00	1.00000	.50000	.79846	420.39146
4.00	1.25000	.62500	.74489	399.23190
4.00	1.50000	.75000	.69036	377.69360
4.00	1.75000	.87500	.63510	355.86539
4.00	2.00000	1.00000	.57938	333.85391

Injection Temperature= -55000000e+03 deg. F

.25	.25000	.12500	.72976	426.74255
.50	.25000	.12500	.64492	400.85645
.50	.50000	.25000	.62518	383.20590
.50	.75000	.37500	.27285	226.41631
.75	.25000	.12500	.87975	496.48679
.75	.50000	.25000	.73217	431.26025
.75	.75000	.37500	.54964	349.59320
.75	1.00000	.50000	.31527	245.29724
.75	1.25000	.62500	.05144	127.99197
1.00	.25000	.12500	.86849	504.78943
1.00	.50000	.25000	.79166	452.33396
1.00	.75000	.37500	.64654	392.71112
1.00	1.00000	.50000	.48965	322.89612
1.00	1.25000	.62500	.30991	242.90974
1.00	1.50000	.75000	.12097	153.93163
1.00	1.75000	.87500	.00335	106.49166
1.25	.25000	.12500	.91042	510.13596
1.25	.50000	.25000	.81071	465.76593
1.25	.75000	.37500	.69662	416.32935

1.25	1.00000	.50000	.57607	361.35313
1.25	1.25000	.62500	.43988	300.74524
1.25	1.50000	.75000	.29353	235.52140
1.25	1.75000	.87500	.14746	170.61824
1.25	2.00000	1.00000	.03298	119.67415
1.50	.25000	.12500	.91898	513.94617
1.50	.50000	.25000	.83059	474.61063
1.50	.75000	.37500	.73428	431.75357
1.50	1.00000	.50000	.62972	385.22729

1.50	1.25000	.62500	.51707	335.34503
1.50	1.50000	.75000	.34749	231.28094
1.50	1.75000	.87500	.27435	227.04583
1.50	2.00000	1.00000	.15556	174.22437
1.75	.25000	.12500	.92548	516.83807
1.75	.50000	.25000	.84523	481.15009
1.75	.75000	.37500	.75918	442.83533
1.75	1.00000	.50000	.64712	401.34937
1.75	1.25000	.62500	.56936	358.36392
1.75	1.50000	.75000	.46666	312.66553
1.75	1.75000	.87500	.36076	265.53934
1.75	2.00000	1.00000	.25498	213.46571
2.00	.25000	.12500	.93063	519.12982
2.00	.50000	.25000	.85471	486.23304
2.00	.75000	.37500	.77813	451.29126
2.00	1.00000	.50000	.69510	414.31741
2.00	1.25000	.62500	.60772	375.43637
2.00	1.50000	.75000	.51666	334.91150
2.00	1.75000	.87500	.42298	293.22824
2.00	2.00000	1.00000	.32856	251.21046
2.25	.25000	.12500	.93484	521.00397
2.25	.50000	.25000	.86594	490.34262
2.25	.75000	.37500	.79330	458.01743
2.25	1.00000	.50000	.71703	424.07855
2.25	1.25000	.62500	.63740	388.04254
2.25	1.50000	.75000	.55448	351.52132
2.25	1.75000	.87500	.47025	314.26166
2.25	2.00000	1.00000	.38472	276.19971
2.50	.25000	.12500	.93837	522.57349
2.50	.50000	.25000	.87353	493.74457
2.50	.75000	.37500	.80569	463.53296
2.50	1.00000	.50000	.73483	431.99799
2.50	1.25000	.62500	.66123	399.24861
2.50	1.50000	.75000	.58531	365.46121
2.50	1.75000	.87500	.50764	330.90140
2.50	2.00000	1.00000	.42611	295.45316
2.75	.25000	.12500	.94138	523.91290
2.75	.50000	.25000	.84015	486.52390
2.75	.75000	.37500	.81609	458.16223
2.75	1.00000	.50000	.74564	438.59015
2.75	1.25000	.62500	.68092	408.00797
2.75	1.50000	.75000	.61026	376.56573
2.75	1.75000	.87500	.53815	344.47659
2.75	2.00000	1.00000	.45524	312.03329
3.00	.25000	.12500	.94399	525.07361
3.00	.50000	.25000	.84562	489.10139
3.00	.75000	.37500	.82499	472.11978
3.00	1.00000	.50000	.74222	444.16851
3.00	1.25000	.62500	.69753	415.40027
3.00	1.50000	.75000	.63120	385.88501
3.00	1.75000	.87500	.56364	355.81912
3.00	2.00000	1.00000	.49536	325.43570

3.25	.25000	.12500	.64627	526.09196
3.25	.50000	.25000	.89048	501.26422
3.25	.75000	.37500	.33270	475.55362
3.25	1.00000	.50000	.77306	449.01993
3.25	1.25000	.62500	.71179	421.74747
3.25	1.50000	.75000	.64910	393.95019
3.25	1.75000	.87500	.58534	365.47769
3.25	2.00000	1.00000	.52095	336.32132
3.50	.25000	.12500	.94630	526.39475
3.50	.50000	.25000	.89477	503.17233
3.50	.75000	.37500	.83948	478.56995
3.50	1.00000	.50000	.78257	453.24496
3.50	1.25000	.62500	.72421	427.27451
3.50	1.50000	.75000	.66463	400.75977
3.50	1.75000	.87500	.60411	373.82983
3.50	2.00000	1.00000	.54302	346.64572
3.75	.25000	.12500	.95012	527.30255
3.75	.50000	.25000	.89859	504.37253
3.75	.75000	.37500	.84550	481.24710
3.75	1.00000	.50000	.79097	456.93056
3.75	1.25000	.62500	.73515	432.14386
3.75	1.50000	.75000	.67826	406.32773
3.75	1.75000	.87500	.62055	381.14467
4.00	2.00000	1.00000	.56232	355.25355
4.00	.25000	.12500	.95175	526.53076
4.00	.50000	.25000	.90202	506.40012
4.00	.75000	.37500	.85039	483.64423
4.00	1.00000	.50000	.79846	460.31442
4.00	1.25000	.62500	.74499	436.47644
4.00	1.50000	.75000	.69036	412.21179
4.00	1.75000	.87500	.63510	387.62051
4.00	2.00000	1.00000	.57936	362.82275

APPENDIX G
PLOTS OF LABORATORY RESULTS

EFFECT OF CO₂ ON STEAM DRIVE RECOVERY

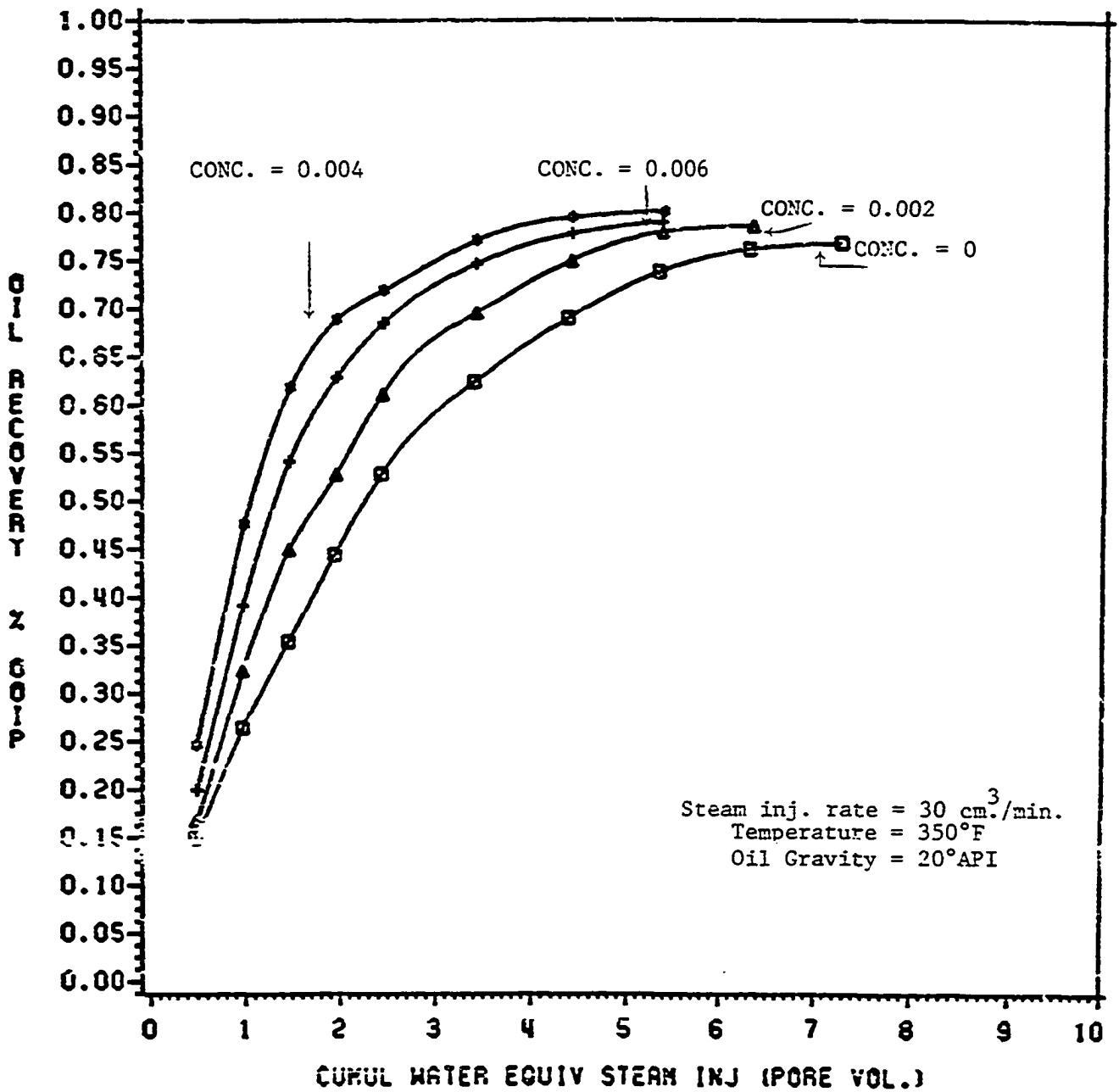


FIGURE G1: EFFECT OF CO₂ ON STEAM DRIVE RECOVERY

CONC. = CO₂/STEAM RATIO (SCF CO₂/CM³ STEAM INJ.)

EFFECT OF CO₂ ON STEAM DRIVE RECOVERY

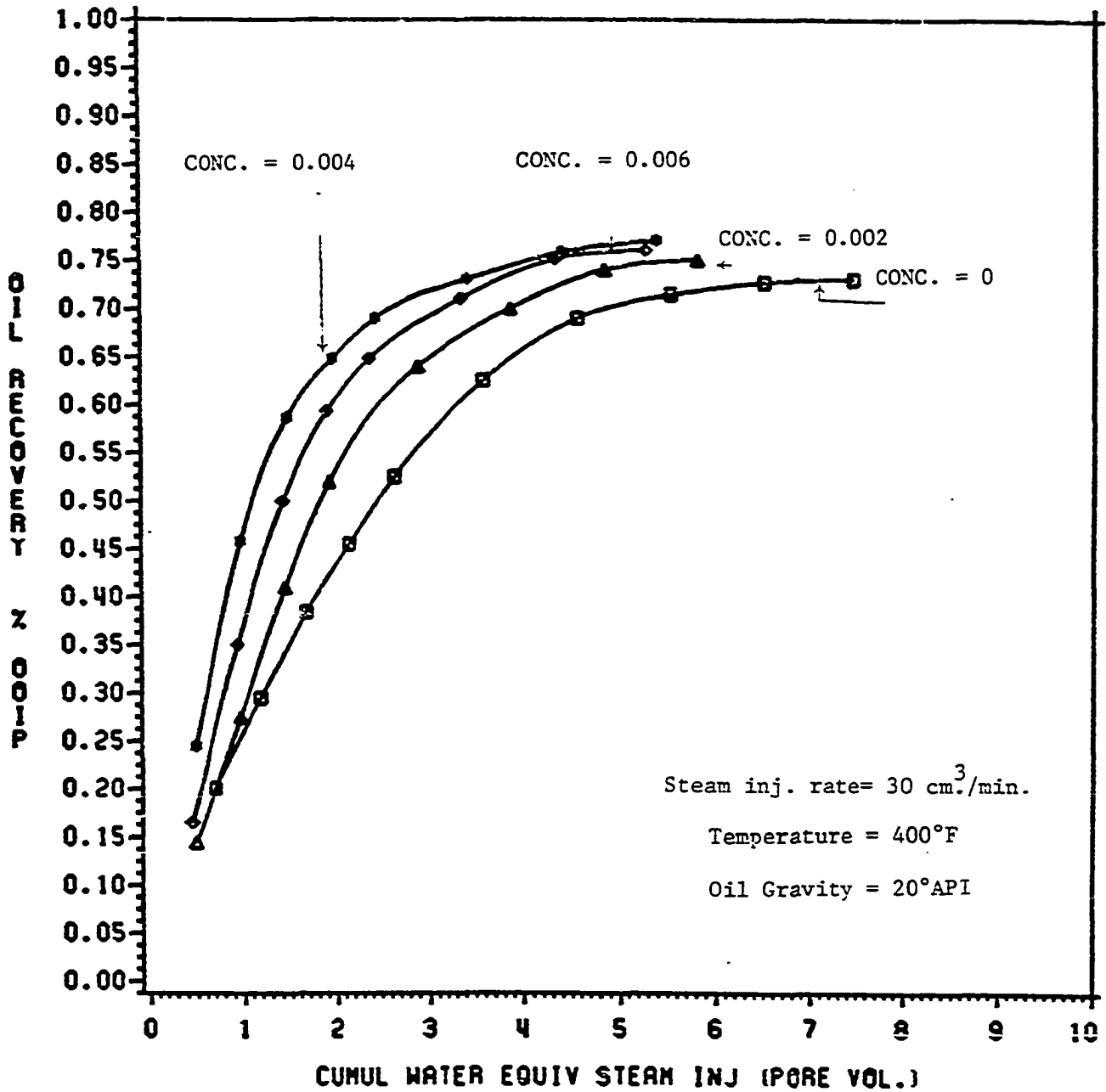


FIGURE G2: EFFECT OF CO₂ ON STEAM DRIVE RECOVERY

CONC. = CO₂/STEAM RATIO (SCF CO₂/CM³ STEAM INJ.)

EFFECT OF CO₂ ON STEAM DRIVE RECOVERY

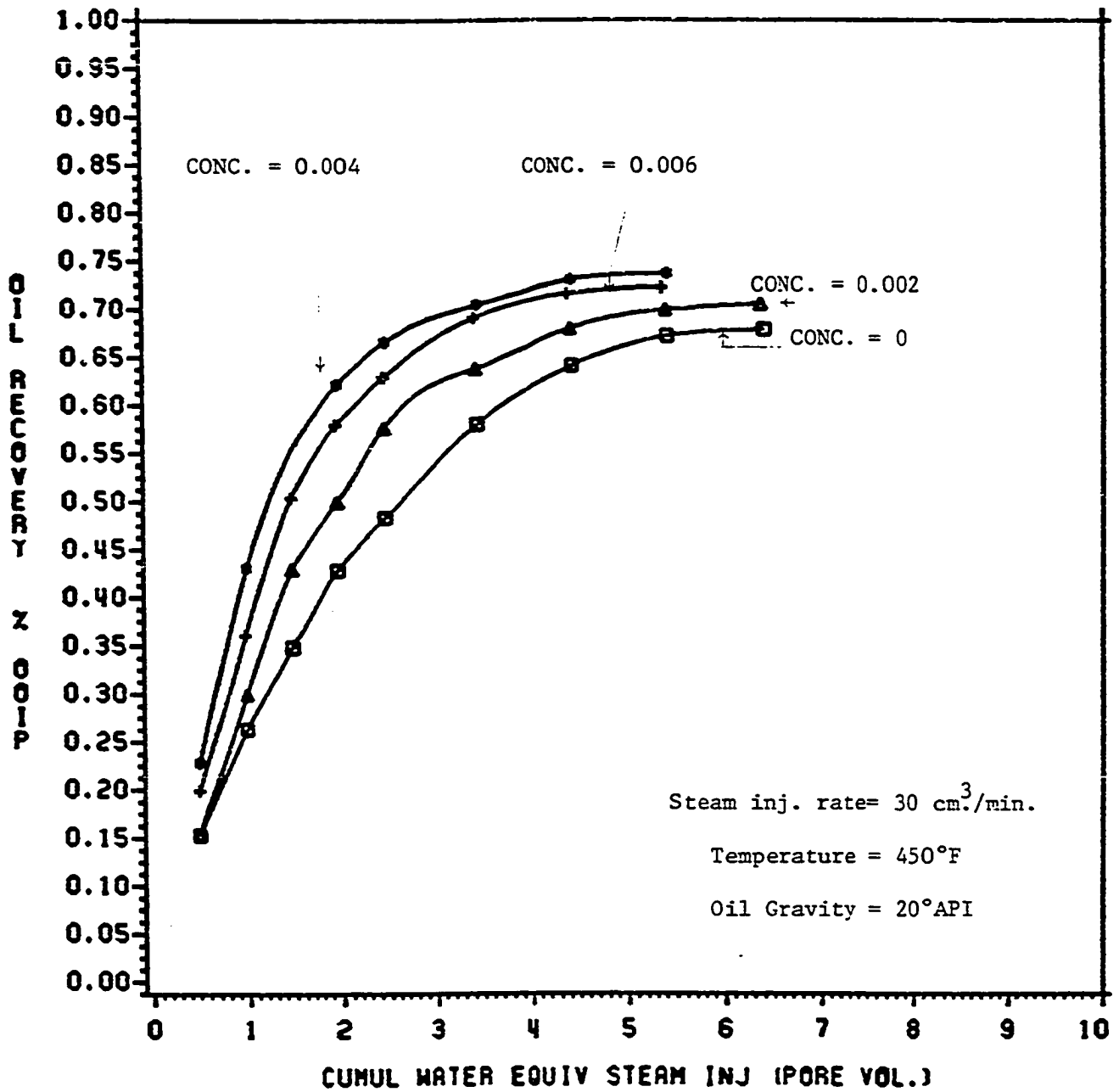


FIGURE G3: EFFECT OF CO₂ ON STEAM DRIVE RECOVERY

CONC. = CO₂/STEAM RATIO (SCF CO₂/CM³ STEAM INJ.)

EFFECT OF CO₂ ON STEAM DRIVE RECOVERY

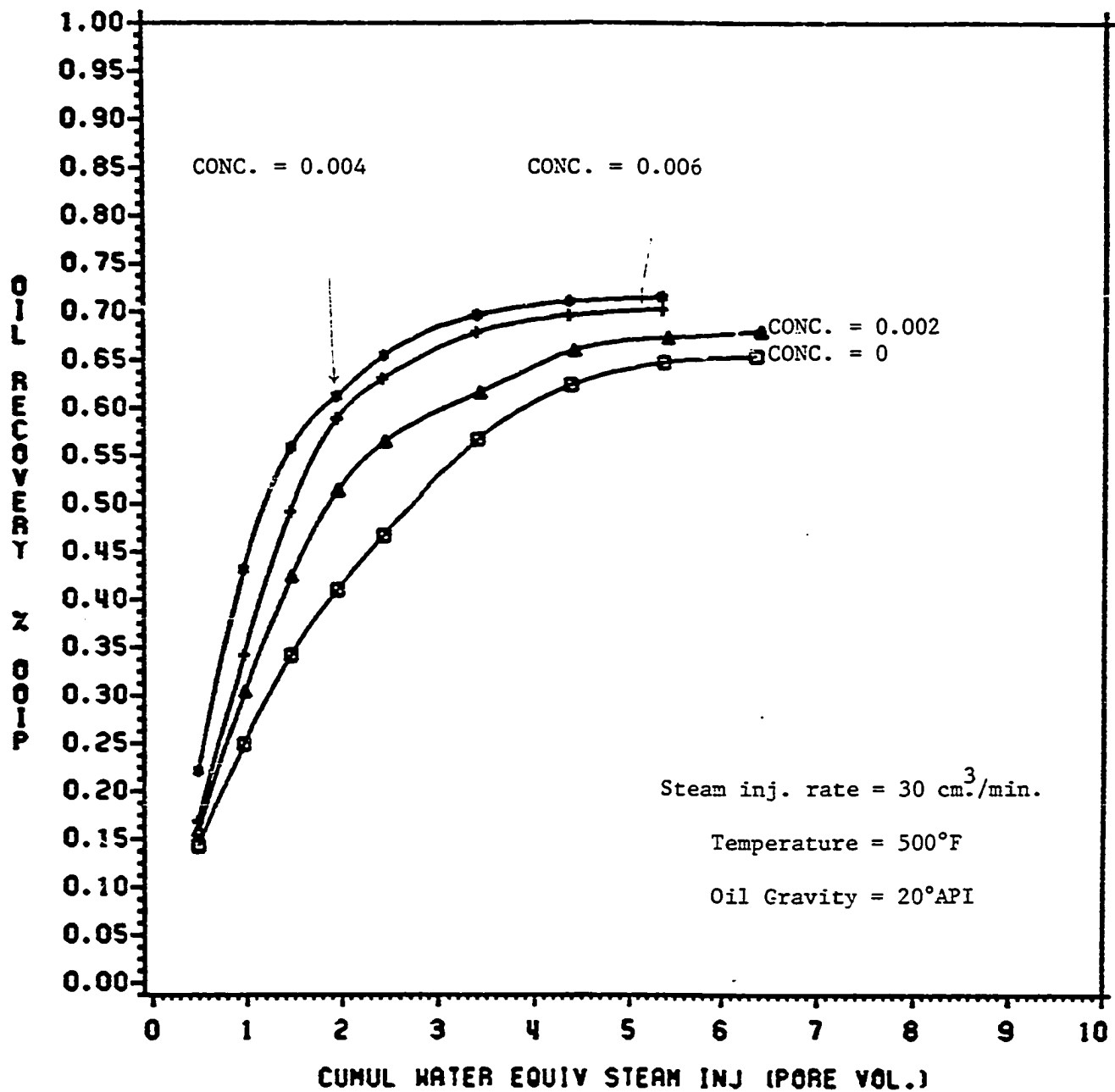


FIGURE G4: EFFECT OF CO₂ ON STEAM DRIVE RECOVERY
 CONC. = CO₂/STEAM RATIO (SCF CO₂/CM³ STEAM INJ.)

EFFECT OF CO₂ ON STEAM DRIVE RECOVERY

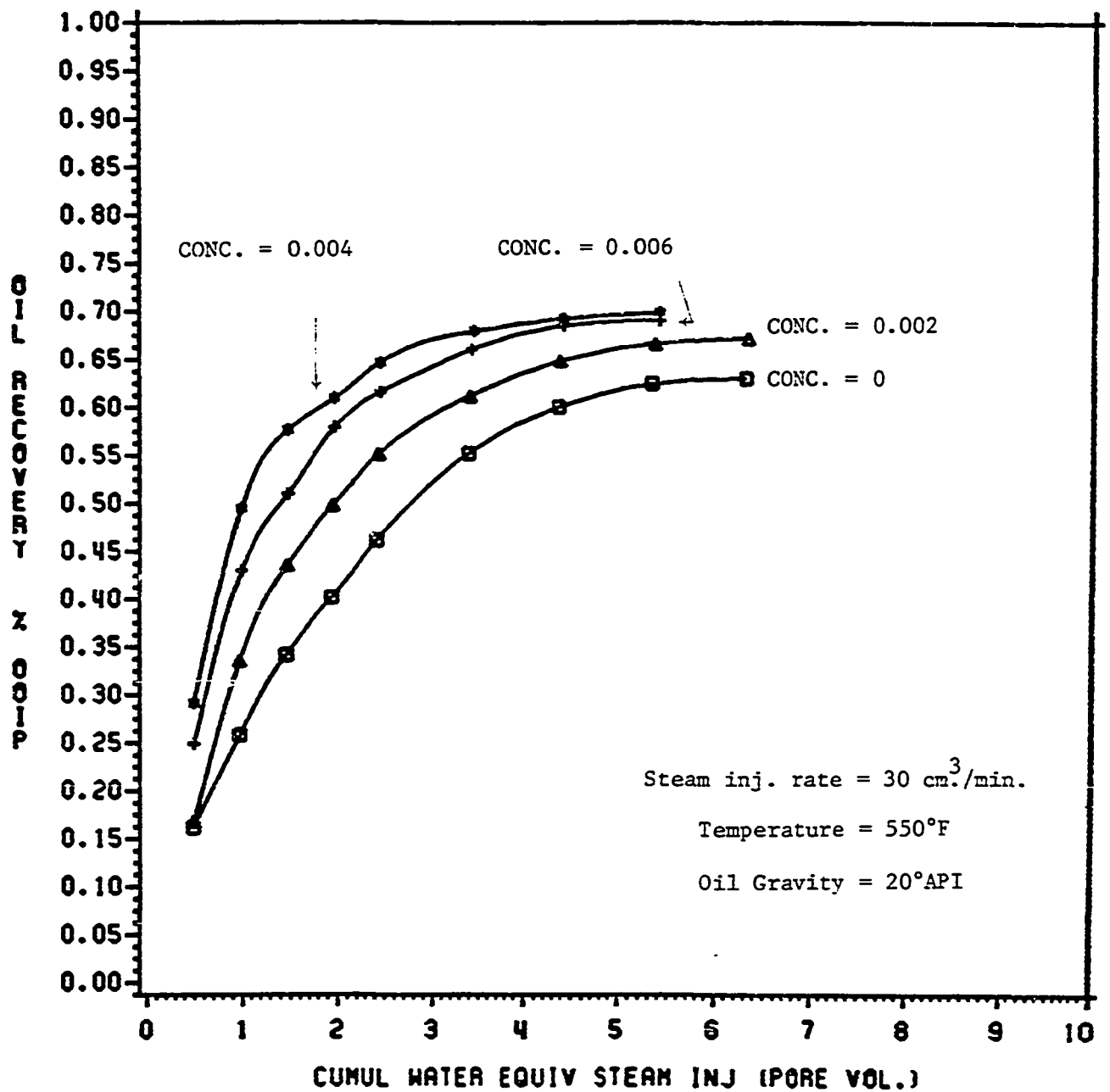


FIGURE G5: EFFECT OF CO₂ ON STEAM DRIVE RECOVERY

CONC. = CO₂/STEAM RATIO (SCF CO₂/CM³ STEAM INJ.)

EFFECT OF CO2 ON STEAM DRIVE RECOVERY

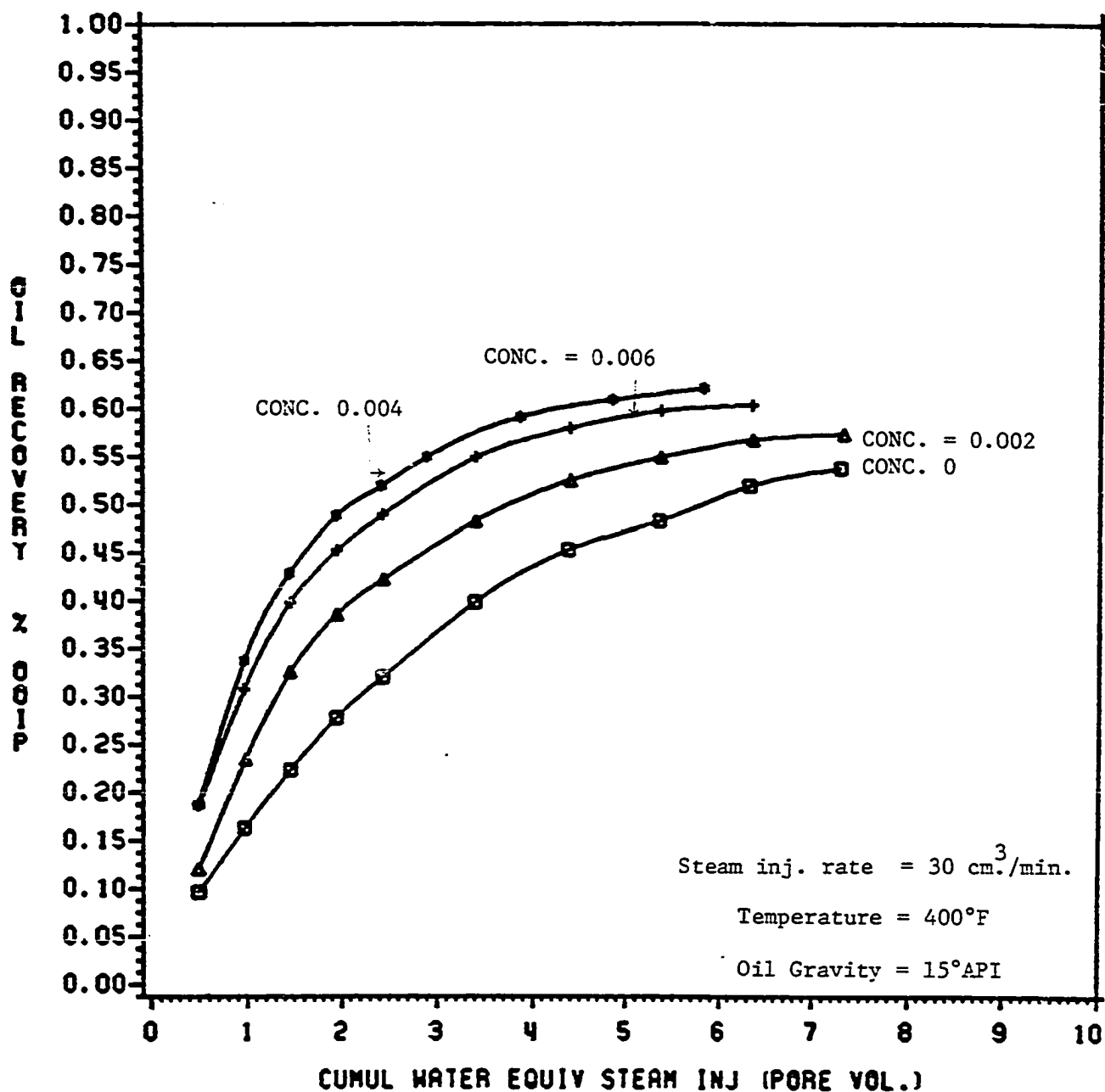


FIGURE G6: EFFECT OF CO₂ ON STEAM DRIVE RECOVERY

CONC. = CO₂/STEAM RATIO (SCF CO₂/CM³ STEAM INJ.)

EFFECT OF CO2 ON STEAM DRIVE RECOVERY

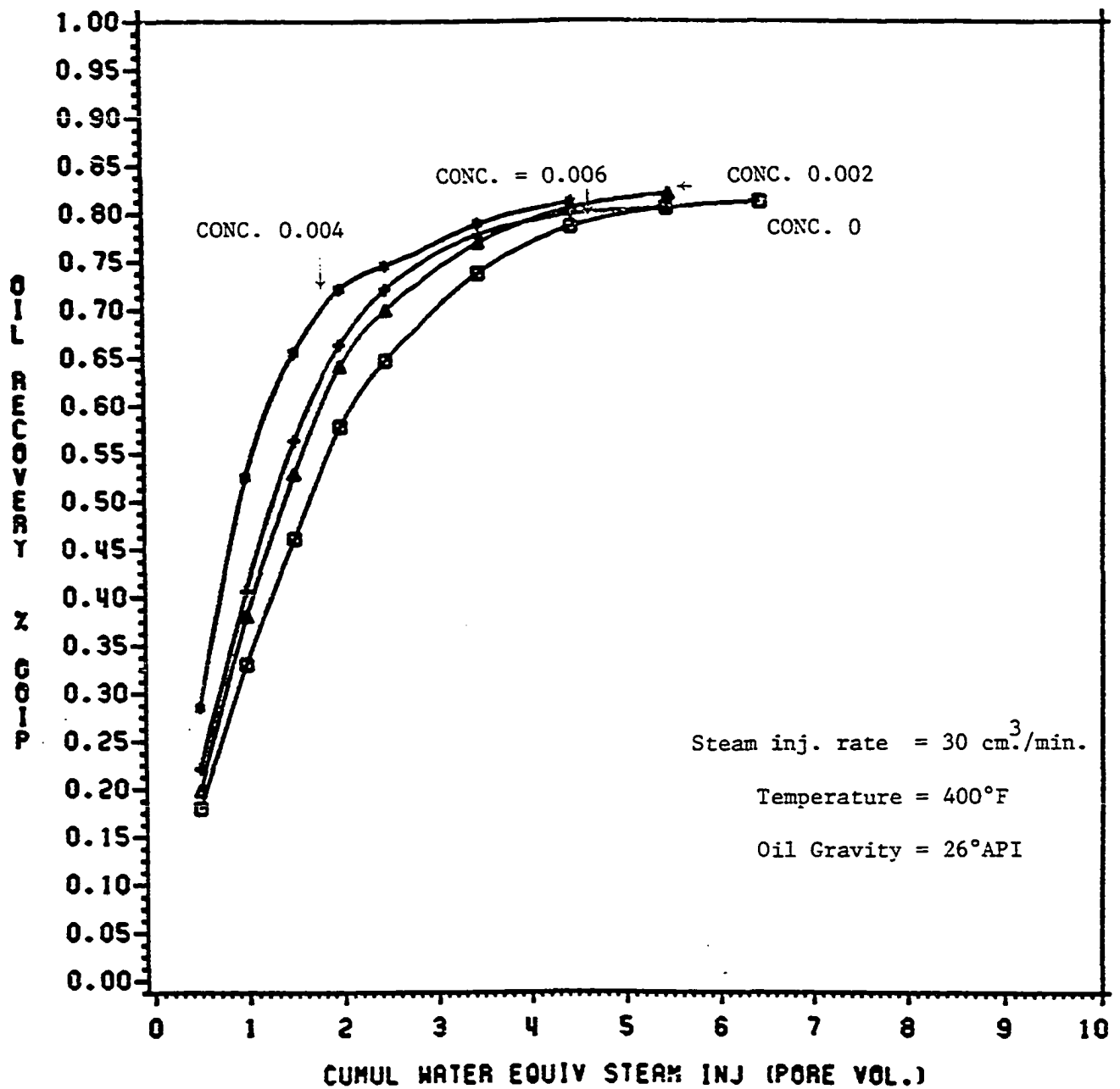


FIGURE G7: EFFECT OF CO₂ ON STEAM DRIVE RECOVERY

CONC. = CO₂/STEAM RATIO (SCF CO₂/CM³ STEAM INJ.)

EFFECT OF PH ON STEAM DRIVE RECOVERY

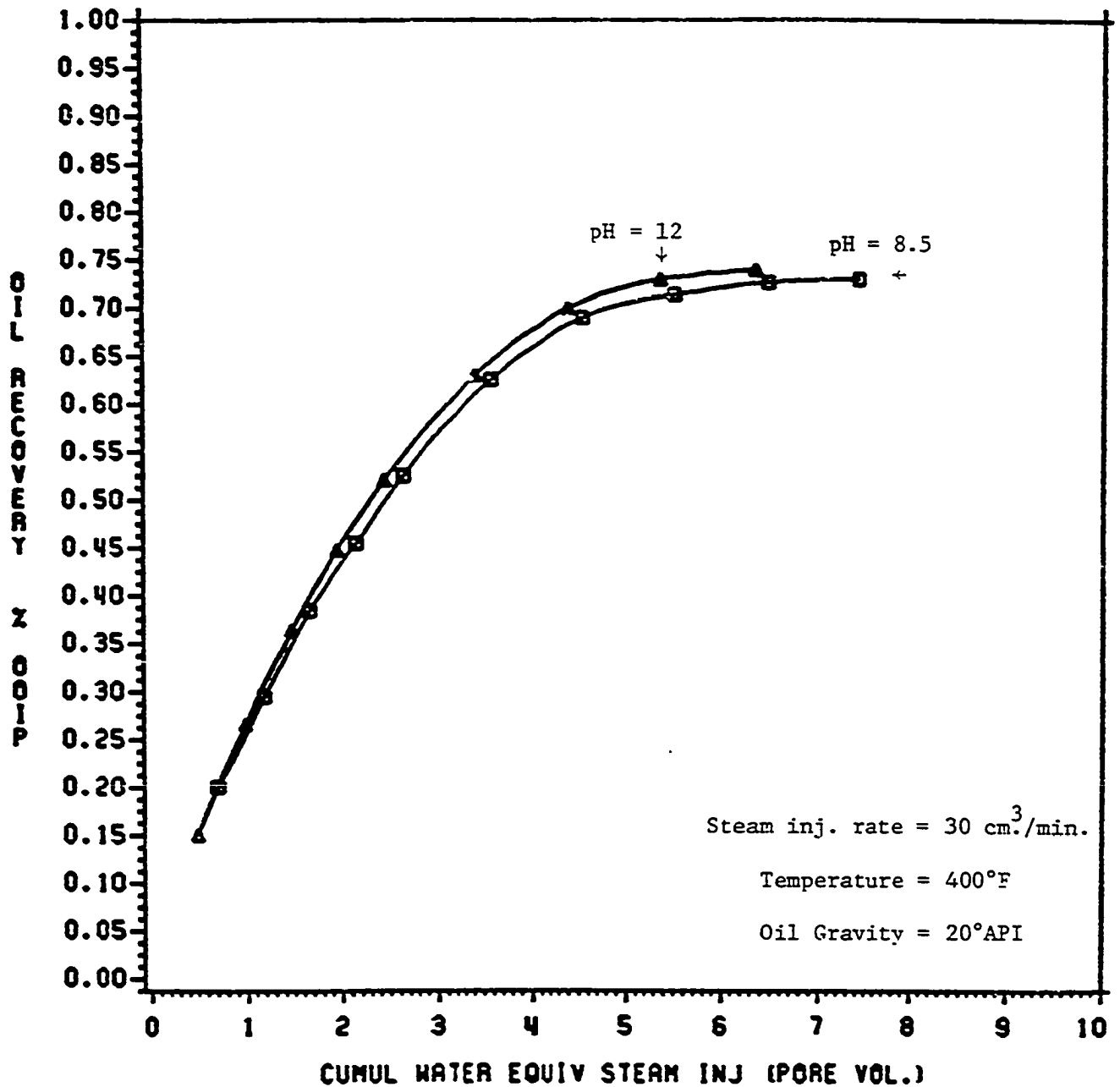


FIGURE G8: EFFECT OF pH ON STEAM DRIVE RECOVERY

CO₂/STEAM RATIO = 0.00 SCF CO₂/CM³ STEAM INJ.

EFFECT OF PH ON STEAM DRIVE RECOVERY

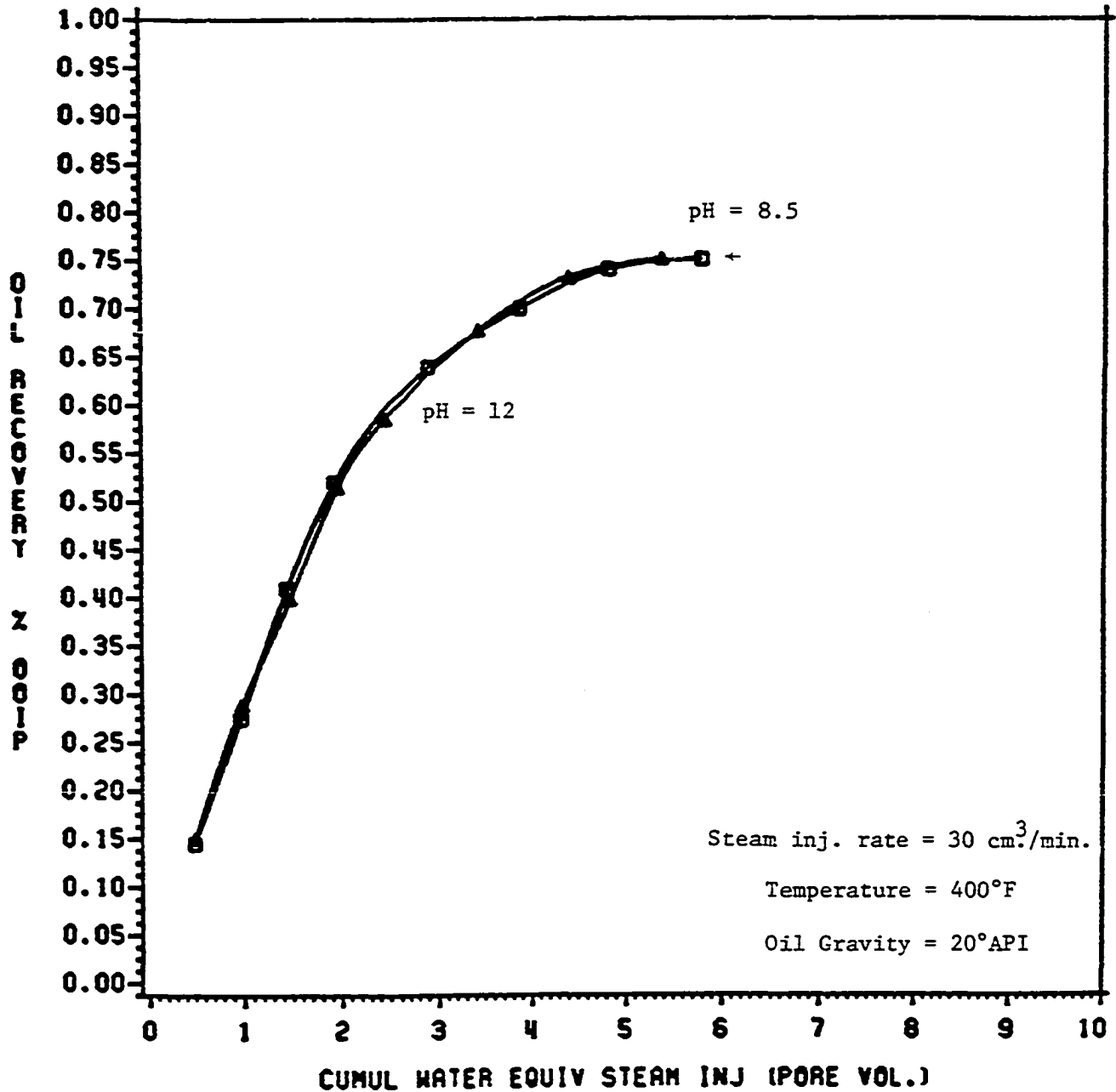


FIGURE G9: EFFECT OF pH ON STEAM DRIVE RECOVERY

TEMPERATURE = 400°F

GRAVITY OF OIL = 20°API

CO₂/STEAM RATIO = .002 SCF CO₂/CM³ STEAM INJ.

EFFECT OF PH ON STEAM DRIVE RECOVERY

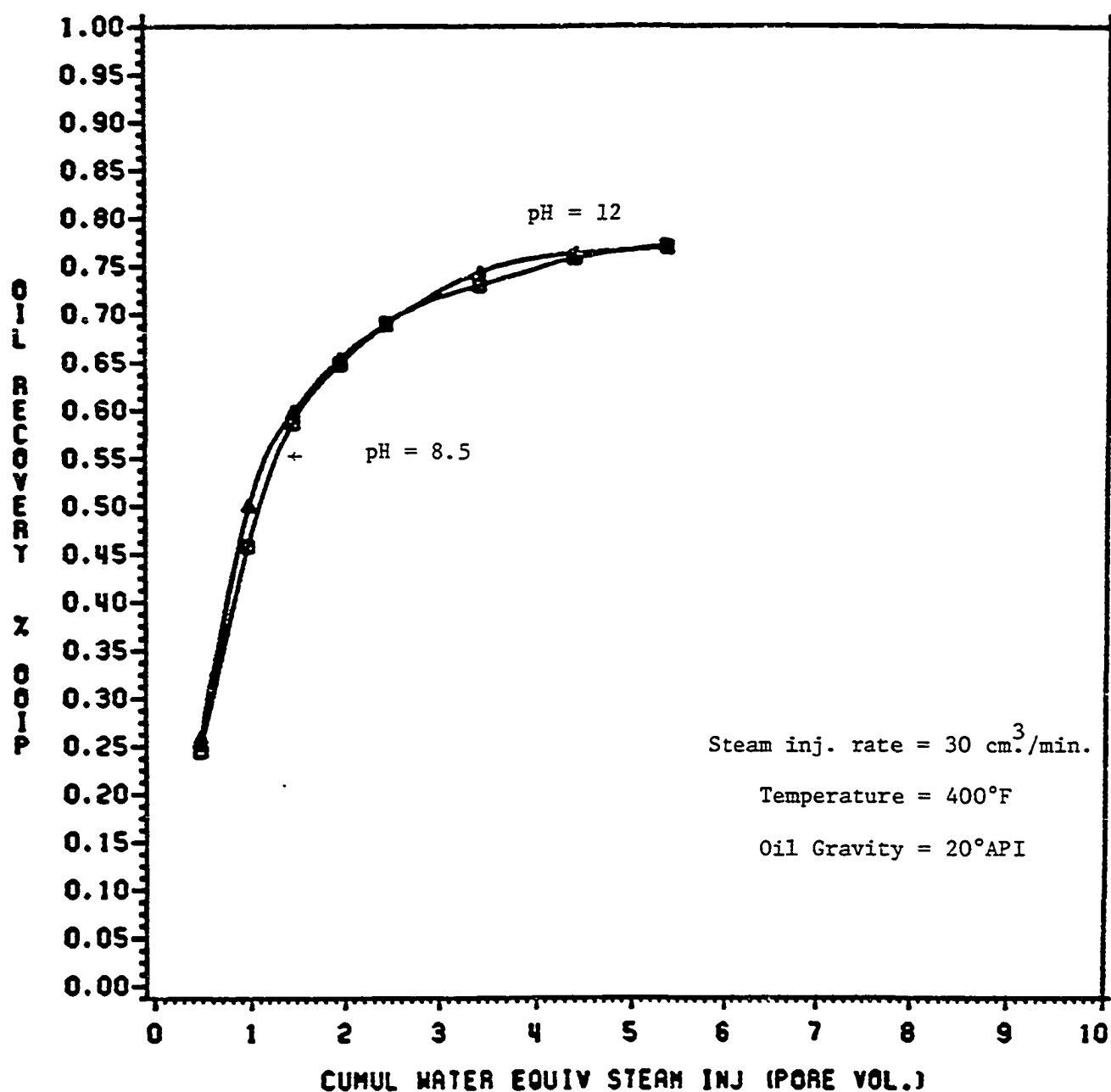


FIGURE G10: EFFECT OF pH ON STEAM DRIVE RECOVERY

TEMPERATURE = 400°F

GRAVITY OF OIL = 20 °API

CO₂/STEAM RATIO = .004 SCF CO₂/CM³ STEAM INJ.

EFFECT OF PH ON STEAM DRIVE RECOVERY

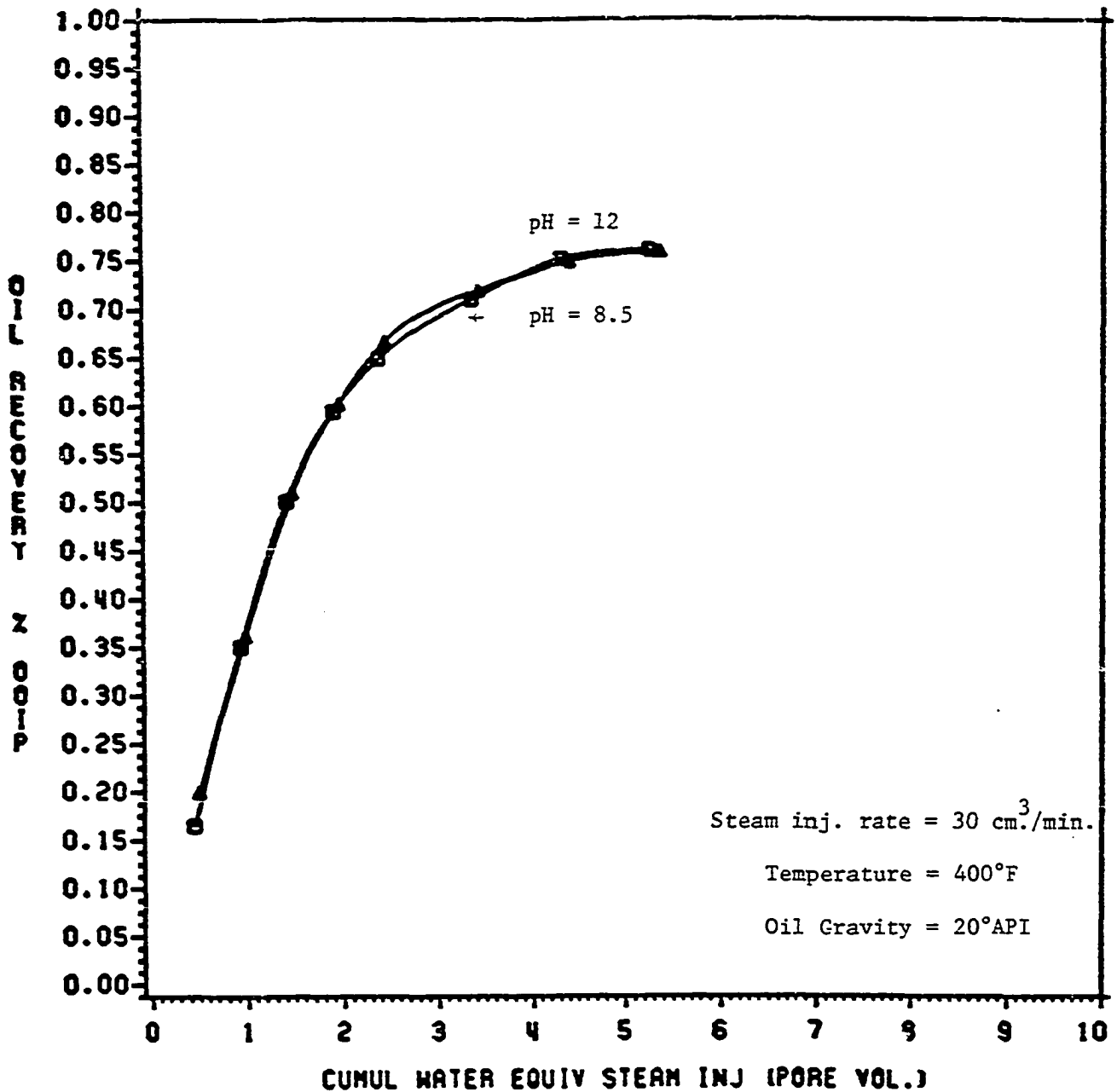


FIGURE G11: EFFECT OF pH ON STEAM DRIVE RECOVERY

CO₂/STEAM RATIO = .006 SCF CO₂/CM³ STEAM INJ.

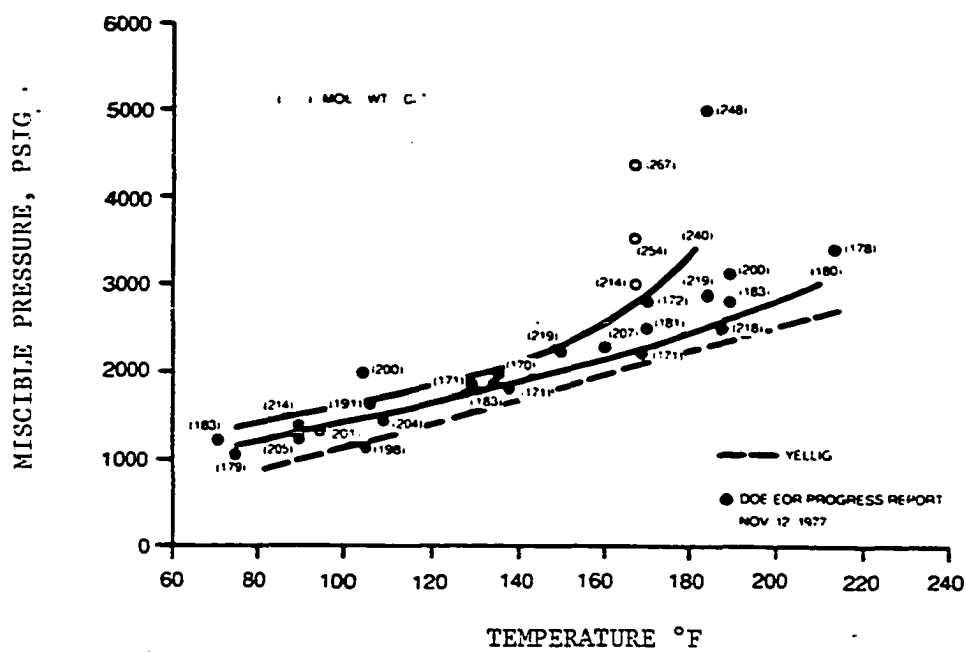


FIGURE G12: HOLM-JOSENDAL DYNAMIC MISCIBILITY DISPLACEMENT CORRELATION
FOR CO₂ (AFTER REF. 67)

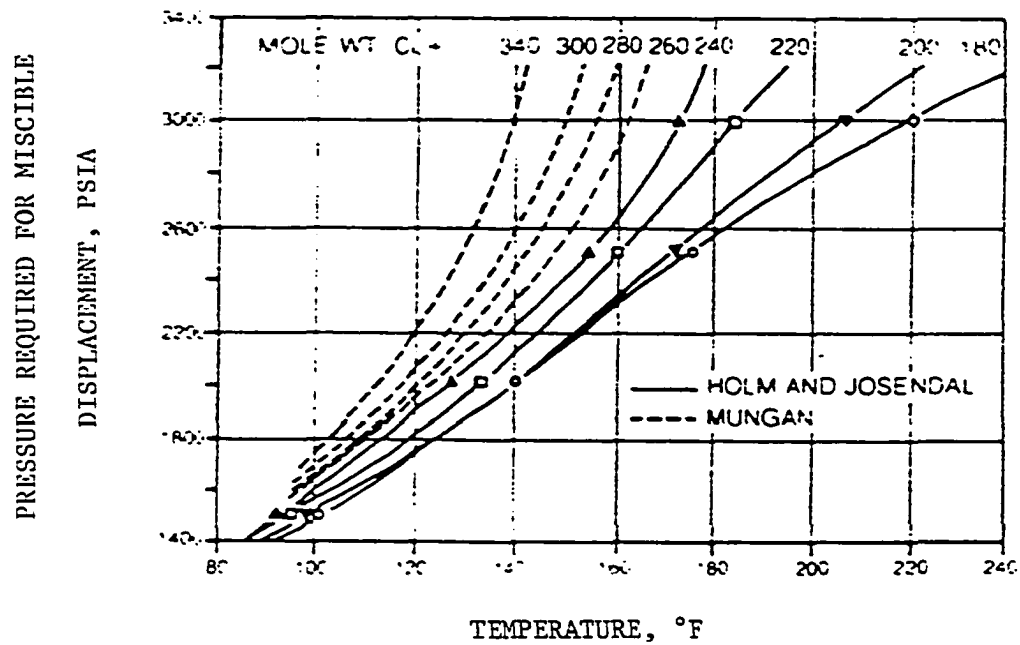


FIGURE G13: PRESSURE REQUIRED FOR MISCIBLE DISPLACEMENT IN CO₂ FLOODING
(AFTER REF.68)

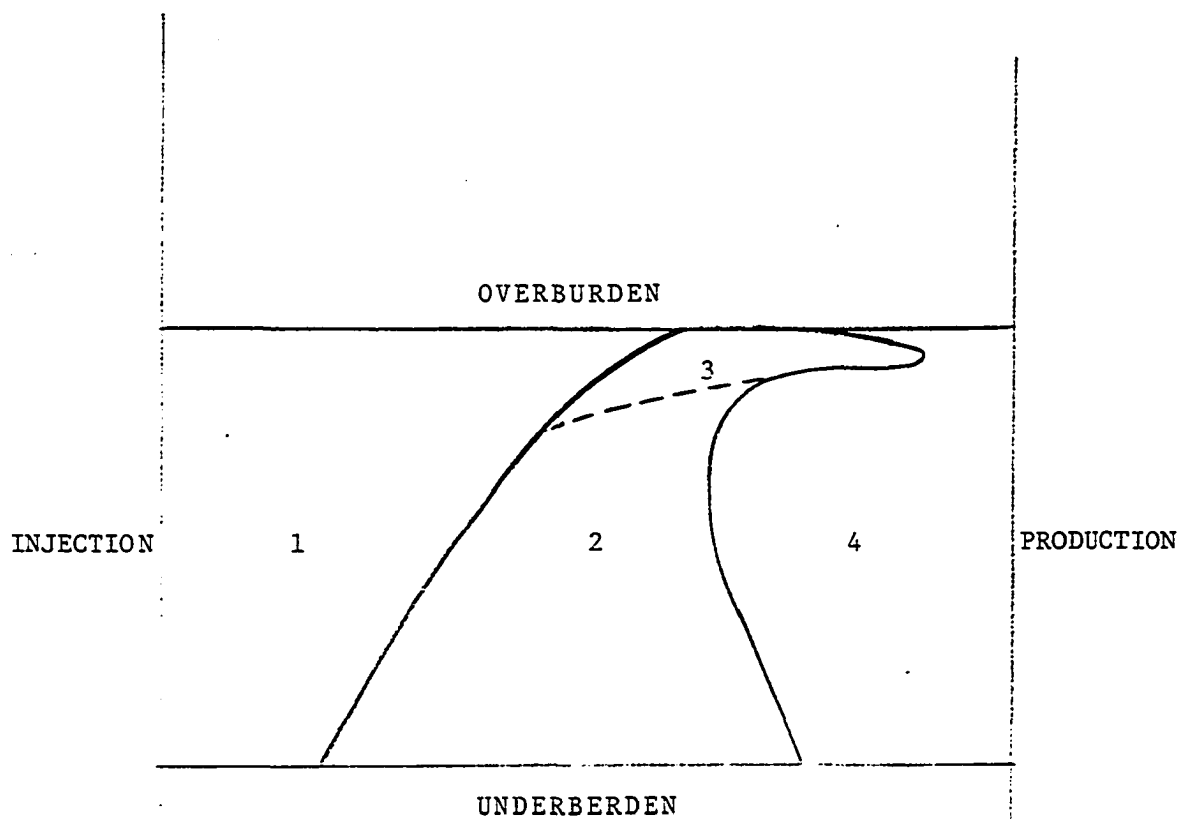


Fig. G14: Physical system representing CO_2 /steam flooding.

1. Steam + CO_2 zone
2. Hot liquid zone
3. CO_2 zone
4. Initial cold region

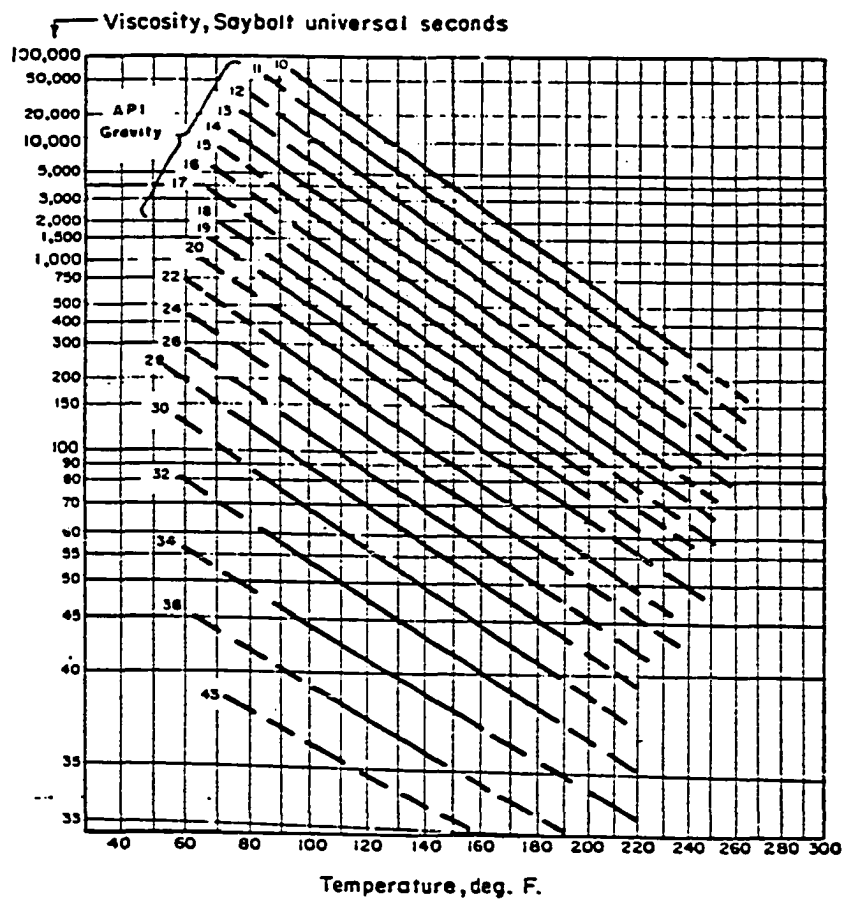


FIGURE G15: CHART FOR TEMPERATURE VARIATION OF CRUDE OIL VISCOSITY
(AFTER REF. 69)

VERTICAL DISTANCE (DIMENSIONLESS)

VERTICAL DISTANCE (DIMENSIONLESS)

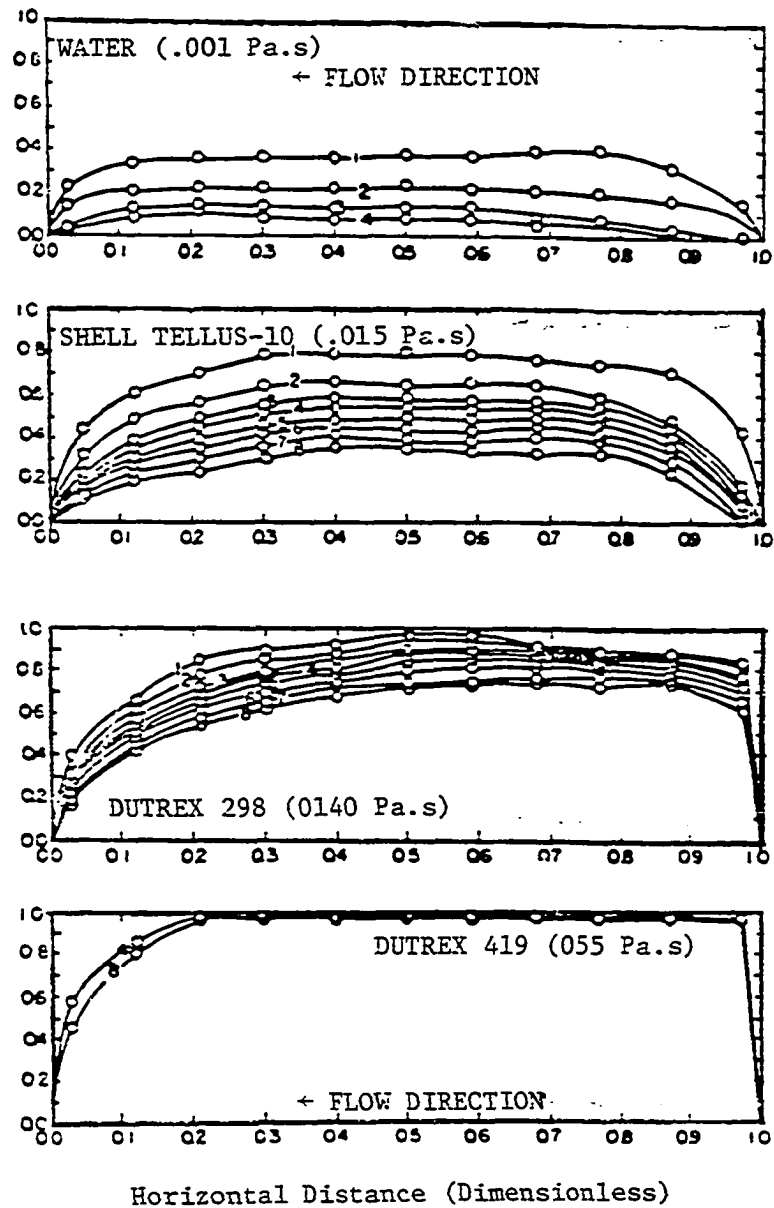


FIGURE G16: EFFECT OF OIL VISCOSITY ON DEVELOPMENT OF VERTICAL SWEEP
(AFTER REF. 70)

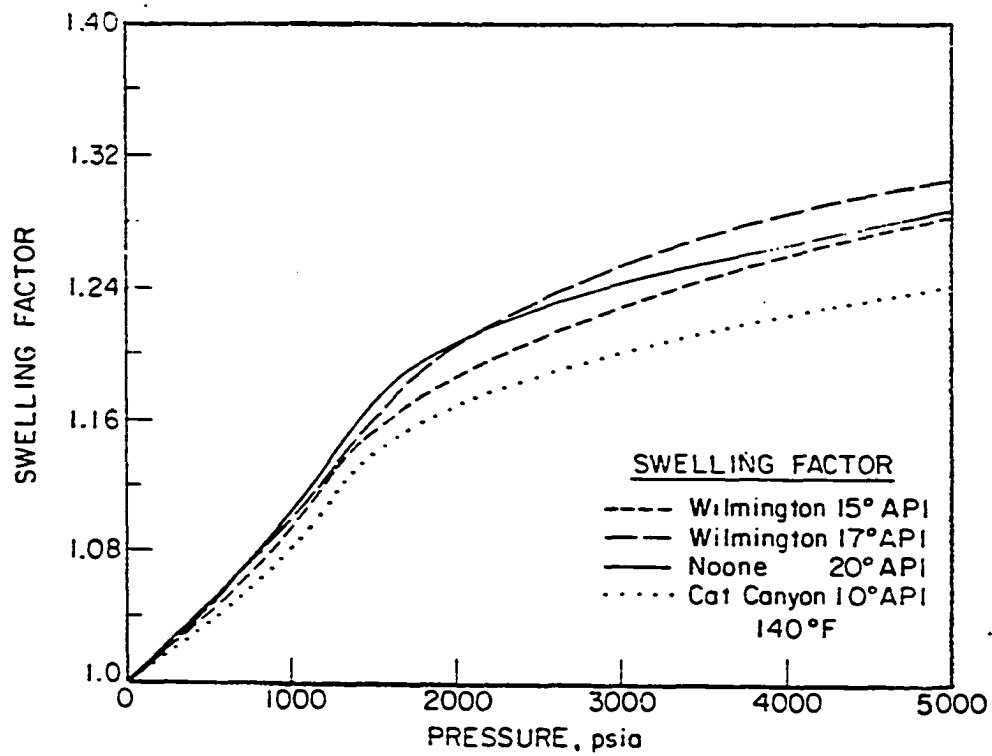


FIGURE G17: Swelling factor comparison of heavy oils at 140°F (after Ref. 71)

TEMPERATURE DISTRIBUTION

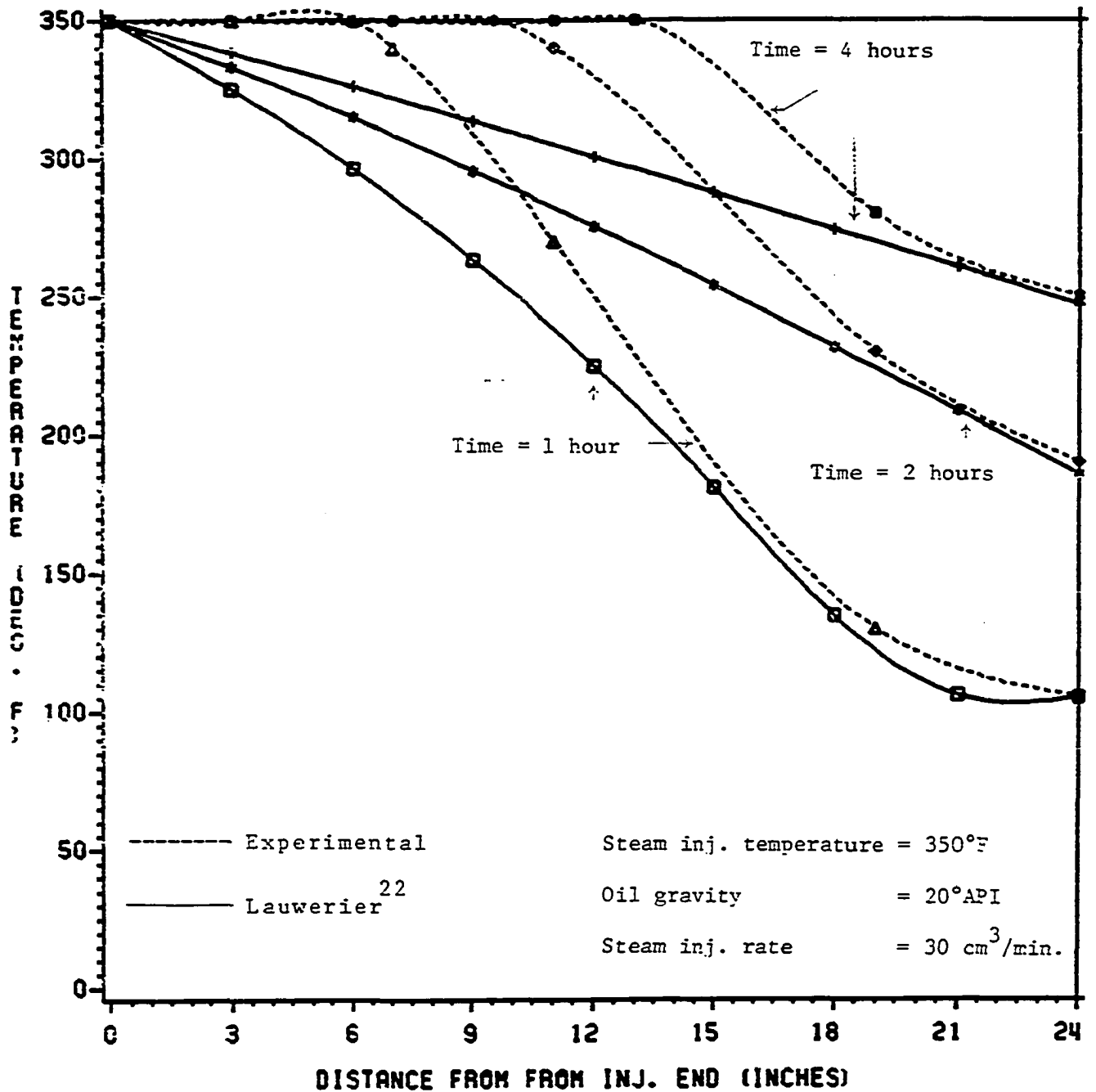


FIGURE G18: TEMPERATURE DISTRIBUTION WITH DISTANCE FOR RUN NO. 2

TEMPERATURE DISTRIBUTION

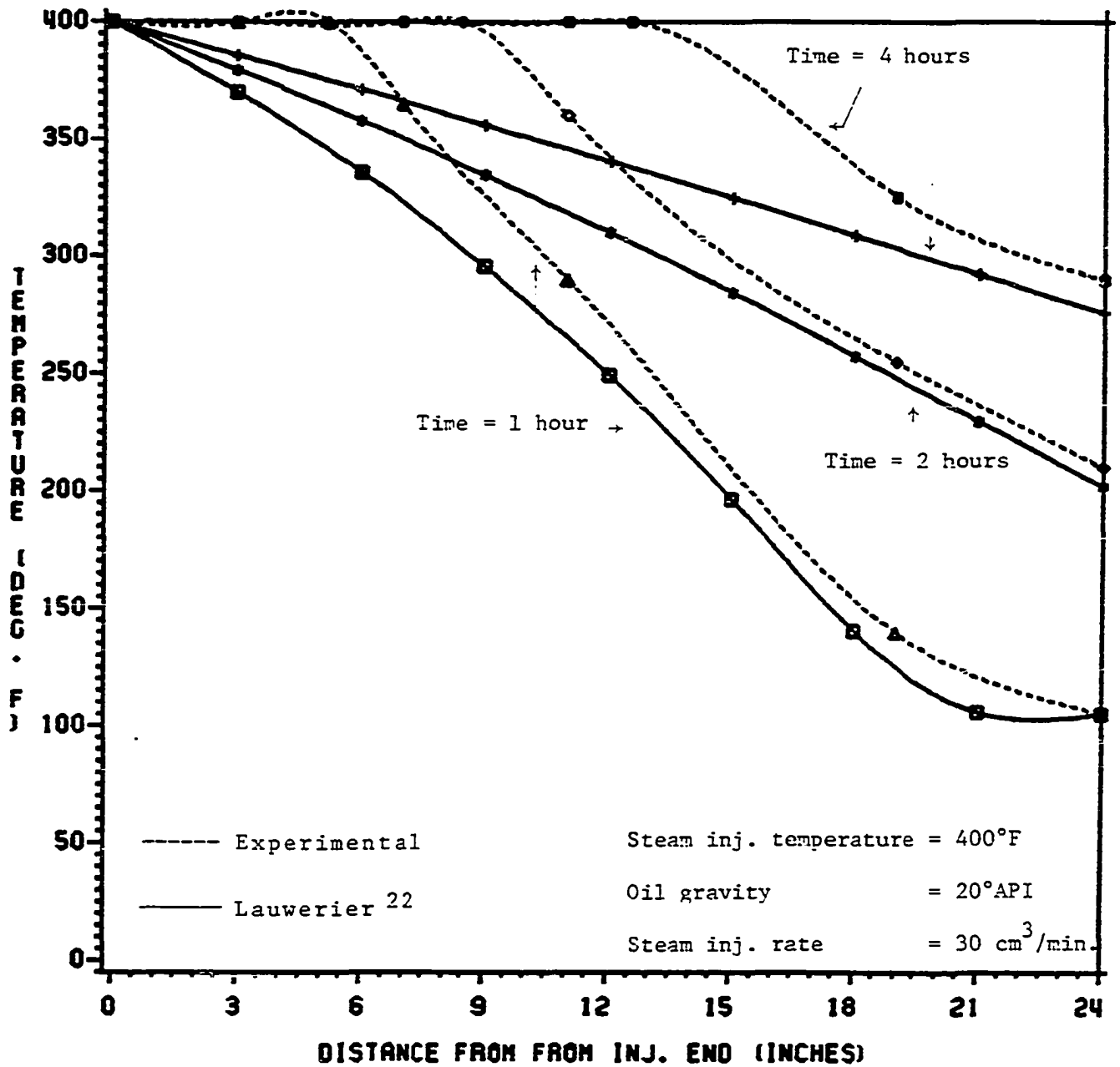


FIGURE G19: TEMPERATURE DISTRIBUTION WITH DISTANCE FOR RUN NO. 3

TEMPERATURE DISTRIBUTION

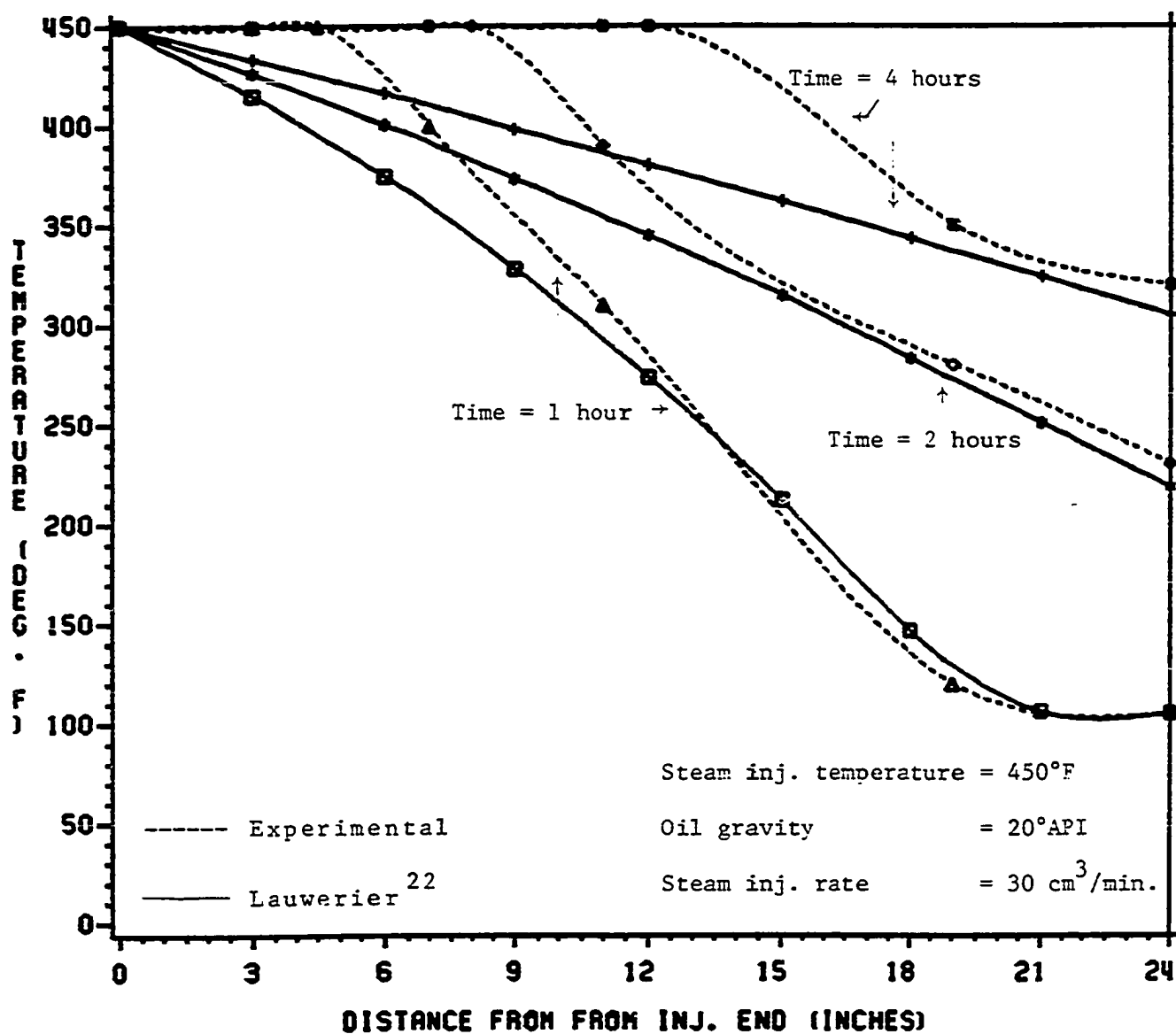


FIGURE G20: TEMPERATURE DISTRIBUTION WITH DISTANCE FOR RUN NO. 4

TEMPERATURE DISTRIBUTION

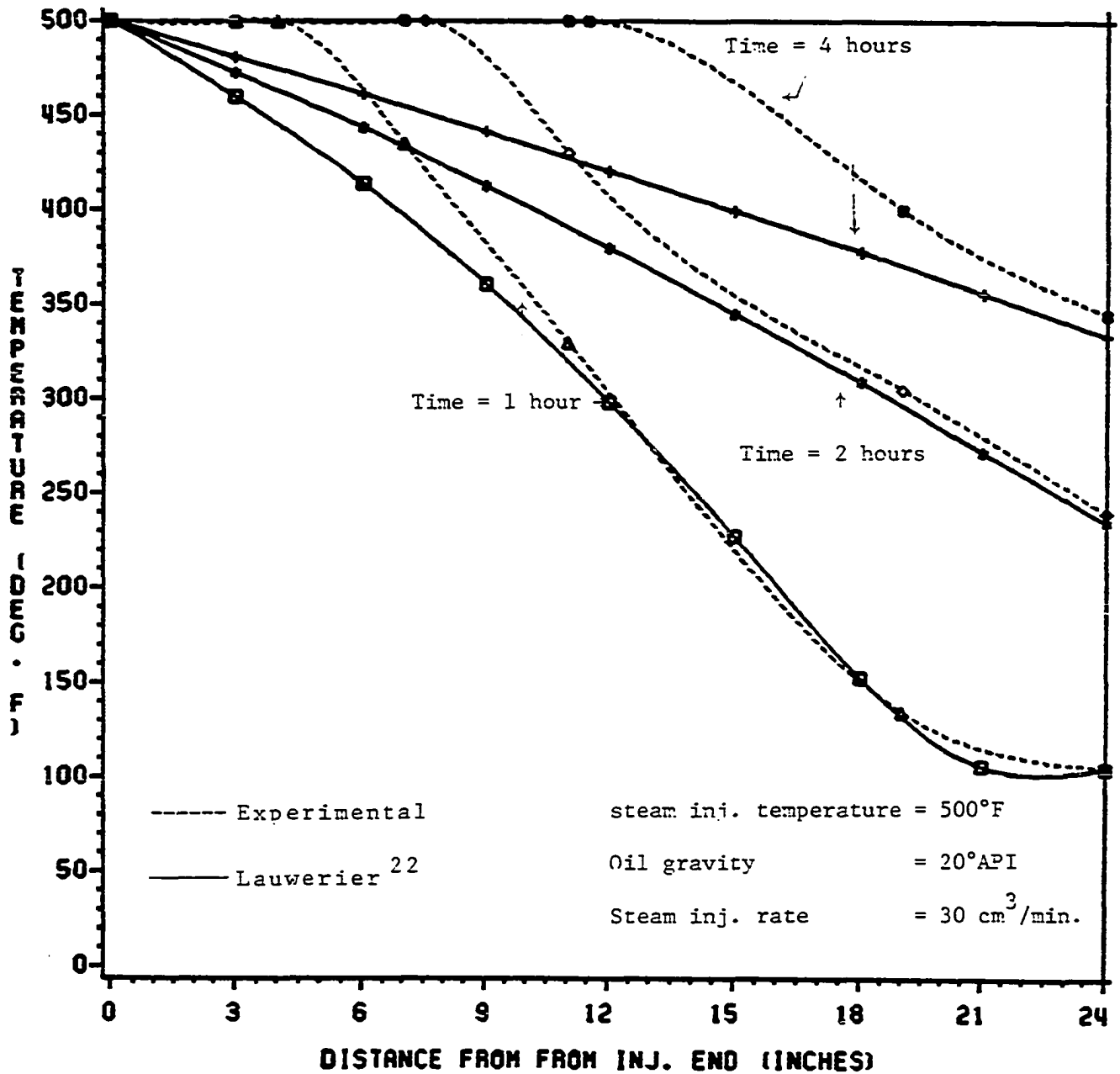


FIGURE G21: TEMPERATURE DISTRIBUTION WITH DISTANCE FOR RUN NO. 5

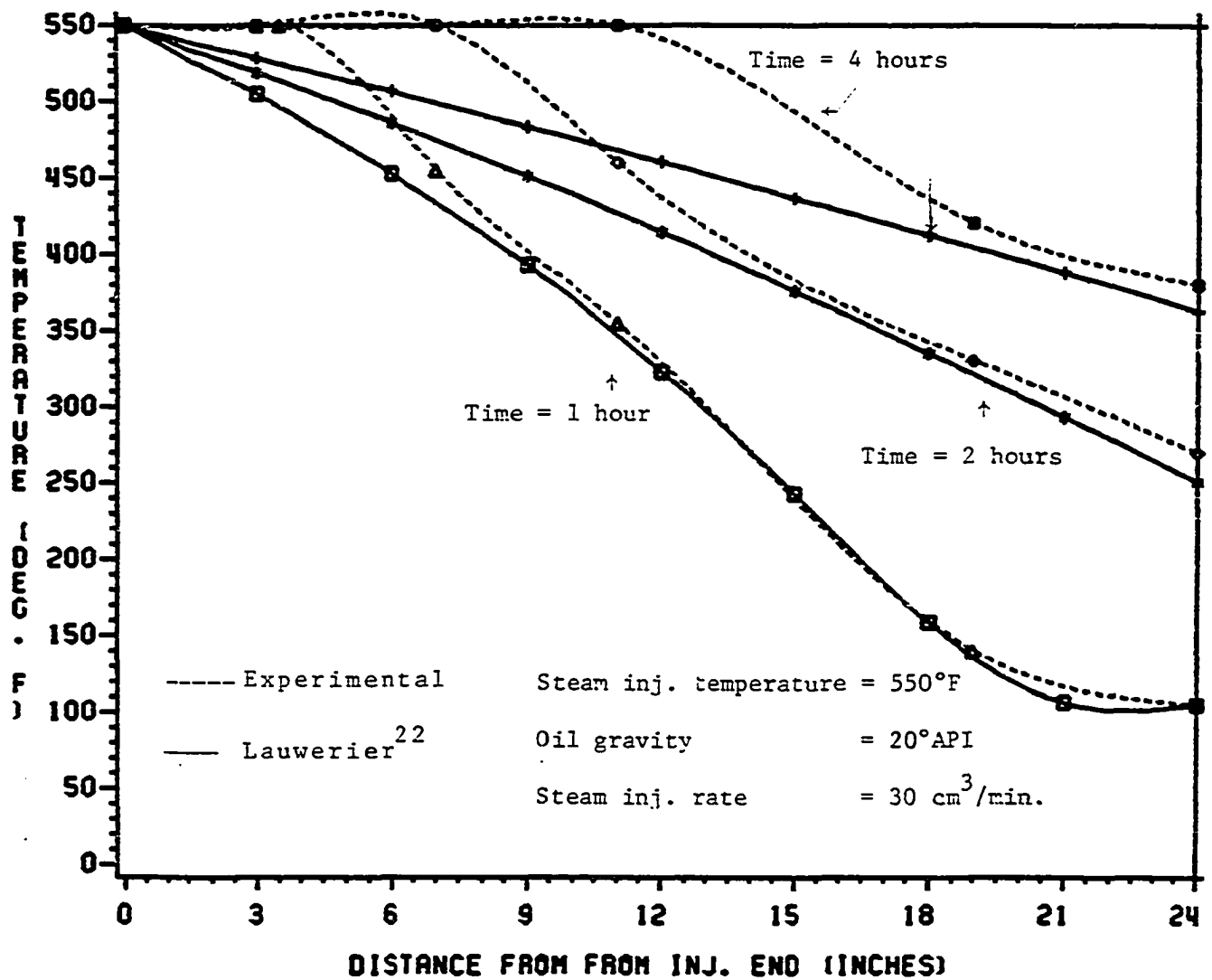


FIGURE G22: TEMPERATURE DISTRIBUTION WITH DISTANCE FOR RUN NO. 6

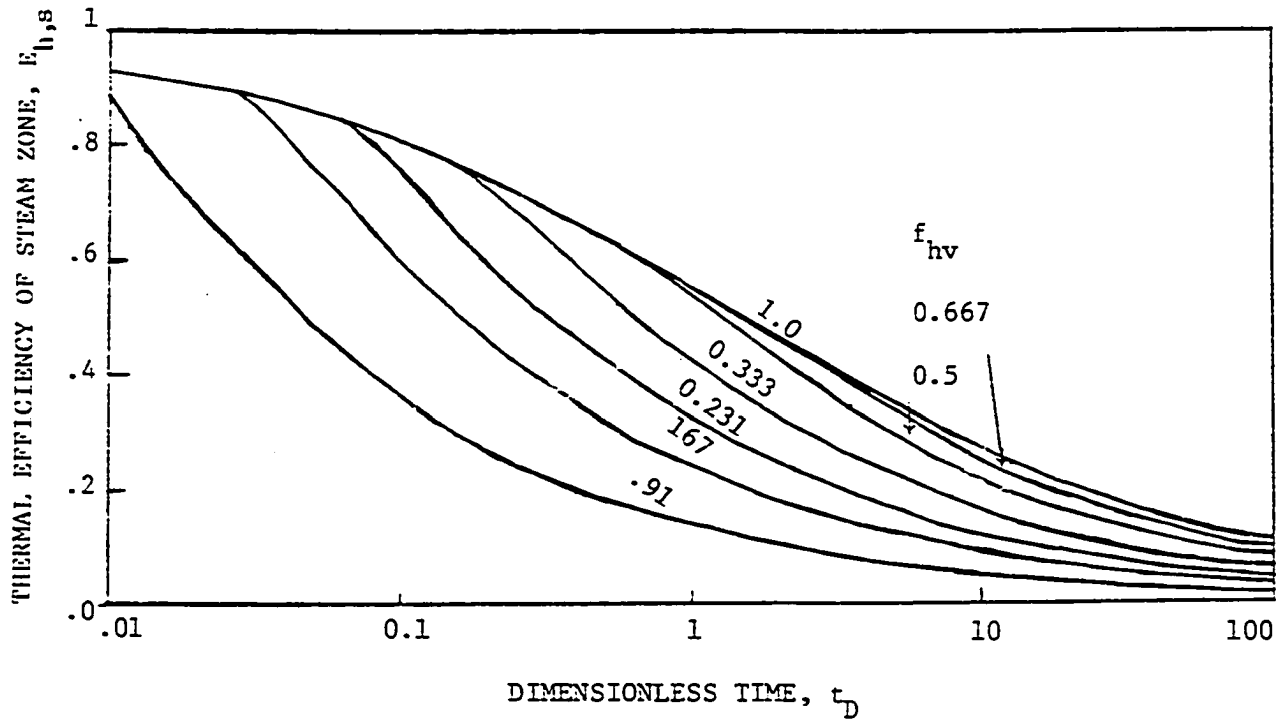


FIGURE G23: FRACTION OF HEAT INJECTED IN STEAMFLOOD REMAINING IN STEAM ZONE. (f_{hv} IS THE RATIO OF LATENT ENERGY TO TOTAL ENERGY INJECTED). (AFTER REF. 47)